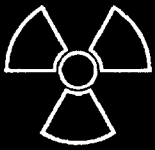
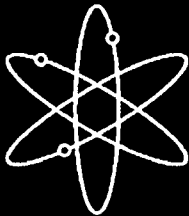




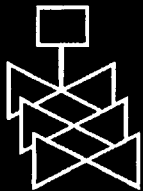
# **Integrated Chemical Effects Test Project: Consolidated Data Report**



**Los Alamos National Laboratory**



**U.S. Nuclear Regulatory Commission  
Office of Nuclear Regulatory Research  
Washington, DC 20555-0001**



## AVAILABILITY OF REFERENCE MATERIALS IN NRC PUBLICATIONS

### NRC Reference Material

As of November 1999, you may electronically access NUREG-series publications and other NRC records at NRC's Public Electronic Reading Room at <http://www.nrc.gov/reading-rm.html>. Publicly released records include, to name a few, NUREG-series publications; *Federal Register* notices; applicant, licensee, and vendor documents and correspondence; NRC correspondence and internal memoranda; bulletins and information notices; inspection and investigative reports; licensee event reports; and Commission papers and their attachments.

NRC publications in the NUREG series, NRC regulations, and *Title 10, Energy*, in the Code of *Federal Regulations* may also be purchased from one of these two sources.

1. The Superintendent of Documents  
U.S. Government Printing Office  
Mail Stop SSOP  
Washington, DC 20402-0001  
Internet: [bookstore.gpo.gov](http://bookstore.gpo.gov)  
Telephone: 202-512-1800  
Fax: 202-512-2250
2. The National Technical Information Service  
Springfield, VA 22161-0002  
[www.ntis.gov](http://www.ntis.gov)  
1-800-553-6847 or, locally, 703-605-6000

A single copy of each NRC draft report for comment is available free, to the extent of supply, upon written request as follows:

Address: U.S. Nuclear Regulatory Commission  
Office of Administration  
Mail, Distribution and Messenger Team  
Washington, DC 20555-0001  
E-mail: [DISTRIBUTION@nrc.gov](mailto:DISTRIBUTION@nrc.gov)  
Facsimile: 301-415-2289

Some publications in the NUREG series that are posted at NRC's Web site address <http://www.nrc.gov/reading-rm/doc-collections/nuregs> are updated periodically and may differ from the last printed version. Although references to material found on a Web site bear the date the material was accessed, the material available on the date cited may subsequently be removed from the site.

### Non-NRC Reference Material

Documents available from public and special technical libraries include all open literature items, such as books, journal articles, and transactions, *Federal Register* notices, Federal and State legislation, and congressional reports. Such documents as theses, dissertations, foreign reports and translations, and non-NRC conference proceedings may be purchased from their sponsoring organization.

Copies of industry codes and standards used in a substantive manner in the NRC regulatory process are maintained at—

The NRC Technical Library  
Two White Flint North  
11545 Rockville Pike  
Rockville, MD 20852-2738

These standards are available in the library for reference use by the public. Codes and standards are usually copyrighted and may be purchased from the originating organization or, if they are American National Standards, from—

American National Standards Institute  
11 West 42<sup>nd</sup> Street  
New York, NY 10036-8002  
[www.ansi.org](http://www.ansi.org)  
212-642-4900

Legally binding regulatory requirements are stated only in laws; NRC regulations; licenses, including technical specifications; or orders, not in NUREG-series publications. The views expressed in contractor-prepared publications in this series are not necessarily those of the NRC.

The NUREG series comprises (1) technical and administrative reports and books prepared by the staff (NUREG-XXXX) or agency contractors (NUREG/CR-XXXX), (2) proceedings of conferences (NUREG/CP-XXXX), (3) reports resulting from international agreements (NUREG/IA-XXXX), (4) brochures (NUREG/BR-XXXX), and (5) compilations of legal decisions and orders of the Commission and Atomic and Safety Licensing Boards and of Directors' decisions under Section 2.206 of NRC's regulations (NUREG-0750).

**DISCLAIMER:** This report was prepared as an account of work sponsored by an agency of the U.S. Government. Neither the U.S. Government nor any agency thereof, nor any employee, makes any warranty, expressed or implied, or assumes any legal liability or responsibility for any third party's use, or the results of such use, of any information, apparatus, product, or process disclosed in this publication, or represents that its use by such third party would not infringe privately owned rights.

# Integrated Chemical Effects Test Project: Consolidated Data Report

---

---

Manuscript Completed: August 2006  
Date Published: December 2006

Principal Investigator: J. Dallman

Prepared by  
J. Dallman, B. Letellier, J. Garcia, J. Madrid, W. Roesch  
Los Alamos National Laboratory  
Los Alamos, NM 87545

D. Chen, K. Howe  
University of New Mexico  
Department of Civil Engineering  
Albuquerque, NM 87110

L. Archuleta, F. Sciacca  
OMICRON Safety and Risk Technologies, Inc.  
2500 Louisiana Blvd. NE, Suite 410  
Albuquerque, NM 87110

B.P. Jain, NRC Project Manager

**Prepared for**  
**Division of Fuel, Engineering and Radiological Research**  
**Office of Nuclear Regulatory Research**  
**U.S. Nuclear Regulatory Commission**  
**Washington, DC 20555-0001**  
**NRC Job Code Y6999**



---

**NUREG/CR-6914, Volume 1, has been  
reproduced from the best available copy.**

---

# INTEGRATED CHEMICAL EFFECTS TEST PROJECT: CONSOLIDATED DATA REPORT

## ABSTRACT

Five tests conducted in the Integrated Chemical Effects Test (ICET) project apparatus attempted to simulate the chemical environment present inside a pressurized-water-reactor containment water pool after a loss-of-coolant-accident. The chemical environment within the tank included boric acid, lithium hydroxide, and hydrochloric acid. Trisodium phosphate, sodium hydroxide, or sodium tetraborate was added to each test. The tests were conducted for 30 days at a constant temperature of 60°C. The materials tested within this environment included representative amounts of submerged and unsubmerged aluminum, copper, concrete, zinc, carbon steel, and insulation samples (either 100% fiberglass or a combination of 80% calcium silicate and 20% fiberglass by volume). Representative amounts of concrete dust and latent debris were also added to the test solution. Water was circulated through the bottom portion of the test chamber during the entire test to achieve representative flow rates over the submerged specimens. Test solution pH ranged from just over 7 in Tests #2 and #3 to just over 8 in Test #5, and it reached almost 10 in Tests #1 and #4. Test solution chemistry varied from test to test, depending on the starting conditions and amount of material corrosion or leaching. Either particulate, flocculent, or film (webbing) deposits were observed in the fiberglass after each test. Visible changes were also seen on the metal coupons in each test. Corrosion was evident on both submerged and unsubmerged coupons. The amount of sediment recovered was directly proportional to the amount of particulate debris added to the test. Tests #3 and #4 had considerably more sediment than did the other tests, primarily because of the cal-sil dust added to the tank. The top layer of Test #3 sediment contained a gel-like material. When cooled to ambient temperature, test solution in Tests #1 and #5 contained precipitates. Test solution from those two tests also exhibited a non-Newtonian tendency for shear thinning with increasing strain rate when the solution was cooled to ambient temperature.



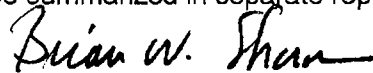
## FOREWORD

The U.S. Nuclear Regulatory Commission (NRC) is engaged in research activities related to resolving Generic Safety Issue (GSI) 191, "Assessment of Debris Accumulation on PWR Sump Performance." During a review of those staff activities, the NRC's Advisory Committee on Reactor Safeguards (ACRS) raised a concern that products attributable to chemical interactions between the emergency core cooling system (ECCS) containment spray water and exposed materials (such as metal surfaces, paint chips, and fiberglass insulation debris) could impede the performance of ECCS recirculation following a loss-of-coolant accident (LOCA) at a pressurized-water reactor (PWR).

In response to that concern, the NRC's Office of Nuclear Regulatory Research (RES) and the nuclear energy industry, represented by the Electric Power Research Institute (EPRI), jointly sponsored an integrated chemical effects test (ICET) program at the University of New Mexico, under the direction of Los Alamos National Laboratory. The objectives of that ICET program were to (1) determine, characterize, and quantify chemical reaction products that may develop in the containment pool in a representative post-LOCA PWR environment, and (2) determine and quantify any gelatinous material that could be produced during the post-LOCA recirculation phase. Toward that end, the ICET program consisted of five tests, with each test representing a unique environment. The intent was that each test would represent a portion of the commercial PWR plant, such that the entire series would broadly characterize containment pool conditions applicable to the existing nuclear fleet.

This six-volume report documents the results of this program. Volume 1 provides a summary and comparison of the important observations and measurements among all of the tests, while Volumes 2–6 provide detailed data reports for each of the five tests. As documented herein, the ICET results indicate that (1) chemical reaction products with varied quantities, consistencies, attributes, and apparent formation mechanisms were found in each unique ICET environment; (2) containment materials (metallic, non-metallic, and insulation debris), pH, buffering agent, temperature, and time are all important variables that influence chemical product formation; and (3) changes to one important environmental variable (e.g., pH adjusting agent, insulation material) can significantly affect the chemical products that form.

This report provides some insights and initial understanding regarding the solution chemistry, as well as the types and amounts of chemical reaction products that may form in the ECCS containment pool. The observed chemical products may potentially contribute to both pressure losses across a debris-laden sump screen and performance degradation of ECCS components downstream of the sump screen. The regulatory application of data and insights gained from this study is to be determined independently by the NRC staff and industry. This report is intended to assist the NRC staff in conducting reviews of licensees' responses to Generic Letter 2004-02 (GL), "Potential Impact of Debris Blockage on Emergency Recirculation During Design-Basis Accidents at Pressurized-Water Reactors," dated September 13, 2004. The staff is conducting additional research to assess head loss implications for chemical products observed in this testing and, with an external peer review group, is identifying outstanding chemical effect issues. The findings from these activities will be summarized in separate reports.



---

Brian W. Sheron, Director  
Office of Nuclear Regulatory Research  
U.S. Nuclear Regulatory Commission



# CONTENTS

ABSTRACT.....	iii
FOREWORD.....	v
EXECUTIVE SUMMARY.....	xix
ACKNOWLEDGMENTS.....	xxiii
ACRONYMS AND ABBREVIATIONS.....	xxv
1. INTRODUCTION.....	1
1.1. Objectives and Test Conditions.....	1
1.2. Information Presented in This Report.....	2
2. TEST PROCEDURES.....	5
2.1. Chemical Test Apparatus Functional Description.....	5
2.2. Pre-Test Preparation.....	6
2.2.1. Test Loop Cleaning.....	6
2.2.2. Test Coupons and Samples.....	7
2.2.3. Quality Assurance (QA) Program.....	11
2.2.4. Test Parameters.....	11
2.3. Test Operation.....	13
3. SUMMARY OF TEST RESULTS.....	15
3.1. Test #1.....	15
3.1.1. Water Samples.....	16
3.1.2. Insulation.....	17
3.1.3. Sediment.....	17
3.1.4. Coupons.....	17
3.2. Test #2.....	18
3.2.1. Water Samples.....	18
3.2.2. Insulation.....	19
3.2.3. Sediment.....	19
3.2.4. Coupons.....	19
3.3. Test #3.....	19
3.3.1. Water Samples.....	19
3.3.2. Insulation.....	20
3.3.3. Sediment.....	21
3.3.4. Coupons.....	22
3.4. Test #4.....	22
3.4.1. Water Samples.....	22
3.4.2. Insulation.....	23
3.4.3. Sediment.....	24
3.4.4. Coupons.....	24
3.5. Test #5.....	24
3.5.1. Water Samples.....	24
3.5.2. Insulation.....	26
3.5.3. Sediment.....	26
3.5.4. Coupons.....	26

4. COMPARISONS OF KEY RESULTS .....	29
4.1. Water Samples .....	29
4.1.1. Water Chemistry .....	29
4.1.2. Precipitates .....	43
4.2. Insulation .....	45
4.2.1. Fiberglass .....	45
4.2.2. Cal-Sil .....	70
4.3. Sediment .....	80
4.3.1. Test #1 Sediment.....	82
4.3.2. Test #2 Sediment.....	86
4.4. Coupons .....	98
4.4.1. Pre- and Post-Test Coupon Photographs .....	98
4.4.2. SEM/EDS.....	112
4.4.3. Passivation of Test #4 Submerged Al Coupons.....	123
4.5. Deposition Products .....	129
4.6. Gel Analysis.....	135
5. CONCLUSIONS.....	143
6. REFERENCES .....	145

## APPENDICES

Appendix A.	ICET Background Information.....	A-1
Appendix B.	Materials Used in ICET Testing.....	B-1
Appendix C.	Test Plan.....	C-1

## FIGURES

Figure 2-1.	Test loop process flow diagram.....	6
Figure 2-2.	Coupon rack configuration in the ICET tank. The blue line represents the surface of the test solution. ....	8
Figure 2-3.	A typical loaded coupon rack in the ICET tank.....	8
Figure 2-4.	Fiberglass samples attached to a coupon rack. ....	9
Figure 2-5.	Solid pieces of cal-sil samples in SS mesh. ....	10
Figure 2-6.	Pulverized cal-sil insulation before addition to the ICET tank.....	10
Figure 4-1.	ICET bench-top pH comparison. ....	30
Figure 4-2.	Day 1 turbidity. ....	31
Figure 4-3.	ICET 60°C turbidity.....	32
Figure 4-4.	ICET 23°C turbidity.....	33
Figure 4-5.	ICET Day-1 TSS.....	34
Figure 4-6.	ICET TSS.....	34
Figure 4-7.	ICET 60°C kinematic viscosity.....	35
Figure 4-8.	ICET 23°C kinematic viscosity.....	36
Figure 4-9.	ICET hydrogen concentration.....	37
Figure 4-10.	ICET Tests #1 and #5 unfiltered aluminum concentration.....	38
Figure 4-11.	ICET unfiltered calcium concentration.....	39
Figure 4-12.	ICET unfiltered copper concentration. ....	39
Figure 4-13.	ICET unfiltered zinc concentration.....	40
Figure 4-14.	ICET Tests #2, #3, and #5 unfiltered magnesium concentration.....	41
Figure 4-15.	ICET unfiltered silica concentration.....	42
Figure 4-16.	ICET unfiltered sodium concentration.....	43
Figure 4-17.	Clean fiberglass before exposure to test chemicals. ....	46
Figure 4-18.	Day 15, sample #4 SEM image (#4037), magnified 2500 times; BSE close-up.....	48
Figure 4-19.	Day 30, sample #3 SEM image (#3003), magnified 250 times, of the fiberglass with surface coating. ....	49
Figure 4-20.	Day 30, sample #3 SEM image (#3007), magnified 500 times, of the film across the fibers.....	49
Figure 4-21.	Day 15, sample #4 counting spectrum (EDS 4-22) for the crust on the fiberglass, as shown in Figure 4-18. ....	50

Figure 4-22.	Day 30, sample #3 counting spectrum (EDS #3003) of the fractured coating, as shown in Figure 4-19.	50
Figure 4-23.	ESEM image, magnified 100 times, of raw fiberglass dipped in ICET Test #1 solution. (rft105.tif, 7/28/05).	51
Figure 4-24.	EDS counting spectrum for the film on fiberglass, as shown in Figure 4-23. (rft106.tif, 7/28/05)	51
Figure 4-25.	ESEM image, magnified 100 times, of raw fiberglass dipped in ICET Test #1 solution and then washed with RO water. (DIfrg15.tif, 8/3/05)	52
Figure 4-26.	ESEM image, magnified 100 times, of raw fiberglass dipped in NaOH solution at pH 9.5. (OHfrg07.tif, 8/3/05)	52
Figure 4-27.	ESEM image, magnified 100 times, of raw fiberglass dipped in the solution containing 2800 mg/L boron and NaOH at pH 9.5. (Bofrg09.tif, 8/3/05)	53
Figure 4-28.	ESEM image, magnified 300 times, of raw fiberglass dipped in the solution containing 2800 mg/L boron and NaOH at pH 9.5. (rfgbn03.tif, 8/5/05)	53
Figure 4-29.	EDS counting spectrum for the film on fiberglass, as shown in Figure 4-28. (rfgbn05.tif, 8/5/05)	54
Figure 4-30.	ESEM image for a Test #2, Day 30, high-flow exterior fiberglass sample.	55
Figure 4-31.	Higher-magnification ESEM image of a Test #2, Day 30, high-flow exterior fiberglass sample.	55
Figure 4-32.	ESEM image for a Test #2, Day 30, high-flow interior fiberglass sample.	56
Figure 4-33.	Higher-magnification ESEM image of a Test #2, Day 30, high-flow interior fiberglass sample.	56
Figure 4-34.	Probe SEM image at 1000× magnification for a Test #2, Day 30, high-flow interior fiberglass sample. (T2D30_HiFlo023)	57
Figure 4-35.	EDS counting spectrum for the deposits on a high-flow exterior fiberglass sample.	57
Figure 4-36.	ESEM image of a Test #3, Day 30, exterior high-flow fiberglass sample, magnified 100 times. (t3hifx33, 5/11/05)	58
Figure 4-37.	EDS counting spectrum for the large masses of particulate deposits shown in Figure 4-36. (t3hifx34, 5/11/05)	59
Figure 4-38.	ESEM image of a Test #3, Day 30, exterior fiberglass sample on the drain collar (away from the drain screen), magnified 1000 times. (t3dcex21, 5/6/05)	59
Figure 4-39.	Comparison of EDS counting spectra between the light particle (EDS1, yellow) and the dark particle (EDS2, red) shown in Figure 4-38. (t3dcex24, 5/6/05)	60
Figure 4-40.	ESEM image of a Test #3, Day 30, interior high-flow fiberglass sample, magnified 100 times. (T3HiF136, 5/11/05)	60

Figure 4-41.	ESEM image of a Test #3, Day 30, interior high-flow fiberglass sample, magnified 1000 times. (t3hifi37, 5/11/05) .....	61
Figure 4-42.	ESEM image of a Test #3, Day 15, high-flow interior fiberglass sample, magnified 2000 times. (T3D15HI3, 4/22/05) .....	61
Figure 4-43.	EDS counting spectrum for the flocculent deposits between the fibers on the ESEM image shown in Figure 4-42. (T3D15HIA, 4/22/05) .....	62
Figure 4-44.	ESEM image, magnified 100 times, of a Test #4, Day 30, exterior high-flow fiberglass sample. (T4HFEx01.jpg) .....	63
Figure 4-45.	ESEM image, magnified 500 times, of a Test #4, Day 30, exterior high-flow fiberglass sample. (t4hfex07.jpg) .....	63
Figure 4-46.	ESEM image, magnified 100 times, of a Test #4, Day 30, exterior fiberglass sample on the drain collar (away from the drain screen). (t4dcox05.jpg) .....	64
Figure 4-47.	ESEM image, magnified 1000 times, of a Test #4, Day 30, exterior fiberglass sample on the drain collar (away from the drain screen). (t4dcox03.jpg) .....	64
Figure 4-48.	EDS counting spectrum for the large mass of particulate deposits on fiberglass shown in Figure 4-47. (t4dcox04.jpg) .....	65
Figure 4-49.	ESEM image, magnified 100 times, of a Test #4, Day 30, interior high-flow fiberglass sample. (t4hfin01.jpg) .....	65
Figure 4-50.	ESEM image, magnified 500 times, for a Test #4, Day 30, interior high-flow fiberglass sample. (t4hfin04.jpg) .....	66
Figure 4-51.	ESEM image, magnified 100 times, of a Test #4, Day 30, interior high-flow fiberglass sample. The sample was gently pre-rinsed with RO water. (T4Rnd01.jpg) .....	66
Figure 4-52.	ESEM image, magnified 500 times, for a Test #4, Day 30, interior high-flow fiberglass sample. The sample was gently pre-rinsed with RO water. (t4rnd05.jpg) .....	67
Figure 4-53.	ESEM image, magnified 100 times, of a Test #5, Day 30, high-flow exterior fiberglass sample. (T5D30HX1.jpg) .....	68
Figure 4-54.	ESEM image, magnified 500 times, of a Test #5, Day 30, high-flow exterior fiberglass sample. (t5d30hx3.jpg) .....	68
Figure 4-55.	ESEM image, magnified 100 times, of a Test #5, Day 30, high-flow interior fiberglass sample. (T5D30HI4.jpg) .....	69
Figure 4-56.	ESEM image, magnified 500 times, of a Test #5, Day 30, high-flow interior fiberglass sample. (t5d30hi6.jpg) .....	69
Figure 4-57.	ESEM image, magnified 500 times, of a Test #5, Day 30 high-flow interior fiberglass sample in a nylon mesh. ....	70
Figure 4-58.	EDS counting spectrum for the deposits between the fibers shown in Figure 4-57. ....	70
Figure 4-59.	SEM image, magnified 1000 times, of an unused, unbaked cal-sil sample. (T3~RawCal_Sil008) .....	72
Figure 4-60.	SEM image, magnified 1000 times, of an unused, baked cal-sil sample. (T3~BakedCal~Sil011) .....	72

Figure 4-61.	XRD results for the unused, unbaked cal-sil sample. ....	73
Figure 4-62.	XRD results for the unused, baked cal-sil sample. ....	73
Figure 4-63.	Annotated ESEM image, magnified 1000 times, of the exterior of a Test #3, Day 30, submerged high-flow baked cal-sil sample. (t3bcal40).....	75
Figure 4-64.	EDS counting spectrum for the light particles (EDS1) shown in Figure 4-63. (T3bcal41).....	75
Figure 4-65.	EDS counting spectrum for the dark particles (EDS2) shown in Figure 4-63. (t3bcal42).....	76
Figure 4-66.	Annotated ESEM image, magnified 500 times, of the exterior of a Test #3, Day 30, unbaked cal-sil sample submerged in the birdcage. (T3Calx22).....	76
Figure 4-67.	EDS counting spectrum for the particles shown in Figure 4-66. (t3calx23) .....	77
Figure 4-68.	Annotated ESEM image, magnified 500 times, of the interior of a Test #3, Day 30, unbaked cal-sil sample submerged in the birdcage. (T3CalI25).....	77
Figure 4-69.	EDS counting spectrum for the particles shown in Figure 4-68. (T3cali26).....	78
Figure 4-70.	ESEM image, magnified 500 times, of a Test #4, Day 30, low-flow exterior baked cal-sil sample. (t4bcex08.jpg).....	79
Figure 4-71.	EDS counting spectrum for the whole image shown in Figure 4-70. (t4bcex09.jpg).....	79
Figure 4-72.	ESEM image, magnified 500 times, of a Test #4, Day 30, low-flow interior baked cal-sil sample. (t4bcin11.jpg).....	80
Figure 4-73.	EDS counting spectrum for the whole image shown in Figure 4-72. (t4bcin12.jpg).....	80
Figure 4-74.	Sediment from south quadrant of tank after Test #1.....	83
Figure 4-75.	SEM overview image, magnified 40 times, of a Test #1, Day 30, sediment sample. ....	83
Figure 4-76.	SEM image with a higher magnification on a Test #1, Day 30, sediment sample.....	84
Figure 4-77.	SEM image, magnified 1000 times, of a Test #1, Day 30, sediment sample.....	84
Figure 4-78.	XRD result on a Test #1, Day 30, mixed-sediment sample.....	85
Figure 4-79.	Picture of a Test #2, Day 30, sediment sample.....	86
Figure 4-80.	SEM image of a Test #2, Day 30, sediment sample. ....	87
Figure 4-81.	Higher-magnification SEM image of a Test #2, Day 30, sediment sample. ....	87
Figure 4-82.	EDS counting spectrum for the porously structured material shown in Figure 4-81.....	88
Figure 4-83.	XRD results for Test #2, Day 30, mixed sediment. ....	88
Figure 4-84.	Sediment removed from the tank after Test #3.....	89
Figure 4-85.	ESEM image of a Test #3, Day 30, pink sediment, magnified 100 times. (t3pnkp31, 5/6/05).....	90

Figure 4-86.	EDS counting spectrum for the pink sediment shown in Figure 4-85. (t3pnkp30, 5/6/05).....	90
Figure 4-87.	ESEM image of a Test #3, Day 30, yellow sediment, magnified 100 times. (t3ylwp34, 5/6/05).....	91
Figure 4-88.	EDS counting spectrum for the particles shown in Figure 4-87. (t3ylwp35, 5/6/05).....	91
Figure 4-89.	XRD results for the Test #3, Day 30, mixed sediment. ....	92
Figure 4-90.	Sediment removed from the tank after Test #4.....	93
Figure 4-91.	Annotated SEM image, magnified 500 times, for a Test #4, Day 30, sediment sample at the bottom of the tank. (T4D30SEDMT027.bmp) .....	93
Figure 4-92.	EDS counting spectrum for the white snow-like deposits (EDS1) shown in Figure 4-91. (T4D30SEDMT16.jpg) .....	94
Figure 4-93.	EDS counting spectrum for the dark deposits (EDS2) shown in Figure 4-91. (T4D30SEDMT17.jpg).....	94
Figure 4-94.	XRD results for the possible matching crystalline substances in the Test #4, Day 30, sediment. ....	95
Figure 4-95.	Sediment sample removed from the tank after Test #5. ....	96
Figure 4-96.	SEM image, magnified 70 times, of the Test #5, Day 30, sediment at the bottom of the tank. ....	96
Figure 4-97.	EDS counting spectrum for the big particulate deposit shown in Figure 4-96.....	97
Figure 4-98.	XRD results for the possible matching crystalline substances in Test #5, Day 30, sediment. ....	97
Figure 4-99.	ICET Test#1 Al-91 post-test (left); ICET Test#2 Al-96 post-test (right).....	98
Figure 4-100.	ICET Test#3 Al-155 submerged, post-test (left); ICET Test#4 Al-237 submerged, post-test, (right). ....	98
Figure 4-101.	ICET Test #5 Al-93 submerged, post-test. ....	99
Figure 4-102.	Unused Al coupon.....	99
Figure 4-103.	ICET Test #1 GS-328 submerged, post-test (left); ICET Test #2 GS-335 submerged, post-test (right). ....	99
Figure 4-104.	ICET Test #3 GS-468 submerged, post-test (left); ICET Test #4 GS-130 submerged, post-test (right). ....	100
Figure 4-105.	ICET Test #5 GS-332 submerged, post-test. ....	100
Figure 4-106.	Unused GS coupon. ....	100
Figure 4-107.	ICET Test #1 IOZ-77 submerged, post-test (left); ICET Test #2 IOZ-79 submerged, post-test (right). ....	101
Figure 4-108.	ICET Test #3 IOZ-156 submerged, post-test (left); ICET Test #4 IOZ-233 submerged, post-test (right). ....	101
Figure 4-109.	ICET Test #5 IOZ-310 submerged, post-test.....	102
Figure 4-110.	Unused IOZ-coated coupon. ....	102
Figure 4-111.	ICET Test #1 CU-80 submerged, post-test (left); ICET Test #2 CU-105 submerged, post-test (right). ....	102

Figure 4-112. ICET Test #3 CU-207 submerged, post-test (left); ICET Test #4 CU-100 submerged, post-test (right).	103
Figure 4-113. ICET Test #5 CU-100 submerged, post-test.	103
Figure 4-114. Unused CU coupon.	103
Figure 4-115. ICET Test #1 US-8 submerged, pre-test (left); ICET Test #2 US-7 submerged, post-test (right).	104
Figure 4-116. ICET Test #3 US-11 submerged, post-test (left); ICET Test #4 US-17 submerged, post-test (right).	104
Figure 4-117. ICET Test #5 US-14 submerged, post-test.	104
Figure 4-118. Unused US coupon.	105
Figure 4-119. ICET Test #1 Conc-6 submerged, post-test (left); ICET Test #2 Conc-2 submerged, post-test (right).	105
Figure 4-120. ICET Test #3 Conc-5 submerged, post-test (left); ICET Test #4 Conc-4 submerged, post-test (right).	105
Figure 4-121. ICET Test #5 Conc-003 submerged, post-test.	106
Figure 4-122. Unused concrete coupon.	106
Figure 4-123. Test #1 Al-42 unsubmerged (left); Test #2 Al-101 unsubmerged (right).	107
Figure 4-124. Test #3 Al-159 unsubmerged (left); Test #4 Al-3 unsubmerged (right).	107
Figure 4-125. Test #5 Al-247 unsubmerged.	108
Figure 4-126. Test #1 GS-223 unsubmerged (left); Test #2 GS-366 unsubmerged (right).	108
Figure 4-127. Test #3 GS-503 unsubmerged (left); Test #4 GS-33 unsubmerged (right).	108
Figure 4-128. Test #5 GS-167 unsubmerged.	109
Figure 4-129. Test #1 CU-76 unsubmerged (left); Test #2 CU-196 unsubmerged (right).	109
Figure 4-130. Test #3 CU-291 unsubmerged (left); Test #4 CU-584 unsubmerged (right).	109
Figure 4-131. Test #5 CU-587 unsubmerged.	110
Figure 4-132. Test #1 IOZ-48 unsubmerged (left); Test #2 IOZ-26 unsubmerged (right).	110
Figure 4-133. Test #3 IOZ-199 unsubmerged (left); Test #4 IOZ-275 unsubmerged (right).	110
Figure 4-134. Test #5 IOZ-356 unsubmerged.	111
Figure 4-135. Test #1 US-1 unsubmerged (left); Test #2 US-10 unsubmerged (right).	111
Figure 4-136. Test #3 US-13 unsubmerged (left); Test #4 US-16 unsubmerged (right).	111
Figure 4-137. ICET Test #5 US-18 unsubmerged.	112
Figure 4-138. Unused aluminum coupon (left); Test #1 submerged aluminum coupon (right).	114
Figure 4-139. Test #2 submerged aluminum coupon (left); Test #3 submerged aluminum coupon (right).	115
Figure 4-140. Test #4 submerged aluminum coupon (left); Test #5 submerged aluminum coupon (right).	115
Figure 4-141. Test #1 unsubmerged aluminum.	115
Figure 4-142. Test #2 unsubmerged aluminum (left); Test #3 unsubmerged aluminum (right).	116

Figure 4-143. Test #4 unsubmerged aluminum (left); Test #5 unsubmerged aluminum (right). .....	116
Figure 4-144. Unused copper coupon (left); Test #1 submerged copper coupon (right). .....	117
Figure 4-145. Test #2 submerged copper coupon (left); Test #3 submerged copper coupon (right). .....	117
Figure 4-146. Test #4 submerged copper coupon (left); Test #5 submerged copper coupon (right). .....	117
Figure 4-147. Test #1 unsubmerged copper. ....	118
Figure 4-148. Test #2 unsubmerged copper (left); Test #3 unsubmerged copper (right). .....	118
Figure 4-149. Test #4 unsubmerged copper (left); Test #5 unsubmerged copper (right). .....	118
Figure 4-150. Unused galvanized steel coupon (left); Test #1 submerged galvanized steel (right). .....	119
Figure 4-151. Test #2 submerged galvanized steel (left); Test #3 submerged galvanized steel (right). .....	119
Figure 4-152. Test #4 submerged galvanized steel (left); Test #5 submerged galvanized steel (right). .....	119
Figure 4-153. Test #1 unsubmerged galvanized steel. ....	120
Figure 4-154. Test #2 unsubmerged galvanized steel (left); Test #3 unsubmerged galvanized steel (right). .....	120
Figure 4-155. Test #4 unsubmerged galvanized steel (left); Test #5 unsubmerged galvanized steel (right). .....	120
Figure 4-156. Unused carbon steel coupon (left); Test #1 submerged carbon steel (right). .....	121
Figure 4-157. Test #2 submerged carbon steel (left); Test #3 submerged carbon steel (right). .....	121
Figure 4-158. Test #4 submerged carbon steel (left); Test #5 submerged carbon steel (right). .....	122
Figure 4-159. Test #1 unsubmerged carbon steel. ....	122
Figure 4-160. Test #2 unsubmerged carbon steel (left); Test #3 unsubmerged carbon steel (right). .....	122
Figure 4-161. Test #4 unsubmerged carbon steel (left); Test #5 unsubmerged carbon steel (right). .....	123
Figure 4-162. Aluminum concentration in ICET Test #1 and Test #4 daily water samples. ....	124
Figure 4-163. Silica concentration in ICET Test #1 and Test #4 daily water samples. ....	125
Figure 4-164. SEM image, magnified 100 times, of a Test #4, Day 30, submerged aluminum coupon sample. (T4D30AlSubm004.bmp) .....	125
Figure 4-165. Annotated SEM image, magnified 1000 times, of a Test #4, Day 30, submerged aluminum coupon sample. (T4D30AlSubm006.bmp) .....	126
Figure 4-166. EDS counting spectrum for the deposits (EDS3) on the coupon surface shown in Figure 4-165. (T4D30AlSubm03.jpg) .....	126
Figure 4-167. EDS counting spectrum for the flat coupon surface (EDS4), as shown in Figure 4-165. (T4D30AlSubm04.jpg) .....	126

Figure 4-168. SEM image, magnified 300 times, of a Test #1, Day 30, submerged aluminum coupon sample. (Test1submA1015.bmp).....	127
Figure 4-169. SEM image, magnified 1000 times, of a Test #1, Day 30, submerged aluminum coupon sample. (Test1submA1016.bmp).....	128
Figure 4-170. EDS counting spectrum for the light spot (EDS1) on the coupon surface shown in Figure 4-169. (T1AIEDS10.tif).....	128
Figure 4-171. EDS counting spectrum for the grey coupon surface (EDS2) shown in Figure 4-169. (T1AIEDS11.tif).....	128
Figure 4-172. SEM image at 650× magnification of a Test #2, Day 30, sample of fine powder on a vertical piece of the submerged PVC rack. (T2D30_Cor_Prod003_Fine Powder).....	130
Figure 4-173. SEM image at 1000× magnification of a Test #2, Day 30, sample of fine powder on a vertical piece of the submerged PVC rack. (T2D30_Cor_Prod002_Fine Powder).....	130
Figure 4-174. EDS counting spectrum for the entire SEM image shown in Figure 4-173. (T2D30EDS1-Fine Powder) .....	130
Figure 4-175. SEM image (130×) of a Test #2, Day 30, sample of white residue on a horizontal piece of the submerged CPVC rack. (T2D30_Cor_Prod004_White Powder on Rack).....	131
Figure 4-176. EDS counting spectrum for the white residue shown in Figure 4-175. (T2D30EDS2).....	131
Figure 4-177. SEM image, magnified 200 times, of a Test #3, Day 30, powder on the submerged rack. (T3~RackPowder013) .....	132
Figure 4-178. EDS counting spectrum for the powder on the submerged rack shown in Figure 4-177. (T3RackPowder09).....	133
Figure 4-179. SEM image, magnified 1000 times, of a Test #4, Day 30, fine powder on the submerged rack. (T4D30RackPowder030.bmp).....	133
Figure 4-180. EDS counting spectrum for the particles (whole image) shown in Figure 4-179. (T4D30RackPowder18.jpg) .....	134
Figure 4-181. SEM image, magnified 100 times, of the Test #5 Day 30, fine yellow powder on the submerged rack. (T5D30YellowDeposits001.bmp) .....	134
Figure 4-182. Annotated SEM image, magnified 1000 times, for the Test #5, Day 30, fine yellow powder on the submerged rack. (T5D30YellowDeposits003.bmp).....	135
Figure 4-183. EDS counting spectrum for the particulate deposit shown in Figure 4-182. (T5D30yllw~partcl02.jpg) .....	135
Figure 4-184. Stainless steel mesh covered with gel-like material. ....	136
Figure 4-185. Gel-like material recovered from the bottom of the tank. ....	136
Figure 4-186. SEM image of a Test #3, Day 30, white gel-like material from the top of the birdcage, magnified 100 times. (T3D30GelMaterial003, 5/9/05) .....	137
Figure 4-187. SEM image of a Test #3, Day 30, white gel-like material from the top of the birdcage, magnified 1000 times. (T3D30GelMaterial004, 5/9/05) .....	138

Figure 4-188. EDS counting spectrum for the white, gel-like material (whole image) shown in Figure 4-187. (T3D30Gel02, 5/9/05) .....	138
Figure 4-189. ESEM image of a Test #3, Day 30, white gel-like material from the top of the birdcage, magnified 1000 times. (t3Gel08, 5/6/05).....	139
Figure 4-190. EDS counting spectrum for the white, gel-like material shown in Figure 4-189. (t3geled6, 5/6/05) .....	140
Figure 4-191. XRD results for a Test #3, Day 30, white gel-like sample. ....	141

## TABLES

Table 1-1. Test Series Parameters .....	2
Table 2-1. Quantity of Each Coupon Type in Every Test.....	7
Table 2-2. Material Quantity/Sump Water Volume Ratios for the ICET Tests.....	12
Table 2-3. Physical Parameters for the ICET Tests .....	12
Table 2-4. Chemical Parameters for the ICET Tests.....	12
Table 4-1. Test Conditions in the ICET Tests.....	29
Table 4-2. Composition of Precipitates from Test #1 .....	44
Table 4-3. Composition of Precipitates from Test #5 .....	44
Table 4-4. Distribution of Main Elemental Components of Precipitates from Tests #1 and #5 .....	44
Table 4-5. Relative Amounts of Particle Deposits in Fiberglass .....	47
Table 4-6. Dry Mass Composition (%) of Unused Cal-Sil Samples by XRF Analysis .....	74
Table 4-7. Elemental Composition of the Sediment Samples from Different Tests Based on XRF Analysis.....	81
Table 4-8. Elemental Composition of the Fiberglass Samples Based on XRF Analysis.....	82
Table 4-9. Mean Weight Gain/Loss Data for Submerged Coupons (g).....	106
Table 4-10. Mean Gain/Loss Data for Unsubmerged Coupons (g) .....	112
Table 4-11. Standard Redox Potential of the Metals Used in the ICET Tests.....	113
Table 4-12. Elemental Compositions (by Mass %) of the Deposits and the Aluminum Coupon Surface, as Shown in Figure 4-163 .....	127
Table 4-13. Elemental Compositions (by Mass %) of the Light and Grey Coating on the Aluminum Coupon Surface, as Shown in Figure 4-167 .....	129
Table 4-14. Elemental Composition of Deposition Products Collected from Horizontal Surfaces on CPVC Coupon Racks after Tests Were Complete.....	132
Table 4-15. The Chemical Compositions for Figure 4-188 .....	139
Table 4-16. Dry Mass Composition (%) of a Test #3 Day 30, White Gel-Like Sample by XRF Analysis.....	140



# INTEGRATED CHEMICAL EFFECTS TEST PROJECT: CONSOLIDATED DATA REPORT

## EXECUTIVE SUMMARY

The U.S. Nuclear Regulatory Commission (NRC) Office of Nuclear Regulatory Research has developed a comprehensive research program to support resolution of Generic Safety Issue (GSI)-191. GSI-191 addresses the potential for debris accumulation on pressurized-water-reactor (PWR) sump screens and the consequent loss of net-positive-suction-head margin in the emergency-core-cooling-system (ECCS). Among the GSI-191 research program tasks is the experimental investigation of chemical effects that may exacerbate sump-screen clogging.

The Integrated Chemical Effects Test (ICET) project was a joint effort by the U.S. NRC and the nuclear utility industry undertaken through the Memorandum of Understanding on Cooperative Nuclear Safety between the NRC and Electrical Power Research Institute, "Addendum on Integral Chemical Effects Testing for PWR ECCS Recirculation." The ICET tests attempted to simulate the chemical environment present inside a containment water pool after a loss-of-coolant accident (LOCA) and monitored the chemical system for 30 days to identify the presence, composition, and physical characteristics of chemical products that formed during the tests. The ICET test series was conducted by Los Alamos National Laboratory at the University of New Mexico, with the assistance of professors and students in the Departments of Civil and Mechanical Engineering. The primary objectives for the ICET test series were (1) to determine, characterize, and quantify chemical-reaction products that may develop in the containment sump under a representative post-LOCA environment and (2) to identify and quantify any gelatinous material that might be produced during the post-LOCA recirculation phase.

This report volume presents the principal findings of the five tests conducted in the ICET test series. The five individual test data reports are included as additional Volumes 2–6. This volume consolidates observations and findings from the individual data reports and compares trends and key results.

All of the ICET tests were conducted in an environment that attempted to simulate containment pool conditions during recirculation. A Project Test Plan, jointly developed by EPRI and NRC, provides a complete rationale for the ICET test conditions. For Tests #1–#4, the initial chemical environment contained 2800 mg/L of boron, 100 mg/L of hydrochloric acid, and 0.7 mg/L of lithium hydroxide. (For some tests, the hydrochloric acid and a small portion of the boron and/or lithium hydroxide were added during the spray phase.) For Test #5, the initial chemical environment contained 2400 mg/L of boron, 43 mg/L of hydrochloric acid, and 0.3 mg/L of lithium hydroxide. Sodium hydroxide was added in Tests #1 and #4, trisodium phosphate was added in Tests #2 and #3, and sodium tetraborate was added in Test #5. All tests were conducted for 30 days at a constant temperature of 60°C. The materials tested within this environment included representative amounts of submerged and unsubmerged aluminum, copper, concrete, zinc, carbon steel, and insulation samples. Representative amounts of concrete dust and latent debris (dirt) were also added to the test solution. The tests included an initial 4-hour spray phase to simulate containment spray interaction with the unsubmerged samples. Water was circulated

through the bottom portion of the test chamber during the entire test to achieve representative flow rates over the submerged specimens.

Insulation samples consisted of scaled amounts of NUKON™ fiberglass and calcium silicate (cal-sil) material. In Tests #1, #4, and #5, only NUKON™ fiberglass was included. In Tests #2 and #3, the samples were 80% cal-sil and 20% NUKON™ fiberglass by volume. In addition, the tank contained 373 metal coupon samples (40 submerged) and 1 submerged concrete sample. Process control consisted of monitoring online measurements of recirculation flow rate, test solution temperature, and pH. Flow rate and temperature were controlled to maintain the desired values of 25 gpm and 60°C. The value of 25 gpm was chosen to yield fluid velocities over the submerged coupons from 0–3 cm/s. Daily water samples were obtained for measurements of pH, turbidity, total suspended solids, kinematic viscosity, shear-dependent viscosity, and for chemical analyses. In addition, microscopic evaluations were conducted on water-sample filtrates, precipitates, fiberglass, cal-sil, metal coupons, and sediment.

Test preparation included heating a specified volume of water to 65°C, which was 5°C higher than the required test temperature to offset the 5°C heat loss that occurred when the test coupons were added. Upon reaching the desired temperature, test-specific chemicals were dissolved into the heated water. Latent debris, concrete, test coupons, and insulation samples were then placed in the tank. Once the solution temperature reached the required test temperature of 60°C, the test commenced with initiation of the tank sprays. During the 4-hour spray period, additional chemicals were added if required. After the addition of all chemicals, the test volume equaled 250 gal. The tests ran for 30 days, while the conditions were maintained within the accepted flow and temperature ranges, with only short periods of slight deviation. Water samples, insulation samples, and metal coupons were analyzed after the test. Sampling and analyses were conducted in accordance with approved project instructions.

Initial test solution pH was different in each test, and it varied from ~7.3 in Test #2 to ~9.8 in Test #4. The pre-determined amounts of chemicals were added for each test, and no attempt was made to control or alter the resulting pH. Solution samples from Tests #1 and #5 produced precipitates upon cooling to room temperature, whereas samples from Tests #2, #3, and #4 did not. The Test #1 precipitates occurred much more quickly and were present in greater quantities than the Test #5 precipitates. Except for precipitates seen on the first day of Test #3, no precipitates were visible in the test solution at the test temperature. Turbidity measurements were taken at 60°C and 23°C. In Tests #2, #3, and #4, measurements at both temperatures produced similar results. During the first 4 hours of Test #3, a large increase in turbidity was seen, which corresponded to the visible precipitates. In Tests #1 and #5, the turbidity at 23°C rose higher than the 60°C values. Total suspended solids (TSS) were also measured in each test. With the exception of Test #5, all tests reached a maximum TSS value by the first day and decreased to a value relatively close to the base-line measurement for the duration of the test. Test #5 TSS measurements varied between the baseline and the maximum value throughout the test. Measurements were made of suspended particles in the test solution. The particle size distribution in the Test #1 test solution indicated diameters <1 µm. For Tests #2–#5, the particle size ranged from 1 to 100 µm, and the size distributions within that range differed from test to test.

In all tests, daily measurements of the constant-shear kinematic viscosity revealed an approximately constant value at both the test and room temperatures. This was true for both filtered and unfiltered samples. Shear-dependent viscosity measurements indicated that the Tests #2, #3, and #4 solutions were representative of a Newtonian fluid. However, in Tests #1 and #5, shear thinning was observed when the solutions were cooled to room temperature.

Throughout the ICET test series, daily water samples were taken for inductively coupled plasma (ICP) analysis of a standard list of elements (plus silica) to determine the composition of the solution. As expected, boron was present in high concentrations in all tests. In Test #1, aluminum and sodium were present in greater concentrations than were all other tested elements. In Test #2, silica and sodium were the dominant elements in solution. Silica, sodium, and calcium were present in the greatest concentrations with the Test #3 solution. In Test #4, silica, sodium, calcium, and potassium were present in solution in the greatest concentrations. Sodium, aluminum, calcium, and silica were the elements of highest concentration in the Test #5 solution.

Insulation debris, which was composed of fiberglass or a mixture of fiberglass and cal-sil, was analyzed after completion of each test. Fiberglass samples were present in all tests. Cal-sil samples were present in only Tests #3 and #4. Three types of deposits were found on the fiberglass samples by electron microscopy: (1) particulates deposited on the exterior of the insulation; (2) flocculence, which was more prevalent on the interior of the insulation (flocculence may have been formed by the chemical byproducts existing in the test or may have been caused by precipitation during the drying process, which was required for most analyses); and (3) film or webbing, which resulted from precipitation of soluble species from Tests #1 and #4 during the drying process. The amount of deposits seen on the fiberglass insulation varied from test to test because of differing solution chemistry. Comparisons revealed that the greatest degree of deposition occurred in Test #3, followed in order by Tests #1, #4, and #2. Test #5 samples had the fewest deposits. Analysis of the cal-sil samples showed large amounts of phosphorous on the exterior of samples obtained from Test #3, but the phosphorus did not penetrate to the interior of the samples.

The system effect on the metal coupons was different for each test. Test #1 experienced the largest amount of corrosion on the submerged coupons. Tests #2–#5 conditions did not cause significant submerged coupon corrosion. None of the tests showed significant corrosion on the unsubmerged coupons. The sediment on the tank bottom at the end of the tests also varied. Tests #3 and #4 had the most sediment, which consisted of chemical precipitate, as well as sediment attributable to the large amount of crushed cal-sil added to the tank. Tests #1, #2, and #5 produced the smallest amount of sediment, which was composed largely of materials from the insulation used (fiberglass) and debris added to the tank.



## ACKNOWLEDGMENTS

The principal authors of this report gratefully acknowledge the assistance of the following persons, without whom successful completion of the Integrated Chemical Effects Test series could not have been accomplished. John Gisclon, representing the Electric Power Research Institute (EPRI), contributed much practical, timely advice on preparation of the quality assurance (QA) procedures, experimental project instructions, and chemical additions. He also provided the insulation and metallic coupons, as well as some of the test chemicals, and Appendix B of this NUREG/CR volume. Tim Andreychek, from Westinghouse, coordinated development of the test plan for the project, that is included as Appendix C of this NUREG/CR volume. Michael Niehaus, from Sandia National Laboratories (SNL), conducted a characterization of time-dependent strain-rate viscosity for the circulating solution. Jim Young, of LANL's Institutional Quality program (QA-IQ), provided valuable reviews and inputs to QA documentation and practices. The authors also express their gratitude for the contributions and participation of numerous Nuclear Regulatory Commission staff members who reviewed the project test plan, project instructions, preliminary data, and test data reports to ensure relevance to plant safety, high-quality defensible results, and timely execution of these tests. Alicia Aragon of SNL provided reviews of the last three test data reports and this NUREG/CR volume.

The authors acknowledge Lisa Rothrock, Eileen Patterson, and Jeanne Bowles of IRM-CAS, LANL, for their editing and composition support. Finally, sincere appreciation is given to Nancy Butner of LANL Group D-5 for her invaluable support with project management, planning, budget analysis, contract administration, administrative reporting, and overall coordination throughout the entire ICET project.



## ACRONYMS AND ABBREVIATIONS

ACRS	Advisory Committee on Reactor Safeguards (NRC)
BSE	Back Scattered Electrons
cal-sil	Calcium Silicate
CPVC	Chlorinated Polyvinyl Chloride
CS	Coated Steel
DAS	Data Acquisition System
DHR	Decay Heat Removal
ECCS	Emergency Core-Cooling System
EDS	Energy-Dispersive Spectroscopy
EPA	Environmental Protection Agency
EPRI	Electric Power Research Institute
ESEM	Environmental Scanning Electron Microscopy
gpm	Gallons per Minute
GS	Galvanized Steel
GSI	Generic Safety Issue
HCl	Hydrochloric Acid
ICET	Integrated Chemical Effects Tests
ICP	Inductively Coupled Plasma
ICP-AES	Inductively Coupled Plasma—Atomic Emission Spectroscopy
IOZ	Inorganic Zinc
LANL	Los Alamos National Laboratory
LiOH	Lithium Hydroxide
LOCA	Loss-of-Coolant Accident
NIST	National Institute of Standards and Technology
NRC	Nuclear Regulatory Commission
NTU	Nephelometric Turbidity Unit
PI	Project Instruction
PVC	Polyvinyl Chloride
PWR	Pressurized Water Reactor
QA	Quality Assurance
QC	Quality Control
RES	Office of Nuclear Regulatory Research (NRC)
RO	Reverse Osmosis
SEM	Scanning Electron Microscopy

SNL	Sandia National Laboratories
SS	Stainless Steel
TEM	Transmission Electron Microscopy
TOC	Total Organic Carbon
TSP	Trisodium Phosphate
TSS	Total Suspended Solids
UNM	University of New Mexico
US	Uncoated Steel
XRD	X-Ray Diffraction
XRF	X-Ray Fluorescence

# 1. INTRODUCTION

The Integrated Chemical Effects Test (ICET) project was a joint effort by the United States Nuclear Regulatory Commission (NRC) and the Electric Power Research Institute (EPRI) to simulate the chemical environment present inside a containment water pool after a loss-of-coolant accident (LOCA) and to monitor the chemical system for an extended time to identify the presence, composition, and physical characteristics of chemical products that may form. The ICET series was conducted by Los Alamos National Laboratory (LANL) at the University of New Mexico (UNM), with the assistance of professors and students in the Departments of Civil and Mechanical Engineering.

## 1.1. Objectives and Test Conditions

Containment buildings of pressurized water reactors (PWRs) are designed to accommodate the energy release following a postulated accident. They also permit recirculation of reactor coolant and emergency-core-cooling-system (ECCS) water to the decay heat removal (DHR) heat exchangers. Water collected in the sump from the reactor coolant system, the safety injection system, and the containment spray system is recirculated through the reactor core to remove residual heat. The recirculation sump contains a screen to protect components that are in the reactor coolant, containment spray, and ECCS flow paths from the effects of debris that could be transported to the sump. Concerns have been raised that fibrous material could form a mat on the screen, obstructing flow, and that chemical reaction products such as gelatinous or crystalline precipitates could migrate to the screen, causing further blockage and increased head losses across the debris bed. Another potential adverse chemical effect is increased bulk fluid viscosity that could also increase head losses through a debris bed.

The primary objectives for the ICET test series were (1) to determine compositions, characterize properties, and quantify masses of chemical reaction products that may develop in the containment sump under a representative post-LOCA environment and (2) to identify and quantify any gelatinous material that might be produced during the post-LOCA recirculation phase.

The ICET test series was conceived as a limited-scope suite of five different 30-day tests with different constituents. The conditions selected for each test are shown in Table 1-1. It should be noted that the Test #5 initial boron concentration and buffering agent were different from the other four tests.\* All tests in the series included metal coupons with surface areas scaled to those in representative PWR containment and sump systems.

The ICET project was a joint effort by the U.S. NRC and the nuclear utility industry, undertaken through the Memorandum of Understanding on Cooperative Nuclear Safety between the NRC and EPRI, "Addendum on Integral Chemical Effects Testing for PWR ECCS Recirculation." EPRI supplied many of the materials used in the ICET tests, and Appendix B provides

---

\*An important distinction exists between the chemical reagents used to achieve bulk solution pH and those used to stabilize or "buffer" the pH within a desired range. However, there was no intent to control pH during the course of the tests. In this report series, discussions of additives that influenced pH refer exclusively to the sodium hydroxide, trisodium phosphate, and sodium tetraborate that, in addition to boric acid, were used to initiate the test conditions. The term "buffer" or "buffering agent" is sometimes used informally to refer to these chemicals.

descriptions of the materials used in the testing. EPRI and NRC also wrote a Project Test Plan (Appendix C, Ref. 1) that provides a complete rationale for the selection of the ICET test conditions.

**Table 1-1. Test Series Parameters**

Run	Temp (°C)	TSP <sup>a</sup>	NaOH	Sodium Tetraborate	pH <sup>b</sup>	Boron (mg/L)	Notes
1	60	N/A	Yes	N/A	10	2800	100% fiberglass insulation test. High pH, NaOH concentration as required by pH.
2	60	Yes	N/A	N/A	7	2800	100% fiberglass insulation test. Low pH, trisodium phosphate (TSP) concentration as required by pH.
3	60	Yes	N/A	N/A	7	2800	80% calcium silicate/20% fiberglass insulation test. Low pH, TSP concentration as required by pH.
4	60	N/A	Yes	N/A	10	2800	80% calcium silicate/20% fiberglass insulation test. High pH, NaOH concentration as required by pH.
5	60	N/A	N/A	Yes	8 to 8.5	2400	100% fiberglass insulation test. Intermediate pH, sodium tetraborate (Borax) buffer.

<sup>a</sup>TSP was added in hydrate form, i.e., Na<sub>3</sub>PO<sub>4</sub>·12H<sub>2</sub>O.

<sup>b</sup>Values shown were the target pH for Tests #1–#4. The value for Test #5 is the expected range.

The ICET test apparatus consisted of a large stainless steel (SS) tank with heating elements, spray nozzles, and associated recirculation pump and piping to simulate the post-LOCA chemical environment. Samples of structural metals, concrete, and insulation debris are scaled in proportion to the relative surface areas found in containment and in proportion to a maximum test dilution volume of 250 gal. of circulating fluid. Representative chemical additives, temperature, flow rates, and material combinations were established in each test, and the system was then monitored while corrosion and fluid circulation occurred for a time comparable to the ECCS recirculation mission time.

## 1.2. Information Presented in This Report

Information on the ICET project is presented in six volumes. Volume 1 (this report) provides a compilation and comparison of key results from ICET Tests #1–#5. Volumes 2–6 (Refs. 2–6) are the test data reports for Tests #1–#5. The test data reports included detailed test information, and highlights from those data reports were assembled here to illustrate similarities and differences between the tests. Section 2 of this volume contains a brief description of the test apparatus and samples used in the tests. Test procedures, quality assurance, and test parameters are also presented. Section 3 summarizes for each individual test the results for daily water samples, insulation, sediment, and coupons. Section 4 contains comparisons of the test results for water samples, insulation, sediment, metal coupons, aluminum coupon passivation, and deposition products. Section 5 discusses conclusions, and Section 6 itemizes references. Appendix A

contains detailed background information on the test apparatus, test samples, analytical methods and measurements, and quality assurance (QA) program. Appendix B describes materials used in the ICET testing, and Appendix C is the Project Test Plan.



## 2. TEST PROCEDURES

The functional description and physical attributes of the ICET apparatus are presented in detail in Appendix A. That appendix includes the Project Test Plan requirements, the test apparatus design, analytical methods and measurements, and the project QA program. The experimental apparatus is briefly described here, followed by a summary of the QA program, test parameters, and test operation.

### 2.1. Chemical Test Apparatus Functional Description

The test apparatus was designed to meet the functional requirements of the Project Test Plan (Appendix C). Functional aspects of the test apparatus are as follows:

1. The central component of the system was a test tank. The test apparatus was designed to prevent solids from settling in the test piping.
2. The test tank maintained both a liquid and vapor environment, as would be expected in a post-LOCA containment building.
3. The test loop controlled the liquid temperature at 60°C ( $\pm 3^\circ\text{C}$ ).
4. The system circulated water for spray that simulated volumetric containment spray rates per unit area of containment cross section.
5. The test tank contained submerged test coupons and provided a water flow that was representative of the containment pool fluid velocities expected at plants.
6. Piping and related isolation valves were provided such that a section of piping could be isolated without interrupting a test.
7. The pump discharge line was split along two branches, one branch directing flow to the spray header in the tank vapor space and the other branch returning flow to the liquid pool. Each branch was provided with an isolation valve and a flow meter.
8. The pump circulation flow rate was controlled at the pump discharge to be within  $\pm 5\%$  of the flow required to establish target fluid velocities in the tank. Flow was controlled manually by setting a throttle valve, but it was monitored automatically in a continuous data record.
9. The tank accommodated a rack of immersed sample coupons that included the potential reaction constituents identified in the test plan.
10. The tank also accommodated six racks of sample coupons that were exposed to a spray of liquid that simulated the chemistry of a containment spray system. Provisions were made for these racks to be visually inspected through polycarbonate windows.

11. The chlorinated polyvinyl chloride (CPVC) coupon racks provided sufficient space between the test coupons to minimize electrochemical interactions between the coupons. The different metallic test coupons were also electrically isolated from each other and from the test stand to prevent galvanic effects resulting from metal-to-metal contact either between specimens or between the test tank and the specimens.
12. The fluid dilution volumes and the sample corrosion surface areas were selected based on scaling considerations that relate the test conditions to representative plant conditions.
13. All components of the test loop were made of corrosion-resistant material (for example, SS for metallic components and CPVC for spray injection lines).

The as-built test loop consisted of a test tank, a recirculation pump, 2 flow meters, 10 isolation valves, and pipes that connect the major components, as shown schematically in Figure 2-1. The labels P, T, and pH represent pressure, temperature, and pH probes, respectively. Valves are numbered V-1 through V-10.

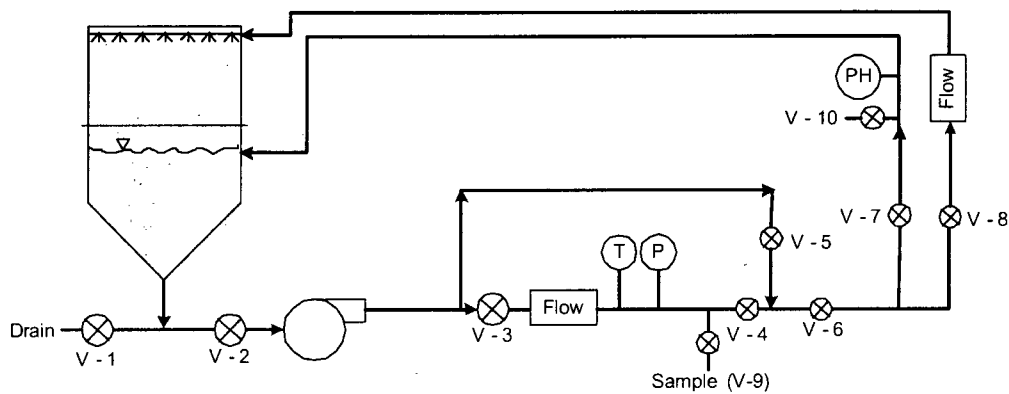


Figure 2-1. Test loop process flow diagram.

## 2.2. Pre-Test Preparation

### 2.2.1. Test Loop Cleaning

Before each test, the experimental loop was thoroughly cleaned to remove all deposits and residues remaining from the previous test. In addition to visual inspections, the apparatus was flushed and cleaned per written directions given in the pre-test operations project instruction (PI). The system was repeatedly flushed with dilute concentrations of ammonium hydroxide, followed by ethanol, then by nitric acid, and finally by reverse osmosis (RO) water, until the effluent water turbidity was less than 0.3 NTU and its conductivity was  $<50 \mu\text{S/cm}$ .

## 2.2.2. Test Coupons and Samples

Each ICET experiment exposed an identical set of metallic and concrete coupons to simulated post-LOCA environments. Each coupon was ~12 in. square. The metallic coupons were ~1/16 in. thick, except for the inorganic zinc-coated steel coupons, which were ~3/32 in. thick. The concrete coupons (one per test) were ~1-1/2 in. thick. Insulation materials were also exposed. NUKON™ fiberglass insulation (hereafter referred to as fiberglass) samples were included in each test. Also, calcium silicate insulation (hereafter referred to as cal-sil) samples were included in Tests #3 and #4. Each test subjected seven racks of coupons to the specified environment, with one being submerged in the lower tank and the remaining six being suspended in the tank vapor space. The number of coupons of each type that were used in every test are listed in Table 2-1.

**Table 2-1. Quantity of Each Coupon Type in Every Test**

<b>Material</b>	<b>No. of Coupons</b>
IOZ coated steel	77
Aluminum (Al)	59
Galvanized steel (GS)	134
Copper (Cu)	100
Uncoated steel (US)	3
Concrete	1

Note: IOZ refers to an inorganic zinc primer coating. IOZ and CS or coated steel (used elsewhere) refer to the same coupon type.

The arrangement of coupon racks in the test tank is schematically illustrated in Figure 2-2. The figure shows a side view of the ICET tank, with the ends of the seven CPVC racks labeled. The normal water level is indicated by the blue line in the figure. Rack 1 was the only submerged rack, and it sat on angle iron supports. It was centered in the tank so that flow from two opposing distribution headers reached it equally. Racks 2–4 were positioned above the water line, supported by angle iron brackets on the side of the tank. Racks 5–7 were positioned at a higher level and were also supported by angle iron brackets. Racks 2–7 were exposed to spray. In Figure 2-2, north is to the right and south is to the left. Compass directions were used subsequently to identify rack locations and sediment sample locations. Appendix A contains more details on the tank internals.

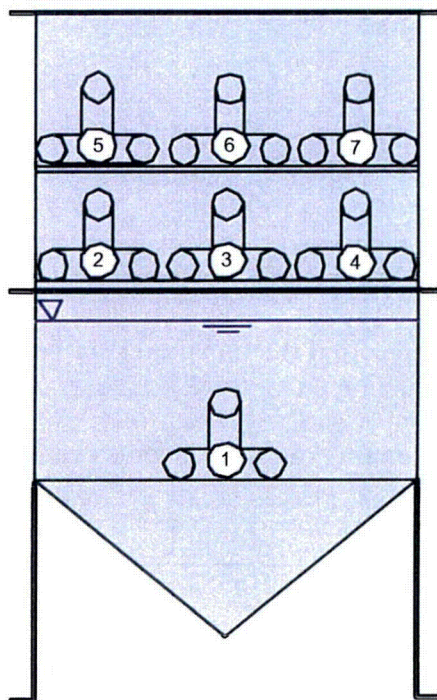


**Figure 2-2. Coupon rack configuration in the ICET tank. The blue line represents the surface of the test solution.**

Figure 2-3 shows the configuration of a typical unsubmerged coupon rack loaded with metal coupons in the ICET tank. The loading pattern of all suspended racks was nearly identical, varying by only one or two coupons. Shown in the figure from left to right, the coupons are arranged as follows: four Cu, four Al, four coated with inorganic zinc (IOZ), seven GS, four Cu, three Al, four IOZ, and seven GS.

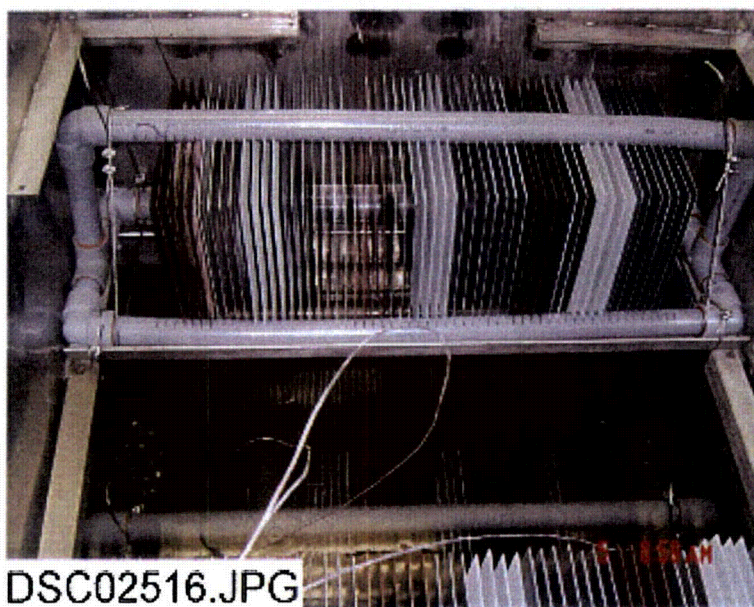


**Figure 2-3. A typical loaded coupon rack in the ICET tank.**

The submerged rack had a slightly different configuration because of the ratios of submerged versus unsubmerged metals. The sole concrete coupon was also placed in the submerged rack. The Rack 1 coupon configuration was originally eight Cu, one Al, one IOZ, two GS, eight Cu, one Al, one IOZ, two GS, one US, nine Cu, one Al, one IOZ, three GS, eight empty slots, concrete, and then eight empty slots. Some copper deposition on the aluminum coupons was observed following Test #2. Subsequently, two of the three Al coupons were moved to empty slots on either side of the concrete coupon in Tests #3–#5.

Several fiberglass samples were placed in the ICET tank. These samples were either submerged or suspended above the water level. The unsubmerged fiberglass samples were positioned so that they would be exposed to sprays. All fiberglass samples were contained in SS wire mesh bags or “pouches” that allowed water flow while confining the fiberglass material. Both loosely packed and more tightly packed samples were used. In addition, some submerged fiberglass samples were located where they would be exposed to relatively high-flow conditions, and others were located in quiescent regions of the tank. Figure 2-4 shows the so-called “sacrificial” fiberglass samples in wire mesh pouches attached to the submerged coupon rack (Rack 1 in Figure 2-2). Each pouch contained ~5 g of fiberglass. Sacrificial samples were attached with SS wire; removed from the tank on Days 4, 15, and 30; and examined for possible time-dependent changes. As shown in the figure, bigger insulation bags were wrapped around the sacrificial specimens during the test. In addition, small sacrificial samples called fiber pucks were added to the solution beginning with Test #3. Fiber puck fabrication and post-test analyses are described in Ref. 5. Appendix A contains more detailed descriptions of the standard fiberglass samples. Appendix B contains additional details on the fiberglass insulation, including heat treating.



Figure 2-4. Fiberglass samples attached to a coupon rack.

Several cal-sil samples were also placed in the ICET tank for Tests #3 and #4. Samples were either submerged or suspended above the water level. The unsubmerged cal-sil samples were positioned so they would be exposed to sprays. In addition to solid cal-sil pieces (Figure 2-5), 43.5 lb of cal-sil dust (Figure 2-6) were added to the tank solution before the test began. As with the fiberglass samples, all of the cal-sil samples (except for the dust) were contained in SS wire mesh that allowed water flow while confining the cal-sil material. Appendix B contains additional details on the cal-sil insulation, including heat treating.



T3D30NRC008.jpg

**Figure 2-5. Solid pieces of cal-sil samples in SS mesh.**



T3D30NRC002.jpg

**Figure 2-6. Pulverized cal-sil insulation before addition to the ICET tank.**

### **2.2.3. Quality Assurance (QA) Program**

A project QA manual was developed to satisfy the contractual requirements that applied to the ICET project. Specifically, those requirements were to provide credible results by ensuring that the QA effort was consistent with the intent of the appropriate sections of 10CFR50, Appendix B, in the areas of test loop design, sampling, chemicals, operation, and analysis.

The 18 criteria of 10CFR50, Appendix B, were addressed separately in a Project QA Manual, and the extents to which they applied to the ICET project were delineated. A resultant set of QA procedures was developed. In addition, project-specific instructions (PIs) were written to address specific operational topics that required detailed, step-by-step guidance. PIs generally applicable to all tests were written for the following topics and were followed for all tests:

- Data Acquisition System (DAS)
- Coupon Receipt, Preparation, Inspection, and Storage
- DAS Alarm Response
- Chemical Sampling and Analysis
- Transmission Electron Microscopy (TEM) Examination of Test Samples
- Scanning Electron Microscopy (SEM) Characterization of Test Samples
- Viscosity Measurements

Project instructions specific to each test were written for the following:

- Pre-Test Operations
- Test Operations
- Post-Test Operations

### **2.2.4. Test Parameters**

ICET test parameters were selected based on literature surveys and on the results of surveys of U.S. nuclear power plants. Quantities of test materials were selected to preserve the scaling of representative ratios between material surface areas and total cooling-water volumes. Chemical additives to the ICET tank simulated the post-LOCA sump environment. The Project Test Plan (Appendix C) is the basis for the following information in this section.

The materials included in the tests were zinc, aluminum, copper, carbon steel, concrete, and fiberglass and cal-sil insulation. The amounts of each material are given in Table 2-2 in the form of material surface area to water volume ratios, with three exceptions: concrete dust, which is presented as a ratio of mass to water volume, and fiberglass and cal-sil insulation, which are presented as a ratio of insulation volume to water volume. Also shown in the table are the percentages of material that were submerged and unsubmerged in the test chamber.

**Table 2-2. Material Quantity/Sump Water Volume Ratios for the ICET Tests**

Material	Ratio Value (ratio units)	Percentage of Submerged Material (%)	Percentage of Unsubmerged Material (%)
Zinc in galvanized steel	8.0 (ft <sup>2</sup> /ft <sup>3</sup> )	5	95
Inorganic zinc primer coating (non-top coated)	4.6 (ft <sup>2</sup> /ft <sup>3</sup> )	4	96
Inorganic zinc primer coating (top coated)	0.0 (ft <sup>2</sup> /ft <sup>3</sup> )	–	–
Aluminum	3.5 (ft <sup>2</sup> /ft <sup>3</sup> )	5	95
Copper (including Cu-Ni alloys)	6.0 (ft <sup>2</sup> /ft <sup>3</sup> )	25	75
Carbon steel	0.15 (ft <sup>2</sup> /ft <sup>3</sup> )	34	66
Concrete (surface)	0.045 (ft <sup>2</sup> /ft <sup>3</sup> )	34	66
Concrete (particulate)	0.0014 (lbm/ft <sup>3</sup> )	100	0
Insulation material (fiberglass or calcium silicate)	0.137 (ft <sup>3</sup> /ft <sup>3</sup> )	75	25

The physical and chemical parameters that were critical for defining the tank environment and that had a significant effect on sump-flow blockage potential and gel formation are summarized in Tables 2-3 and 2-4, respectively. Note that of the chemical parameters listed, only boric acid, lithium hydroxide, and hydrochloric acid were present in all five tests.

**Table 2-3. Physical Parameters for the ICET Tests**

Physical Parameter	Test Value	
Tank water volume	949 L	250 gal.
Circulation flow	100 L/min	25 gpm
Spray flow	15 L/min	3.5 gpm
Sump temperature	60°C	140°F

**Table 2-4. Chemical Parameters for the ICET Tests**

Chemical	Concentration
H <sub>3</sub> BO <sub>3</sub> concentration	2800 mg/L as boron <sup>a</sup>
Na <sub>3</sub> PO <sub>4</sub> ·12H <sub>2</sub> O concentration	As required to reach pH 7 in the simulated sump fluid
NaOH concentration	As required to reach pH 10 in the simulated sump fluid
Sodium tetraborate (Borax)	As required to reach boron concentration of 2400 mg/L in Test #5
HCl concentration	100 mg/L*
LiOH concentration	0.7 mg/L*

<sup>a</sup>Concentrations applicable to Tests #1–#4. Concentrations for Test #5 were 2400 mg/L boron, 43 mg/L HCl, and 0.3 mg/L LiOH.

### 2.3. Test Operation

All of the ICET tests were conducted in environments that attempted to simulate expected containment pool conditions during recirculation. The tests were conducted for 30 days at a constant temperature of 60°C. The materials tested within each environment included representative amounts of submerged and unsubmerged aluminum, copper, concrete, zinc, carbon steel, and insulation samples. Representative amounts of concrete dust (21.2 g) and latent debris (63.7 g) were also added to the test solution. Each test also had representative amounts of insulation debris present, either as fiberglass or a mixture of fiberglass and cal-sil.

Preparation of the tests began with the heating of approximately 250 gal. of RO water to 65°C, which was 5°C above test temperature. This initial temperature was used to offset the 5°C reduction in water temperature caused by the addition of the metal coupons and insulation samples. The required chemicals for each test, pre-measured latent debris, and concrete dust were added to the heated RO water with the recirculation pump operating to ensure complete dissolution. Then the pump was stopped, and the metal coupons and fiberglass samples were put into the tank. Inserting the coupon racks and insulation samples required approximately 2 hours.

After all required items were added to the tank, base-line grab samples and measurements of the test solution were taken. Time zero of the test started with initiation of the tank sprays, which lasted for 4 hours. During the spray phase, additional chemicals were injected directly into the nozzle spray lines or into the recirculation line. The nozzle spray flow was set at 3.5 gpm. The recirculation flow was set at 25 gpm.

The initial 4-hour spray phase simulated containment spray interaction with the unsubmerged samples. The spray pH was controlled to be <12 for all tests. Water was circulated through the bottom portion of the test chamber during the entire test to achieve representative flow rates over the submerged specimens. Any water loss because of water sample removal and evaporation during the tests was replaced with RO water.

Test solution samples were taken during the first 24 hours of the test and daily thereafter. Water chemistry measurements included pH, turbidity, total suspended solids (TSS), kinematic viscosity, and strain-rate viscosity. Additionally, daily measurements of selected elemental concentrations (plus silica) with inductively coupled plasma-atomic emission spectroscopy (ICP-AES) were performed. Weekly size distributions of suspended particles were also determined. Sampling and analyses were conducted in accordance with approved project instructions.

Samples of fiberglass were taken from the tank at several day intervals for SEM/energy-dispersive spectroscopy (EDS) investigations. At test termination, water, insulation, metallic coupon, and sediment samples were obtained and various parameters investigated.



### 3. SUMMARY OF TEST RESULTS

This section summarizes the key results obtained from each ICET test. These test summaries are organized for each test, with brief test descriptions that are supplemental to Section 2.3 and four results sections: (1) water samples, (2) insulation (fiberglass and cal-sil), (3) sediment, and (4) metal coupons.

Elemental chemical analyses with ICP-AES were performed similarly for each test. Daily samples were analyzed for aluminum, calcium, copper, iron, magnesium, nickel, silica, sodium, and zinc. Boron, lithium, potassium, lead, and chloride (analyzed using ion chromatography) were evaluated at the beginning of the tests, at the midpoint, and at the end of the tests. In the test summaries that follow, only those elements that were prevalent in solution (except for boron, which had a high concentration in all tests) are discussed. The water samples were totally digested before the ICP-AES measurements and represented the solution plus any precipitate present. Samples were kept at 4°C between the time they were extracted and when they were digested.

The measurements were within the accepted uncertainties of the laboratory quality control (QC) program (see Appendix A, Section A.4), or the analyses were rerun. Each batch of samples had its own specific uncertainty, depending on the results of the laboratory's QC checks. A typical set of measurement uncertainties are for aluminum,  $\pm 20\%$ ; calcium,  $-14\%$  and  $+19\%$ ; sodium,  $\pm 20\%$ ; magnesium,  $-13\%$  and  $+20\%$ ; and silica,  $-9\%$  and  $+12\%$ .

Deposits on the fiberglass samples were of three types: particulates, flocculence, and film or webbing. Particulate deposits were confined to the exteriors of the samples and were physically attached or retained. Flocculent deposits were found throughout the samples and were more prevalent on the fiberglass interior. It is likely that film or webbing deposits that were observed in Tests #1 and #4 were caused by chemical precipitation during the drying process.

#### 3.1. Test #1

ICET Test #1 was conducted using sodium hydroxide to obtain the target pH of 10. Fiberglass was the only type of insulation used in the test. Boric acid, lithium hydroxide, and hydrochloric acid were also added to the test solution.

Preparation of ICET Test #1 (Run 1 in Table 1-1) began with the heating of 200 gal. of RO water to 60°C. Boric acid, sodium hydroxide, lithium hydroxide, and hydrochloric acid were added to the heated RO water, with the recirculation pump operating to ensure complete dissolution. After the chemicals were observed to be well mixed, an additional 50 gal. of RO water were added to reach the required test volume. The solution again was brought to the desired test temperature. During the first 30 minutes of the spray period, additional sodium hydroxide was injected directly into the nozzle spray lines.

The fiberglass and metal coupons were added on the evening of November 20, 2004. Because of the quantity of the metal mass added to the tank, the solution temperature dropped below the desired test range. The test apparatus was held in recirculation mode for ~12 hours, until the next morning, when the temperature had again reached the desired value. Some settling of the added

particulates was observed overnight, with the turbidity decreasing from 12 to 8 NTU over that time.

The experiment commenced at 10:00 a.m. on Sunday, November 21, 2004, and it ended on Tuesday, December 21, 2004, at 10:00 a.m. Details of ICET Test #1 are reported in Ref. 2.

### **3.1.1. Water Samples**

Test #1 had a target pH of 10. The actual test solution pH at the end of the sodium hydroxide injection during the spray phase was 9.5. The pH decreased slightly during the test, and it was ~9.4 at the end of the test.

No chemical byproducts were visible at the test temperature of 60°C. However, microscopic evaluation revealed the presence of small amorphous particulates, which existed in the test solution before cooling. After the first 8 hours of testing, when the test solution was cooled to room temperature, precipitates became visible. The amount of visible room temperature precipitation increased, and the precipitates formed more quickly during cooling as the test progressed. Reheating of precipitated solution samples led to only partial dissolution of the solid back into solution. Additionally, analysis of the precipitates indicated that they were principally amorphous, and the fundamental particle size was ~10 nm. Much larger agglomerations of these basic particles were also visible.

Turbidity was measured at two temperatures: 60°C and 23°C. At 60°C, the turbidity remained relatively constant at around 1 NTU after 3 days of testing. At 23°C, the turbidity began rising at Day 3 to ~135 NTU at the end of the test.

The TSS increased from the base-line measurement of 27 mg/L to a peak concentration of 43 mg/L after the 30-minute injection of the additional sodium hydroxide. The baseline TSS sample was taken after the addition of the debris to the tank solution. By the end of the first day, the TSS measurement had declined to a value similar to that of the base-line measurement. For the first 13 days of testing, the TSS measurement oscillated within the range of 13–24 mg/L. On the 14th day, the TSS measurement increased notably above the previous range to a value of 29 mg/L. From that point, the TSS measurement fluctuated within the range of 20–29 mg/L.

The test solution was filtered through a 0.7- $\mu$ m filter, and the particle size distribution was determined. After Day 1, the particulates remained <1  $\mu$ m for the duration of the test.

Bulk kinematic viscosity values at 60°C remained steady throughout the test. However, at 23°C the kinematic viscosity began to increase after 5 days of testing and leveled out after ~20 days of testing. Strain-rate viscosity testing clearly demonstrated thinning or reduced viscosity with increasing strain rate for the 25°C samples (strain-rate viscosity was measured at 60°C and 25°C) after Day 23, which is indicative of non-Newtonian behavior. No strain-rate dependency was observed for the 60°C solution.

Results from ICP-AES analyses indicated that aluminum and sodium were present in the test solution in the greatest concentrations. The sodium concentration was ~2000 mg/L at the start of the test and rose to ~4500 mg/L after 3 days of testing. It stayed at that level for the duration of

the test. The aluminum concentration was near zero at the start of the test. It rose to 350 mg/L after ~20 days of testing and then evened out until the end of the test, similar to the behavior of the kinematic viscosity. The aluminum concentration in solution corresponds well with the mass lost from the submerged aluminum coupons.

### **3.1.2. Insulation**

Fiberglass insulation samples were removed from the test tank on Day 15 and Day 30 of the test and examined. The Day-15 samples exhibited evidence of particulate deposits on individual fibers and a web-like material spanning multiple fibers. The Day-30 samples exhibited similar substances that were more prevalent, and contiguous webbing appeared to span multiple fibers. The particulate deposits were observed on only the exterior surfaces of the insulation. The penetration depth spanned a few fiber diameters below the surface. Insulation within the remaining portion of the insulation holder bags was not subject to these deposits, and these fibers appeared relatively pristine after the test.

### **3.1.3. Sediment**

A total of 292 g (wet) of sediment were recovered from the tank bottom after the tank was drained. Photographs and SEM images showed that a large portion of the sediment was composed of fiberglass debris. Elemental composition analysis of the sediment indicated that silicon was the dominant element (27% by mass). This information is consistent with the fact that fiberglass was the only insulation material used in the test. Sodium was the next most prominent element (9% by mass). It should be noted that these compositions are somewhat qualitative because of the difficulty in obtaining an accurate spatial average using a 25- $\mu$ m beam spot.

The latent debris and concrete dust quantities added just before the onset of testing amounted to ~85 g. The additional amount of sediment appeared to be made up of fugitive insulation material that escaped from the insulation sample bags during testing. Generally, the sediment was found to contain no visible chemical byproducts that were similar to the web-like material present in the fibrous insulation. Although the sediment settled to the bottom of the tank during the test, subsequent settling tests revealed that the sediment was easily re-suspended and required a substantial amount of time (hours to days) before completely settling in a quiescent container.

### **3.1.4. Coupons**

The coupons were weighed after drying, and no cleaning was performed before weighing. Therefore, post-test weights included any corrosion products or surface deposits that were present on the test coupons. Weight loss/gain measurements indicated that only the aluminum specimens experienced a significant weight change. The aluminum specimens lost ~25% of their pre-test mass. The carbon steel sample lost ~2% of its pre-test mass, whereas the concrete sample gained ~3% more mass. The concrete weight gain may have resulted from retained water, since the weight measurement was performed after several days of air drying. Other samples either gained or lost much less than 1% of their pre-test mass.

## 3.2. Test #2

ICET Test #2 was conducted using TSP as the buffering agent, with a target pH of 7. Fiberglass was the only type of insulation used in the test. Boric acid, lithium hydroxide, and hydrochloric acid were also added to the test solution.

The test began with 240 gal. of RO water and chemicals in the system. Beginning at 30 minutes into the spray phase, two batches of the TSP solution were metered into the recirculation line. Each batch consisted of boric acid and TSP in 5 gal. of RO water.

The experiment commenced at 9:45 a.m. on Saturday, February 5, 2005, and it ended on Monday, March 7, 2005. Details of ICET Test #2 are reported in Ref. 3.

### 3.2.1. Water Samples

Test #2 had a target pH of 7. After the spray phase and during the first week of testing, the test solution pH averaged 7.2. There was a slight increase in the average pH to a value of 7.3 during the second week. The pH remained constant over the final 2 weeks of the test.

No chemical byproducts were visible in the daily water samples at the test temperature of 60°C or upon cooling to 23°C. Additionally, no precipitates or byproducts became visible as the samples were stored at room temperature after the end of the test.

Turbidity values at both test and room temperatures were very similar; thus, only the 60°C value is explained further. A sharp rise in water sample turbidity occurred after 4 hours, which coincided with the completed introduction of TSP. The maximum turbidity value at both test and room temperatures was reached within 1 day of testing. That value was 20 NTU when the test solution was at 60°C. The turbidity then gradually decreased to a level of 1 NTU by the sixth day of the test. Thereafter, the turbidity remained constant until the end of the test.

The TSS values exhibited similar trends. The TSS value was a maximum (36.2 mg/L) at the end of the 4-hour spray cycle, which coincided with the completed addition of TSP. After the first 24 hours of the test, the TSS sample dropped to 27.5 mg/L and continued to decrease to 10 mg/L by Day 5 of the test. The TSS concentration was constant at that point until the end of the test.

Measurements of water-sample particulate sizes indicated that 80%–90% of the particulates were between 50 and 100  $\mu\text{m}$  during the first 2 days of testing. Measurements of weekly samples thereafter indicated that the suspended particulates were between 1 and 25  $\mu\text{m}$ .

Kinematic viscosity measurements at 60°C and 23°C were constant during the entire test. Strain-rate viscosity measurements indicated that the water samples exhibited common Newtonian behavior, where the shear stress is directly proportional to the strain rate.

ICP-AES results indicated that the elements present in the highest concentrations were silica and sodium. The silica concentration at the beginning of the test was ~3 mg/L; it then increased nearly linearly to 85 mg/L by Day 19 of the test. The silica concentration then remained constant through the end of the test. The initial sodium concentration (after TSP injection) averaged

~900 mg/L during the entire test, but the sodium concentration measurements fluctuated between values of 700 and 1000 mg/L during the course of the test.

### **3.2.2. Insulation**

Fiberglass insulation samples were removed from the test tank on Days 4, 16, and 30 of the test and analyzed. Flocculent deposits were observed in the Day-4 fiberglass samples. The amount of the deposits increased with the test duration. At the end of the test, these deposits were dispersed throughout the insulation samples. However, the amount of deposits was greater on the exterior than on the interior of the samples. The fibers were not encrusted, and the deposits often appeared near the intersection of several fibers.

### **3.2.3. Sediment**

A total of 256 g (wet) of sediment was recovered from the tank bottom after the tank was drained. A large portion of the sediment consisted of fugitive fiberglass debris, and the sediment appeared to be heterogeneous throughout. Elemental composition analysis of the sediment indicated that silicon was the dominant element (18% by mass). This is consistent with the fact that fiberglass was the only insulation material used in the test. Aluminum was the next most prominent element (9% by mass), followed by phosphorus (4% by mass).

### **3.2.4. Coupons**

A copper layer was evident on the submerged aluminum samples. The layer can be attributed to electrochemical ion transfer. Large, white deposits also covered the submerged aluminum coupons. The samples were weighed after drying, and no cleaning was performed before weighing. No significant weight loss or gain occurred except for the submerged galvanized steel coupons and concrete coupon, which gained approximately 3% of their pre-test weights.

## **3.3. Test #3**

ICET Test #3 was conducted using TSP as the buffering agent, with a target pH of 7. A combination of 20% fiberglass and 80% cal-sil (by volume) was the insulation mixture used in the test. Boric acid, lithium hydroxide, and hydrochloric acid were also added to the test solution.

The test began with 240 gal. of RO water and chemicals in the system. Beginning at 30 minutes into the spray phase, two batches of the TSP solution were metered into the recirculation line. Each batch consisted of boric acid and TSP in 5 gal. of RO water. The second batch also included the pre-determined amount of HCl needed for the test.

The experiment commenced at 3:30 p.m. on Tuesday, April 5, 2005, and it ended on May 5, 2005. Details of ICET Test #3 are reported in Ref. 4.

### **3.3.1. Water Samples**

The target system pH was 7. The TSP injection was completed by the end of the spray phase, and the test solution pH was 7.3 at that time. The pH increased to a value of 7.9 by the third day of

testing. After Day 3, the average pH values increased slightly to a value of ~8.0 and remained there until the end of the test.

During the first few hours of the test, precipitates were visible through the tank's viewing window. Otherwise, no chemical byproducts were visible in the daily water samples at the test temperature of 60°C or upon cooling to room temperature. Additionally, no precipitates or byproducts became visible after the samples were stored at room temperature after the end of the test. The ICP-AES analyses of daily water samples did not provide sufficient time resolution to quantify the rapid transient at the beginning of the test.

Turbidity measurements at both test and room temperatures were very similar; thus, only the 60°C values are explained. At test initiation, the turbidity measured 54 NTU, which is attributable to the addition of cal-sil dust. Approximately 1 hour into the test, the turbidity had increased significantly (>200 NTU). By the end of the 4-hour spray phase, the turbidity decreased to 79 NTU. The turbidity continued to decrease, and by the end of the first day, the turbidity fell below 1 NTU and remained near that value for the remainder of the test.

The TSS values exhibited trends similar to those of the turbidity. During the TSP injection, white flocculent particles were visible within the solution. The TSS concentration rose from its baseline value of ~10 mg/L to 268 mg/L midway through the TSP injection. At the end of the 4-hour spray cycle, the concentration had decreased to 73 mg/L. After the first 24 hours of the test, the TSS concentration had dropped to 14 mg/L and remained in the 10–20 mg/L range for the remainder of the test.

Measurements of water-sample particulate sizes indicated that they were relatively unchanged during the test. Measurements of weekly samples indicated that the suspended particulate sizes were between 1 and 50 µm.

Kinematic viscosity measurements at 60°C and 23°C were constant during the entire test. Strain-rate viscosity measurements indicated that the water samples exhibited common Newtonian behavior.

ICP-AES results indicated that the elements present in the highest concentrations were silica, sodium, and calcium. The silica concentration increased quickly to a value of ~100 mg/L after the first day of testing and then remained relatively constant throughout the next 20 days. Starting at Day 20, the silica concentration appeared to decrease slowly, but it remained >82 mg/L by the end of the test. The sodium concentration (after TSP injection) averaged ~1090 mg/L during the entire test, but the sodium concentration measurements fluctuated between values of 900 mg/L and 1620 mg/L. The calcium concentration gradually increased asymptotically from a baseline value of 3 mg/L to a Day-30 value of 109 mg/L.

### **3.3.2. Insulation**

ICET Test #3 had the greatest amount of deposits on the fiberglass of all the ICET tests. In general, the amount of deposits increased as the test progressed, and the greatest amount of deposits was found on the Day-30 exterior samples. The deposits on these samples included particles that had likely been physically captured or attached. Based on EDS analysis, the

particulate deposits on the fiberglass exterior may be classified into two categories according to phosphorous (P) and silicon (Si) content. Particulate deposits of lower P and higher Si content were likely cal-sil particles. The particulate deposits with lower Si and high P, Ca, and O content were likely composed of calcium phosphate precipitates (specific phase was not identified), which explains the composition of the white gel-like cream deposit found on the tank bottom. Calcium phosphate precipitated when pre-dissolved calcium from the cal-sil reacted with phosphate from the TSP. After precipitation, the calcium phosphate was transported to the fiberglass exterior by sedimentation and flowing water. Both kinds of deposits (cal-sil and calcium phosphate precipitates) may be physically transported and/or deposited onto the fiberglass sample exterior in this manner.

In contrast to the exterior regions of the fiberglass, the interior fiberglass samples were relatively pristine, with few particulate deposits. However, the interior samples did contain significant flocculent deposits. EDS analysis indicated that the flocculent deposits contained insignificant amounts of P, meaning that the deposits were not related to the white gel-like cream deposit.

Cal-sil made up 80% by volume of the insulation in Test #3. A Day-30 baked cal-sil sample that had been submerged in the high-flow zone and a Day-30 unbaked cal-sil sample that had been submerged in the birdcage were examined. The exterior surface of the baked cal-sil sample from the high-flow region was examined by environmental scanning electron microscopy (ESEM) and EDS. These results showed a significant amount of phosphorus. Smaller amounts of phosphorus were found on the exterior of the unbaked cal-sil in the birdcage sample. However, almost no phosphorus was present in the interior of the unbaked cal-sil.

### **3.3.3. Sediment**

A large quantity (over 78 kg wet) of sediment was recovered from the bottom of the tank after it was drained. The sediment was ~9 in. deep in some places on the bottom of the test tank after the test. The main reason for the large amount recovered was that ~20 kg of the cal-sil added was in the form of dust. The sediment was similar in consistency to wet mud and was pink and yellow, consistent with the baked and unbaked cal-sil that was originally added to the tank. Calcium was the dominant element present (19% by mass), followed by silicon (17% by mass). Although dominated by cal-sil, the sediment was also likely composed of fiberglass debris and corrosion products. Though an accurate mass comparison is difficult because of the large amount of water retained in the recovered sediment, it is believed that a significant fraction of the sediment mass was composed of secondary chemical precipitates.

Test #3 was unique in that a pinkish-white, gel-like deposit was found after the tank was drained. That deposit had the consistency of face cream and covered portions of the sediment and submerged objects on the tank bottom. No effort was made to isolate all of the gel-like deposit. However, 500 mL were collected separately for analysis. EDS results showed that 92% of the deposit was composed of calcium, oxygen, and phosphorus. Implications of this gel-like material are discussed in Ref. 7.

### **3.3.4. Coupons**

All of the submerged coupons had white particulate deposits on them at the end of the test. As in Test #2, a copper layer was evident on the submerged aluminum samples. The galvanized steel coupons had an average weight gain of 15 g, and the others had weight changes of less than 2 g. The concrete coupon was covered with a white particulate and gained ~3% of its pre-test weight. Overall, the unsubmerged coupons had similar streaking deposits and weight changes of 2 g or less.

## **3.4. Test #4**

ICET Test #4 was conducted using sodium hydroxide to obtain the target pH of 10. A combination of 20% fiberglass and 80% cal-sil (by volume) was the insulation mixture used in the test. Boric acid, lithium hydroxide, and hydrochloric acid were also added to the test solution.

The test began with 249 gal. of RO water and chemicals in the system. Over the first 30 minutes of the test, 1 gal. of RO water containing 614 g of sodium hydroxide was metered into the spray. The test ran for 30 days, with one 2.25-hour interruption caused by a power outage, which occurred on Day 11.

The experiment commenced at 2:30 p.m. on Tuesday, May 24, 2005, and ended on June 23, 2005. Details of ICET Test #4 are reported in Ref. 5.

### **3.4.1. Water Samples**

The target pH for this test was 10, and the actual test solution pH was approximately 9.8 at the end of the sodium hydroxide injection into the spray. The pH of the test solution decreased slightly over the first 2 days of the test to a value of 9.6. After the second day, the pH rose steadily to a value of 9.9 by Day 8. Thereafter, the pH varied between 9.7 and 9.9 over the remainder of the test, and was ~9.8 at the end of the test.

No chemical byproducts were visible in the daily water samples at the test temperature of 60°C or upon cooling to room temperature. Additionally, no precipitates or byproducts became visible after the samples were stored at room temperature following the test.

Turbidity measurements at both test and room temperatures were very similar; thus, only the 60°C values are explained. The turbidity value at the start of the test was high (130 NTU), because of the addition of cal-sil before initiation of the test. Turbidity steadily decreased during the 4-hour spray phase and reached a value of 36 NTU by the end of this phase. The turbidity continued to decrease and, by the end of the first day, fell below 3 NTU and remained largely constant over the remainder of the test.

TSS values generally exhibited trends similar to the turbidity trends. At the start of the test, the TSS was 129 mg/L, which was the highest measured value. At the end of the 4-hour spray cycle, the concentration had decreased to 68 mg/L. After the first 24 hours of the test, the TSS concentration had dropped below 40 mg/L and remained roughly constant during the remainder

of the test. The TSS varied between 29 and 45 mg/L from Day 1 to Day 30, with an average value of ~35 mg/L.

Measurements of water-sample particulate sizes indicated that they were relatively unchanged during the test. Measurements of weekly samples indicated that the particulate sizes were between 1 and 50  $\mu\text{m}$ .

Kinematic viscosity measurements at 60°C and 23°C were constant during the entire test. Strain-rate viscosity measurements indicated that the water samples exhibited common Newtonian behavior.

ICP-AES results indicated that the elements present in the highest concentrations were silica, sodium, calcium, and potassium. The silica concentration increased quickly to a value of ~100 mg/L after the first day of testing and then continued to increase steadily until Day 15, when the concentration was ~170 mg/L. The silica concentration was approximately constant from Day 15 to the end of the test, but individual concentration measurements varied between ~160 and 190 mg/L. The sodium concentration at the start of the test was ~6,000 mg/L and increased fairly steadily over the course of the 30-day test. By Day 17, the sodium concentration variability had increased significantly from day to day. The calcium concentration rose from a 4-hour value of 37 mg/L to ~70 mg/L over the first 5 days of testing. After Day 5, the calcium concentration remained relatively constant for the duration of the test. The potassium concentration was measured five times throughout the duration of the test, and it rose from a baseline value of 7 mg/L to 35 mg/L at the end of the test.

### **3.4.2. Insulation**

The ICET Test #4 fiberglass contained a large amount of deposits. Fiberglass samples exhibited deposits throughout the fiber matrix after they had been exposed in the test solution for 30 days. Particulate deposits were generally found only on the exterior of the fiberglass and were likely physically retained or attached on the fiberglass exterior. EDS analyses indicated that these particulate deposits contained significant amounts of silica and calcium, suggesting they were from cal-sil debris. In contrast, the interior of the fiberglass samples was relatively clean, and only film deposits were observed. To investigate the formation of the film deposits, controlled experiments were performed by gently rinsing the interior fiberglass samples with several drops of RO water before ESEM analysis. After being rinsed with RO water, the film deposits disappeared from the fiberglass samples. These results suggest that the film was actually soluble, which is consistent with the explanation that the film was deposited during the drying process of the fiberglass.

As with Test #3, cal-sil made up 80% by volume of the insulation. However, the significant sodium concentration that was present in solution as a dissolved ion throughout the duration of the test (unlike phosphate in Test #3, which was quickly depleted) was able to diffuse to the interior of the cal-sil (the cal-sil was essentially soaked in a sodium solution for 30 days). Thus, it appears in relatively equal amounts in the interior and exterior cal-sil samples.

### **3.4.3. Sediment**

A large quantity (>86 kg wet) of sediment was recovered from the bottom of the tank after it was drained. The sediment was ~9 in. deep in some places on the bottom of the test tank. The main reason that the amount recovered was so large is that 80% of the fiberglass was replaced by cal-sil insulation, with ~20 kg being in the form of cal-sil dust. The sediment was similar in consistency to wet mud and was pink and yellow, consistent with the baked and unbaked cal-sil that was originally added to the tank. Calcium was the dominant element present in the sediment (20% by mass), followed by silicon (16% by mass). Although dominated by cal-sil, the sediment also contained fiberglass debris and corrosion products. No secondary chemical precipitates were observed during Test #4 that would increase the quantity of sediment. The larger amount of recovered mass from Test #4 compared to Test #3 is indicative of the uncertainty inherent to a bulk mass balance on the ICET tank. The difference in sediment masses may be because the Test #4 sediment was recovered sooner after the tank was drained, and it contained higher water content.

### **3.4.4. Coupons**

The unsubmerged zinc, aluminum, US, and copper samples exhibited evidence of corrosion upon removal from the test chamber. No significant corrosion products were observed on any of the metallic samples contained within the submerged coupon rack. Pre- and post-test weight measurements revealed insignificant changes (<1 g) in the bulk weight of the submerged and unsubmerged metallic coupons. A faint, white film was present on the submerged aluminum and zinc coupons. The film was much less than the corrosion products evident on the unsubmerged specimens. Test #4 was unique in the relatively inert response of the submerged coupons to the high-pH environment. Section 4.4.3 provides an hypothesis for the observed behavior.

## **3.5. Test #5**

ICET Test #5 was conducted using sodium tetraborate (borax) as the buffering agent, with an expected pH of 8–8.5. Fiberglass was the only type of insulation used in the test. Boric acid, lithium hydroxide, and hydrochloric acid were also added to the test solution.

The test began with 248 gal. of RO water and chemicals in the system. After 2 hours, 2 gal. of RO water containing 90.8 mL of hydrochloric acid were metered into the spray.

The experiment commenced at 11:00 a.m. on Tuesday, July 26, 2005, and ended on August 25, 2005. Details of ICET Test #5 are reported in Ref. 6.

### **3.5.1. Water Samples**

A target pH range of 8–8.5 was specified for the onset of this test. The test solution pH was 8.4 before initiation of the sprays, after the initial chemical environment had been established. The pH of the test solution decreased slightly during the last 2 hours of the spray phase to a value of ~8.3 because of the hydrochloric acid addition. The pH was 8.2–8.3 over the first 20 days of the test, and it was between 8.2 and 8.5 over the final 10 days of the test.

No chemical byproducts were visible at the test temperature of 60°C during this test. At room temperature, precipitates became visible at the bottom of the water samples, beginning with the Day-2 sample. The amount of visible room temperature precipitation appeared to increase only slightly in subsequent daily water samples. It should be noted that it required several days at room temperature before the precipitates were visible on the bottom of the sample bottles. The total amount of precipitates in the Day-30 water sample barely covered the bottom of the 250-mL sample bottles. When the precipitates were suspended upon shaking, they were no longer visible, and it required ~2–3 days before they settled back to the bottom of the sample bottles.

Test #5 solution (120 gal.) was archived at 60°C in constant-temperature ovens at the end of the test. After ~2 months of aging, similar small quantities of precipitates were visible at the bottom of the storage containers. Furthermore, it was found that when this test solution was decanted, its rapid cooling to ~40°C could quickly produce small amounts of visible precipitates. These findings are documented in Ref. 8.

Turbidity values at 60°C and 23°C were similar until Day 7. The turbidity values taken before the latent debris and concrete dust were added were less than 1 NTU. After addition of the latent debris and concrete dust samples, the turbidity increased to 14 NTU at the start of the test. During the 4-hour spray phase, the turbidity slowly decreased to 12 NTU at the end of the spray phase. As the test continued, the turbidity measurements at both temperatures continued to decrease and were <1 NTU by Day 8. The 60°C values generally remained below 1 NTU for the remainder of the test and had an average value of 0.7 NTU between Days 8 and 30. Beginning with the Day 8 measurement, the 23°C values began to deviate from, and were slightly higher than, the 60°C values. Between Days 12 and 14, the 23°C turbidity began to increase and reached a value of ~5 NTU by Day 18, where it remained for the remainder of the test.

The baseline TSS before the initiation of sprays was 16 mg/L. At the conclusion of the spray phase, the TSS value was ~27 mg/L. TSS then decreased until Day 5, when it was ~17 mg/L. From Days 5 through 9 of the test, TSS remained approximately constant, with an average value of 17 mg/L. On Day 10 it increased to a value of 25 mg/L. Between Days 10 and 21, the average TSS value was >20 mg/L, but the results were more variable. Individual measurements ranged from a low of 16 mg/L to a high of 32 mg/L during this time frame. After Day 22, the TSS measurements decreased to ~15 mg/L and remained approximately constant over the duration of the test.

Measurements of water-sample particulate sizes indicated that they were between 1 and 50 µm during the first 3 days of testing. Measurements of weekly samples indicated that the particulates were <1 µm until the last measurement, when 90% of the particulates were between 25 and 50 µm.

The bulk kinematic viscosity measurements at 60°C remained constant during the test. The 23°C measurements remained constant over the first 15–17 days of the test. Between Days 16 and 18, the 23°C viscosity increased slightly to ~0.96 mm<sup>2</sup>/second and remained constant until the end of the test. Strain-rate viscosity testing clearly demonstrated that the viscosity varied with the strain

rate for the 25°C samples, which is indicative of non-Newtonian behavior. No strain-rate dependency was observed for the 60°C solution.

ICP-AES results indicated that the elements present in the highest concentrations were sodium, aluminum, calcium, and silica. The sodium concentration was ~1200 mg/L between Days 1 and 17 of the test. On Day 18, the sodium concentration increased to 1400 mg/L and remained at this value through Day 20. Between Days 20 and 30, the sodium concentration gradually decreased to a value of ~1200 mg/L. The aluminum concentration was initially minimal and then rose to ~55 mg/L after ~12 days of testing. The Day 15 measurement indicated a sudden drop in the aluminum concentration to ~45 mg/L. The aluminum concentration remained below 50 mg/L between Days 15 and 20. The Day 21 measurement indicated that the aluminum concentration had dropped again to 37 mg/L. Beginning at the Day 23 measurement, the aluminum concentration rose from 35 to 45 mg/L by the end of the test.

The calcium concentration initially was minimal, but it rose to a value of >15 mg/L by Day 2 and reached 20 mg/L by Day 6. The calcium concentration peaked by Day 11 at ~22 mg/L and at Day 15 decreased slightly to 20 mg/L. Between Days 15 and 24, the concentration remained approximately constant at 20 mg/L. The Day-25 measurement indicated that calcium had increased to 30 mg/L, and it remained above this value for the remainder of the test. The initial silica concentration at test initiation was ~6 mg/L; it rose to 10 mg/L by the end of the spray phase and peaked at 12 mg/L by Day 3 of the test. The concentration slowly decreased after Day 3 until it reached a value of 7 mg/L by Day 22. The silica concentration remained <8 mg/L between Days 22 and 30.

### **3.5.2. Insulation**

ICET Test #5 had the smallest amount of deposits in the fiberglass of any of the ICET tests. Day-30 high-flow fiberglass exterior samples were relatively pristine, and no significant particulate deposits were found. The lack of deposits is likely because of the small amount of suspended particles in the test solution. The interior samples were also relatively pristine, and only flocculent deposits were observed. The flocculent deposits were primarily composed of oxygen, sodium, calcium, magnesium, aluminum, and possibly silicon.

### **3.5.3. Sediment**

A very small quantity of sediment (only 89 g wet) was found on the test tank floor after draining. For reference, that is only slightly higher than the 85 g of concrete dust and latent debris that were added prior to the test initiation. The sediment consisted of fiberglass debris and particulate deposits. Silicon made up 30% by mass of the sediment, and sodium was the next most prominent at 7%.

### **3.5.4. Coupons**

The samples were weighed after drying, and no cleaning was performed before weighing. Weight loss/gain measurements indicated that only the submerged aluminum specimens experienced a significant weight change. The submerged aluminum specimens lost ~5% of their pre-test mass. The concrete sample gained 226 g (3% of its pre-test mass). The concrete weight

gain may have resulted from retained water, since the weight measurement was performed after several days of air drying. Other samples either gained or lost <1% of their pre-test mass.

This page intentionally left blank.

## 4. COMPARISONS OF KEY RESULTS

Samples from the ICET tests were subjected to numerous laboratory analyses. This section presents key results from these analyses and compares them for each test. Section 4.1 presents water chemistry and precipitate analyses, Section 4.2 discusses the findings from examinations of fiberglass and cal-sil samples, Section 4.3 describes the post-test sediment, Section 4.4 compares photographs and microscopic analyses of coupons, Section 4.5 discusses results from deposition product examinations, and Section 4.6 presents analyses of the Test #3 gel-like precipitate.

### 4.1. Water Samples

Daily water samples were obtained during each ICET test. Numerous water chemistry parameters were measured and are presented in Section 4.1.1. Additionally, precipitates were observed in Tests #1 and #5 and are discussed in Section 4.1.2.

#### 4.1.1 Water Chemistry

Throughout the ICET test series, daily measurements of pH, turbidity, TSS, and kinematic viscosity were taken. Additionally, daily measurements of selected elemental concentrations were obtained. In this section, these measurements are compared. Since chemical parameters and insulation debris differed from test to test, Table 4-1 was compiled to serve as a guide to system parameters as the water chemistry results are discussed.

**Table 4-1. Test Conditions in the ICET Tests.<sup>1,2</sup>**

Test #	Boron <sup>3</sup> added (mg/L)	NaOH added (mg/L)	TSP <sup>4</sup> added (mg/L)	Controlling pH buffer system	Insulation <sup>5</sup>	
					Fiberglass	Cal-sil
1	2,800	7,677	-	borate	100%	-
2	2,800	-	4,000	phosphate	100%	-
3	2,800	-	4,000	phosphate	20%	80%
4	2,800	9,600	-	borate	20%	80%
5	2,400	-	-	borate	100%	-

<sup>1</sup>The chemical doses were according to the required parameters given in Table 2-4. To determine the quantities of NaOH and TSP required to meet the target pH values in Table 2-4, water quality modeling using Visual Minteq Version 2.30 was conducted, followed by verification through bench-scale testing prior to the ICET tests.

<sup>2</sup>Temperature was 60°C ± 3°C in all tests. The following chemicals were also added to the solution: LiOH = 0.7 mg/L and HCl = 100 mg/L in Tests #1–#4. LiOH = 0.3 mg/L and HCl = 42.8 mg/L in Test #5. Also, 63.7 g of latent debris and 21.21 g concrete dust was added to the solution prior to the test initiation for each test.

<sup>3</sup>The required concentration of boron was added as 16,000 mg/L H<sub>3</sub>BO<sub>3</sub> in Tests #1–#4, and as 6,848 mg/L H<sub>3</sub>BO<sub>3</sub> and 10,580 mg/L as Na<sub>2</sub>B<sub>4</sub>O<sub>7</sub>·10H<sub>2</sub>O in Test #5.

<sup>4</sup>TSP = Na<sub>3</sub>PO<sub>4</sub>·12H<sub>2</sub>O (Trisodium phosphate).

<sup>5</sup>All tests consisted of 0.137 cu ft of insulation represented per cubic foot of water. For each test, the insulation was present as fiberglass and/or calcium silicate material with the distribution of materials as shown in the table.

Each test had a different pH that was attributable to specific chemical requirements (Table 4-1). As shown in Figure 4-1, although the target pH was different between tests, all tests had a similar consistency with only a slight drift in pH throughout the test. The only exception to this trend was observed in Test #3, where the pH deviated from the initial pH by approximately 0.8 unit. In Test #3, phosphate precipitated out of solution early during the test which resulted in the diminished buffering capacity of the system. Without adequate buffering, the system pH could be more easily affected as varying chemical reactions occurred.

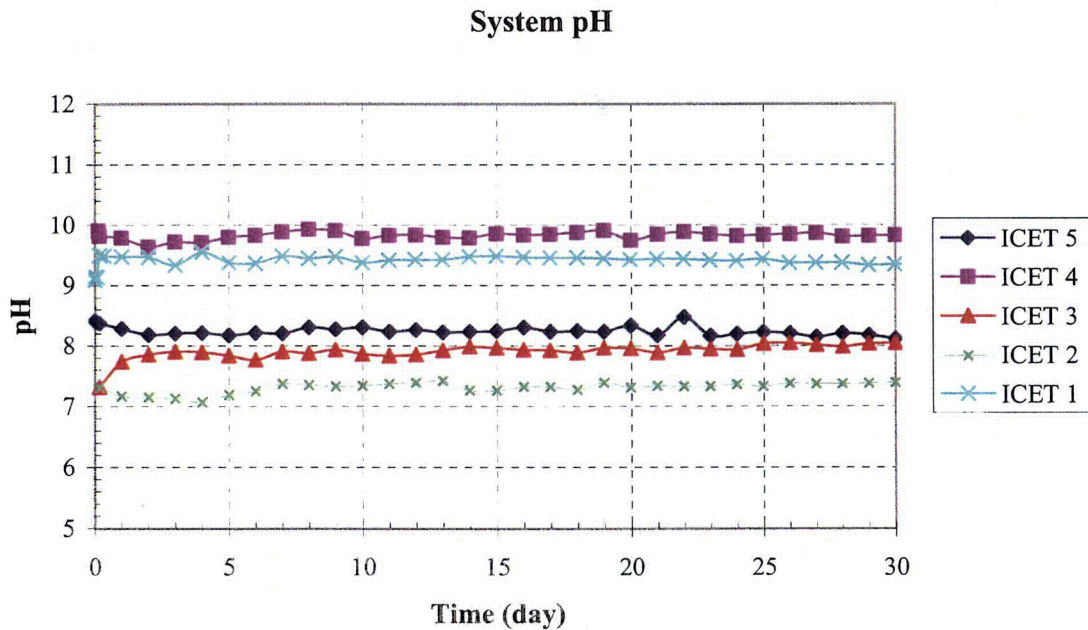


**Figure 4-1. ICET bench-top pH comparison.**

Turbidity measurements were taken frequently at 60°C during the first day of testing and are presented in Figure 4-2. The number of samples taken during the first day of each test varied. The official procedure only specified a time-zero, 4-hour, and 24-hour sample, but as a result of visual observations and varying test ingredients, samples were taken more often for some tests.

### Day One Turbidity

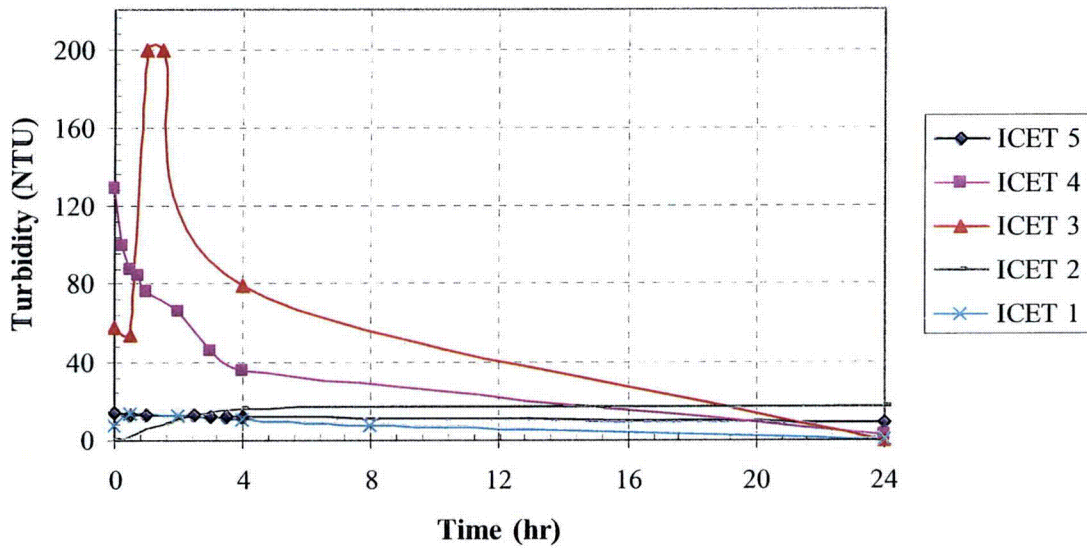


Figure 4-2. Day 1 turbidity.

In all of the tests, turbidity peaked within the first few hours of testing and decreased to lower values within 24 hours. Tests #3 and #4 had higher time zero measurements as compared with the other tests because cal-sil dust was added to the tank before test initiation. The difference in the peak measurements is because of the varying chemical and insulation requirements for each test.

For all tests, the 60°C turbidity values, (Figure 4-3), were relatively similar. Each reached a maximum value during first day of testing and by the second day of testing decreased to very low values which were similar to the baseline measurements. The turbidity measurements remained at these lower values for the duration of the tests.

### 60 °C Turbidity Measurements

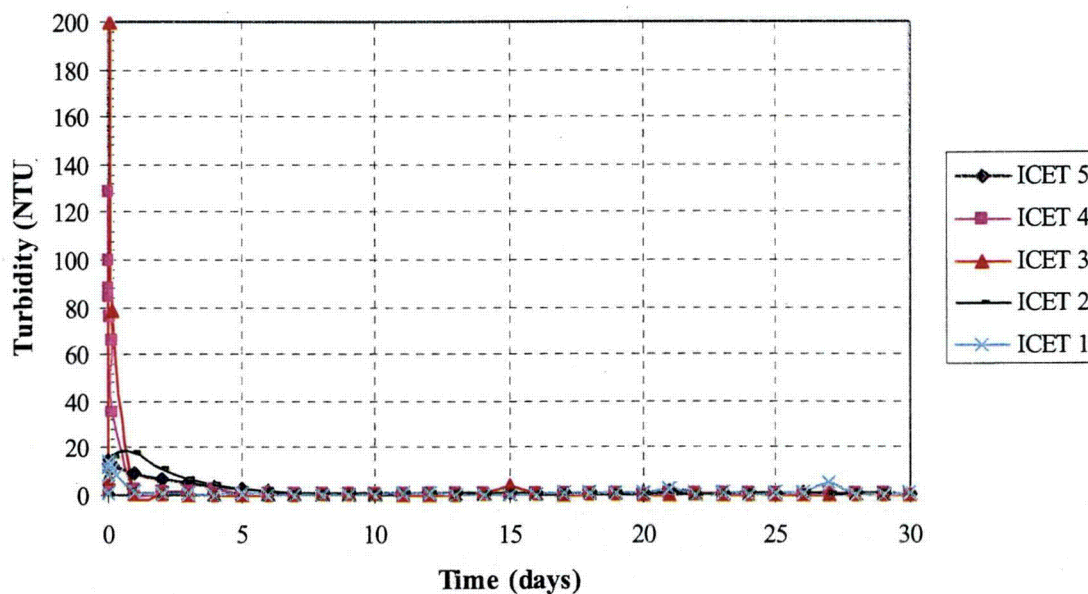


Figure 4-3. ICET 60°C turbidity.

Turbidity measurements at 23°C, as shown in Figure 4-4, were also relatively similar for Tests #2–#4. Turbidity reached a maximum value within the first day of testing and decreased towards the base-line value, with Test #2 having the longest delay time. Tests #1 and #5 turbidity measurements deviated from the previously observed pattern, which may be attributable to temperature-dependent solution behavior. Tests #1 and #5 solutions produced precipitates upon cooling that made the solutions cloudy in nature and consequently provided higher turbidity readings. Since Test #1 had a larger concentration of soluble aluminum and a larger amount of subsequent precipitation, it also experienced a more dramatic deviation in turbidity. As Test #1 progressed, the cloudy nature of the cooled solution became more pronounced, which is indicative of increased soluble aluminum concentration resulting in increased precipitation at room temperature.

### 23 °C Turbidity Measurements

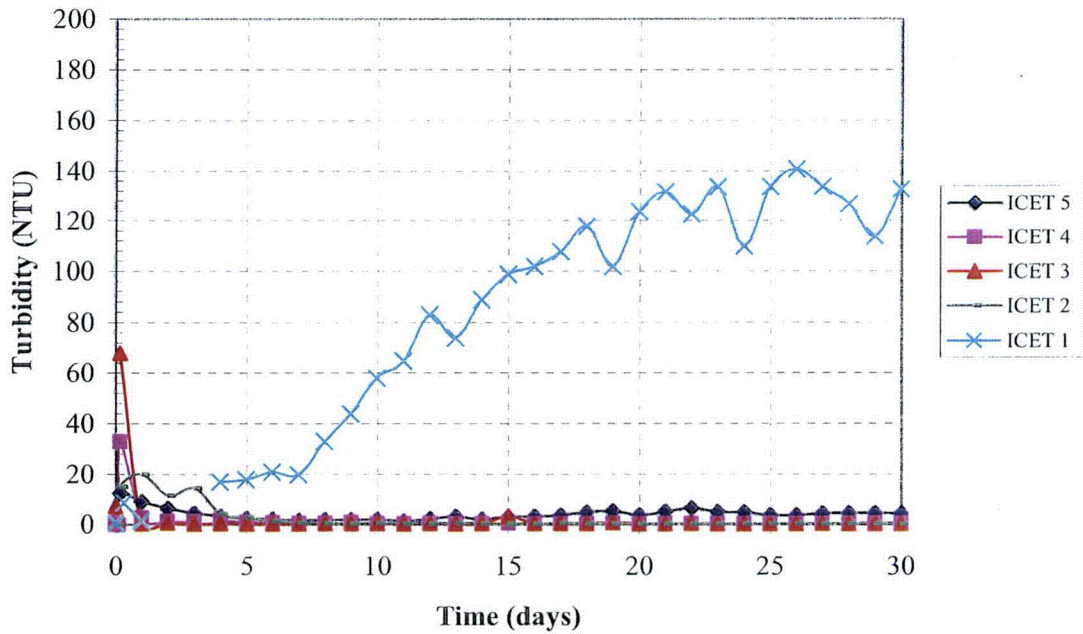


Figure 4-4. ICET 23°C turbidity.

TSS measurements were also taken for each test. As can be seen in Figure 4-5, each test reached a maximum value within the first few hours of testing and declined to a minimum value similar to the base-line measurement. As seen in Figure 4-6, the daily TSS measurements varied within a moderate range around the minimum value obtained during the first day of testing. Tests #3 and #4 provided the largest initial TSS concentrations, which are attributable to the addition of cal-sil into the chemical environment prior to test initiation.

### Day One TSS

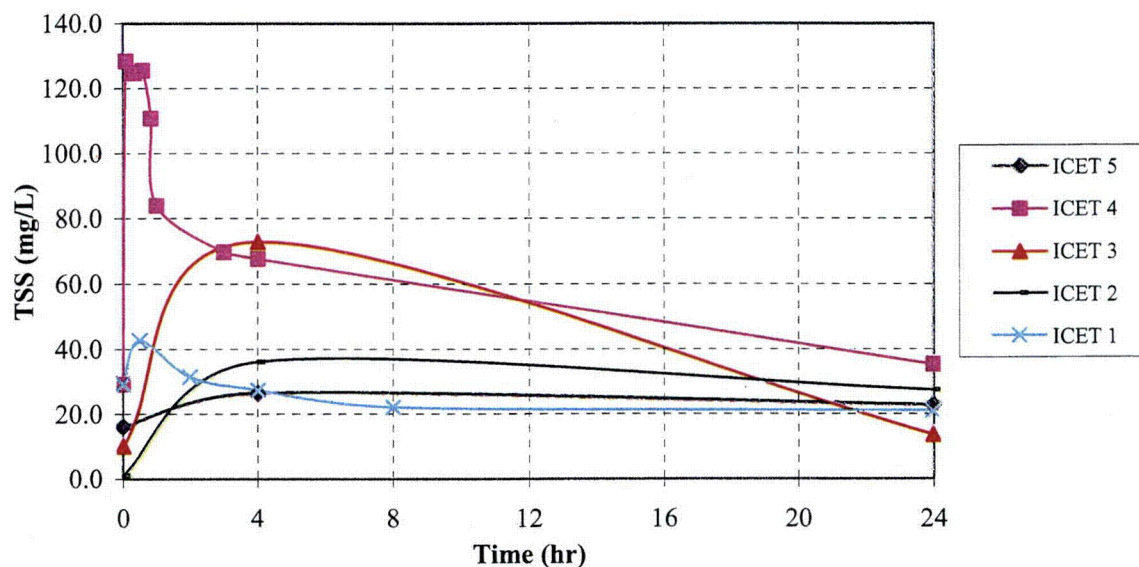


Figure 4-5. ICET Day-1 TSS.

### TSS

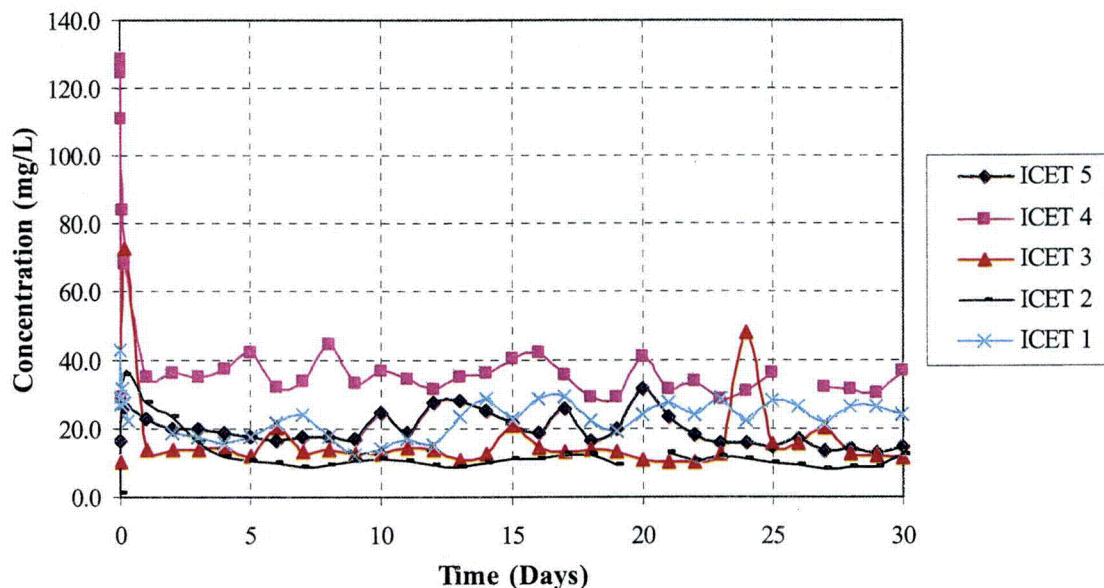


Figure 4-6. ICET TSS.

Measurements of the kinematic viscosity taken at 60°C resulted in approximately constant values, with the exception of Test #1 (Figure 4-7). All values were greater than that of pure water (0.4665 mm<sup>2</sup>/s at 60°C, see Ref. 9). The highest viscosities were obtained in Tests #1 and #4,

which may be attributed to the higher concentrations of suspend solids in solution (Figure 4-6) and/or to the large concentrations of chemicals added to solution (Table 4-1). The viscosity of the bulk solution can be affected by the presence of particulates, electrolytes, and gelatinous substances.

### 60 °C ICET Viscosity

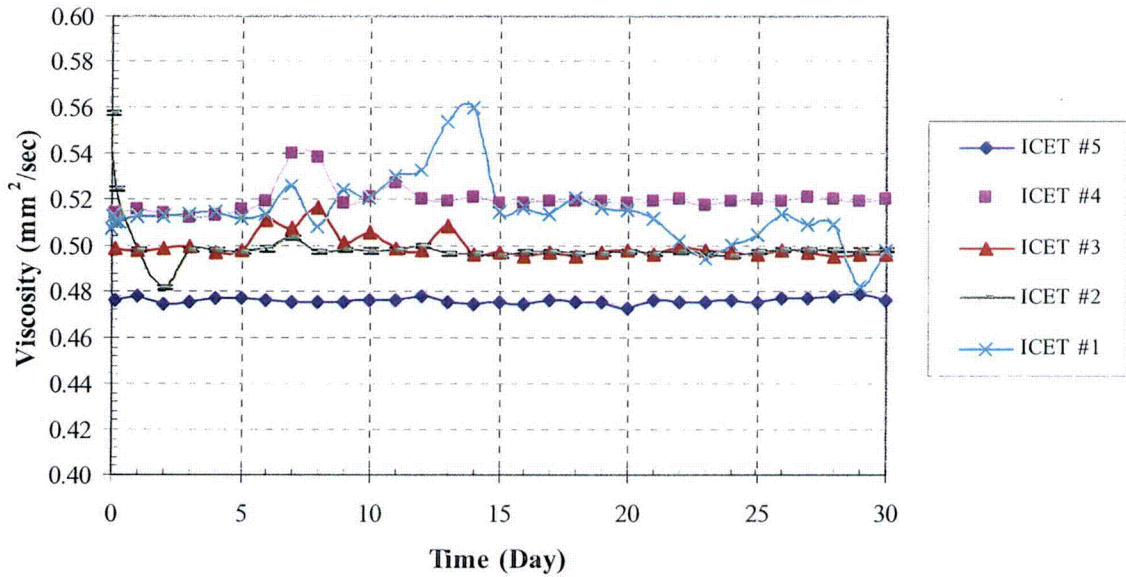


Figure 4-7. ICET 60°C kinematic viscosity.

The room-temperature kinematic viscosities (Figure 4-8) were also relatively constant with the exception of Test #1. Although the room temperature measurements taken during ICET #1 experienced deviations from day to day, the measurements generally increased to a higher value throughout the duration of the test. The increase is attributable to the increase in aluminum concentration and visible precipitates. The variations within the Test #1 viscosity measurements could be attributed to temperature-dependent solution behavior. Following Test #1, daily measurement protocols were refined to report the kinematic viscosity after a 5-minute cooling time in a constant-temperature water bath.

### 23 °C ICET Viscosity

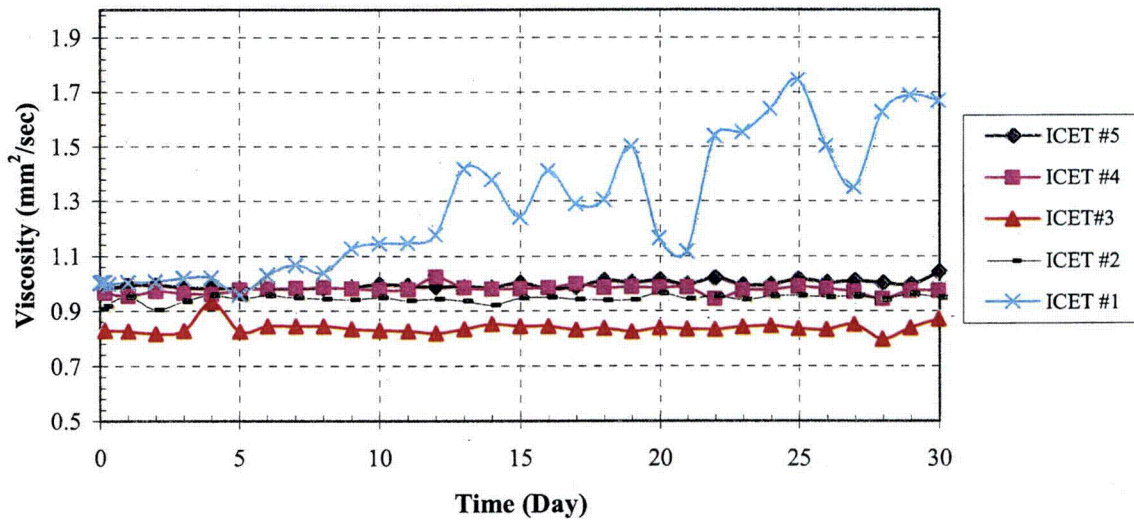


Figure 4-8. ICET 23°C kinematic viscosity.

As previously noted, the Test #1 solution became cloudy when its temperature was reduced. This cloudiness is attributable to chemical product precipitation. The technique used to measure viscosity was not intended to obtain measurements of solution with precipitation present. Consequently, for the systems in which precipitation was observed, the viscosity measurements should only be interpreted qualitatively.

During the ICET test series, the hydrogen concentration was measured in the tank atmosphere. The tank was passively vented during all tests to avoid an unsafe hydrogen buildup. However, as shown in Figure 4-9, differences were noted between tests, with Test #1 having the highest concentration. Because of changes in operational procedures, passive venting, and the simplicity of the measurement tool, these measurements should be used for qualitative interpretations only.

## Hydrogen Generation

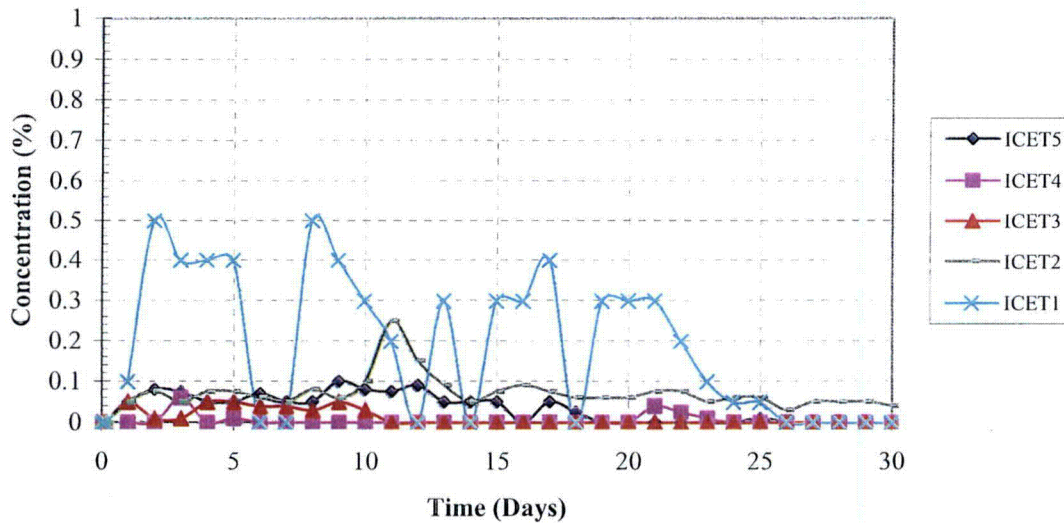


Figure 4-9. ICET hydrogen concentration.

During Test #1, ventilation valves were initially kept closed and only opened for hydrogen measurements and for venting when values reached a level approaching the safety action threshold. Within the first few days of the test, the hydrogen measurements were above the safety action threshold of 0.4%. These measurements were checked by UNM health and safety officials and found to be erroneous, which resulted in a procedural change for hydrogen sampling. An evaluation of the Test #1 hydrogen concentrations was made, keeping in mind the limitations of the measurement and the changes in operational procedures. It is speculated that the zero values on Days 6, 7, 12, 14, and 18 were erroneous. However, the trend seen from Day 20 until the end of the test is qualitatively accurate. Of interest is the hydrogen generation decreasing to zero from Day 21 to Day 26, which corresponds to the leveling off of aluminum concentration on Day 25 (Figure 4-10).

Another procedural change was made at the start of Test #2. For the first 10 days of testing, the vent valves on the tank lid were left open at all times and the hydrogen generation measurements were relatively low (0.05%–0.1%). For Day 11 through Day 12, the vent valves were closed to determine actual hydrogen build-up in the tank which spiked at 0.25%. For Tests #3–#5, the ventilation valves remained open and the hydrogen concentration was monitored daily.

Daily water samples were taken for ICP-AES analyses throughout the ICET test series. Results from those analyses are presented next. Details of the sample preparation process, typical measurement uncertainties, and minimum detection limits are given in Appendix A. Aluminum was one of the elements measured in the test solution. Tests #1 and #5 were the only experiments that produced a detectable amount of aluminum in solution (Figure 4-10). Both tests were in a pH range of high aluminum solubility and both experienced aluminum coupon corrosion. Test #1 had a higher pH which allows for greater corrosion and consequent solubility

than that of Test #5. Although Test #4 also possessed conditions favorable for aluminum corrosion and solubility, it had different overall solution chemistry because it contained cal-sil as 80% of the insulation source. This difference in chemical composition for Test #4 provided a “passivation” (see Section 4.4.3) layer that protected the aluminum coupons from significant corrosion and resulted in lower aluminum concentrations.

### Unfiltered Aluminum Concentration

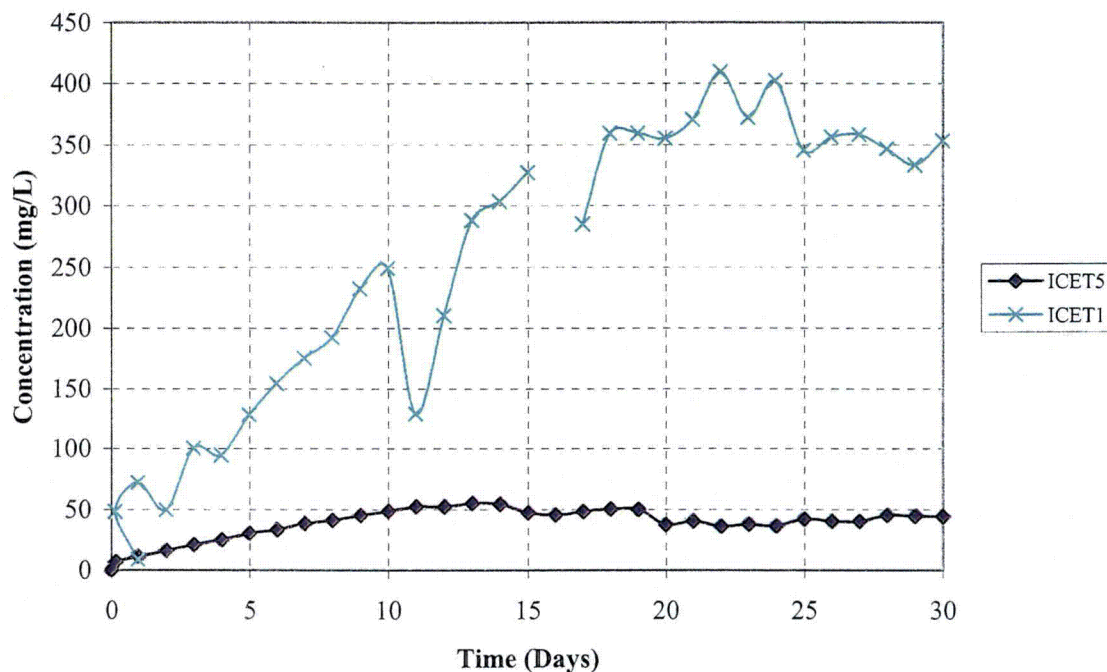


Figure 4-10. ICET Tests #1 and #5 unfiltered aluminum concentration.

As seen in Figure 4-11, Tests #3 and #4 calcium concentrations were the highest of the ICET tests, which is a result of the cal-sil added to solution. Although the amount of cal-sil added was the same for Tests #3 and #4, the systems differed in their initial chemical compositions.

### Unfiltered Calcium Concentration

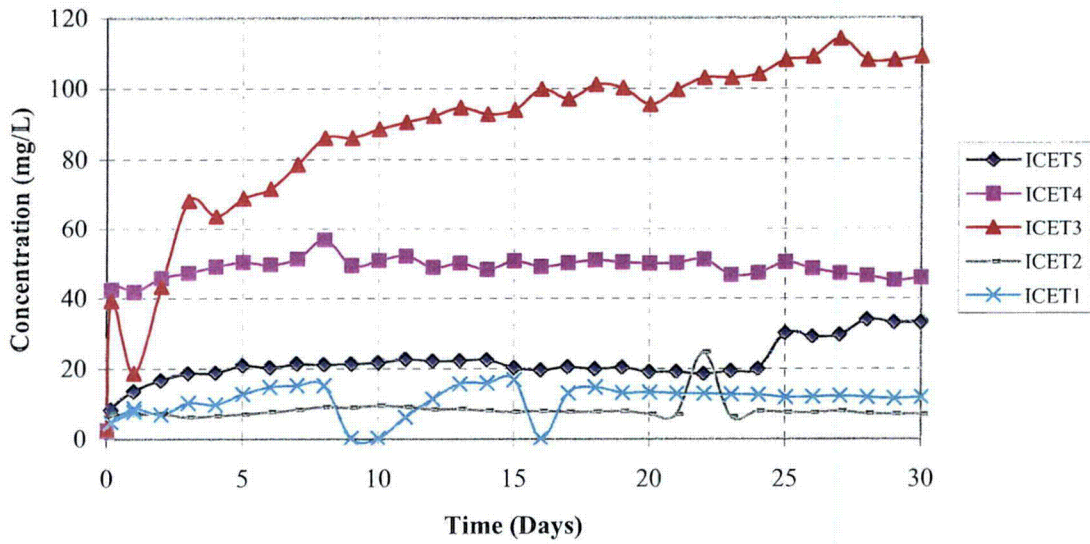


Figure 4-11. ICET unfiltered calcium concentration.

The copper, zinc, and magnesium concentrations, Figures 4-12 through 4-14, were present in low amounts which was not unexpected.

### Unfiltered Copper Concentration

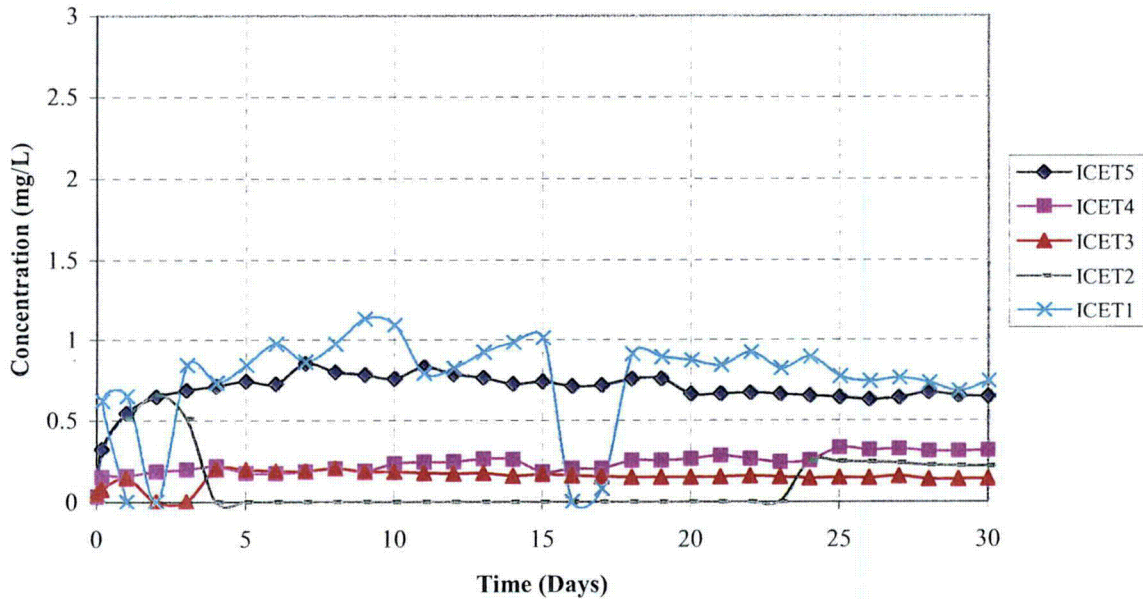


Figure 4-12. ICET unfiltered copper concentration.

Figure 4-13 shows that the highest zinc concentration (up to 10 mg/L) occurred during the first 4 days of Test #2, and then decreased to below 1 mg/L for the remainder of the test. This result was likely caused by a combination of passivation of the zinc surface and settling/precipitation of zinc products. The precipitation was likely caused by phosphate, as the sediment sample from Test #2 contained zinc and phosphate compounds (Figure 4-82).

### Unfiltered Zinc Concentration

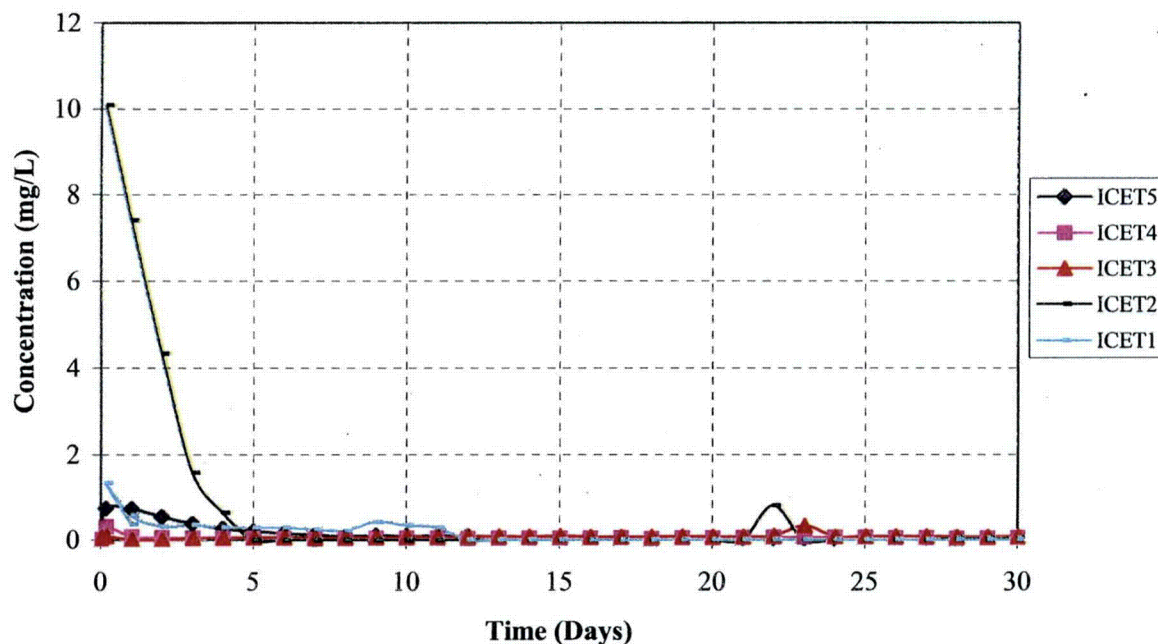


Figure 4-13. ICET unfiltered zinc concentration.

The magnesium concentrations for Tests #2, #3, and #5 are shown in Figure 4-14. The concentrations in Tests #1 and #4 were below minimum detection limits.

### Unfiltered Magnesium Concentration

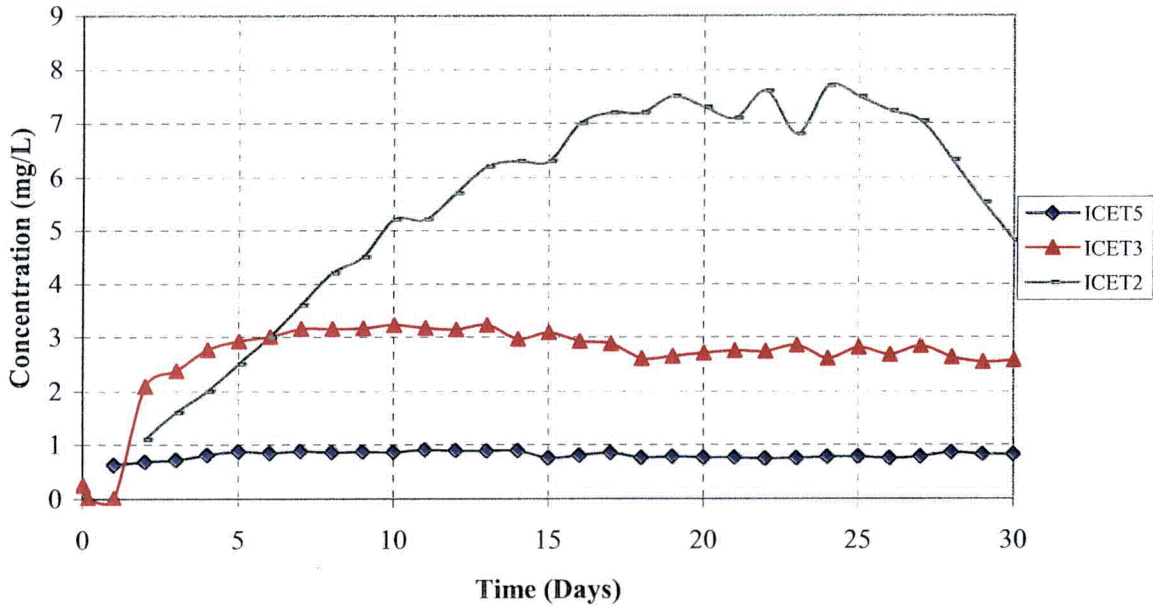


Figure 4-14. ICET Tests #2, #3, and #5 unfiltered magnesium concentration.

As shown in Figure 4-15, Tests #3 and #4 had the largest soluble silica concentrations, which is a result of the presence of cal-sil in the tests. As pH increases, silica solubility increases. Since Test #4 was conducted at a high pH and had cal-sil in solution, it had the highest silica concentrations. Test #2 silica concentrations could be attributed to the dissolution of fiberglass in solution at the system pH. Although Tests #2 and #3 had different sources of insulation, they share similar solution pH and have similar silica concentrations at the end of the tests.

### Unfiltered Silica Concentration

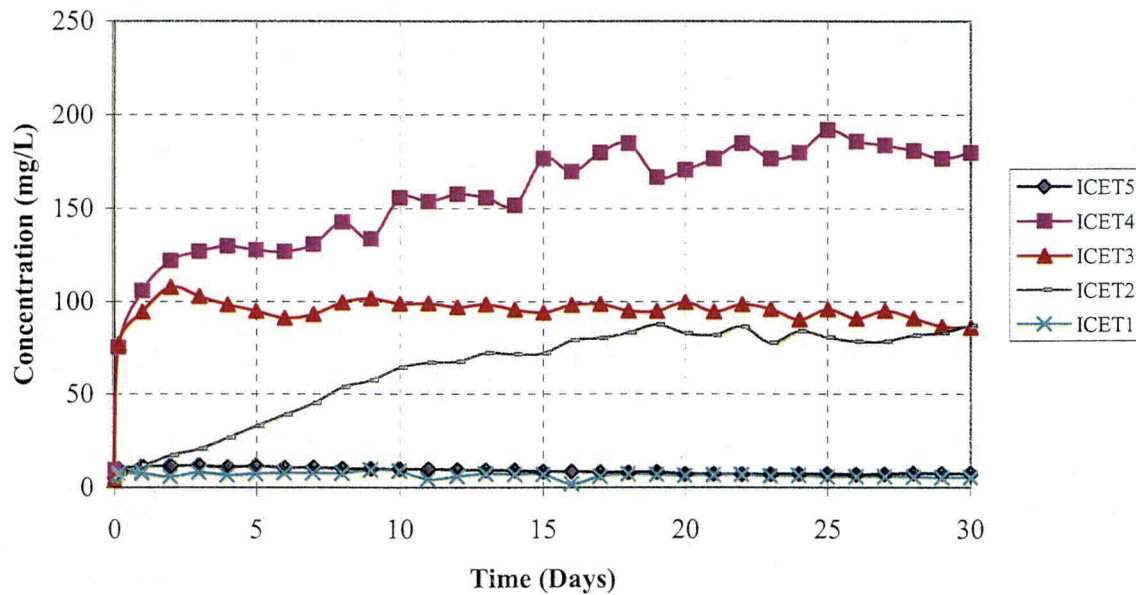


Figure 4-15. ICET unfiltered silica concentration.

Sodium concentrations are presented in Figure 4-16. In Tests #1 and #4, higher concentrations of sodium were detected because sodium hydroxide was added in those tests. A higher concentration of sodium hydroxide was used in Test #4 to obtain a higher pH value than Test #1. An unusually high concentration of sodium was present in Test #4, however, of which only about half can be attributed to the sodium hydroxide addition. The additional sodium could be a result of degrading insulation. At higher pH values as that of Test #4, silica is more soluble (Figure 4-15) which can allow for the insulation, to degraded to a greater degree releasing chemicals such as sodium, into solution.

Tests #1 and #4 had similar system pH values and contained similar constituents. However, the unusually large sodium concentration in Test #4 was not observed in Test #1. It is plausible that the difference in initial silica concentration affected the overall solution chemistry. Test #1 had a smaller amount of initial soluble silica and notable aluminum corrosion. The aluminum could have coated the fiberglass, interacting with the silica content, protecting it from degradation and the subsequent release of silica and sodium into solution. In Test #4, the initial soluble silica resulting from the addition of cal-sil, may have protected the aluminum from corrosion. This phenomenon is discussed in Section 4.4.3. Without corroded aluminum to protect the insulation by interacting with the silica content, the insulation may have been able to dissolve into solution releasing more sodium and silica into solution.

### Unfiltered Sodium Concentration

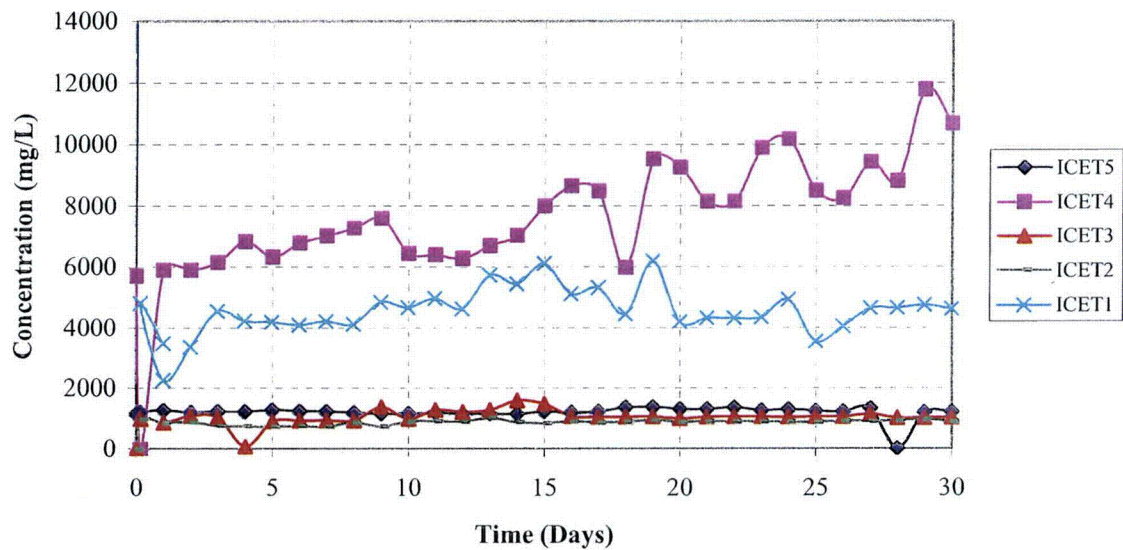


Figure 4-16. ICET unfiltered sodium concentration.

#### 4.1.2. Precipitates

White precipitates were observed in Tests #1 and #5 test solution samples as the solutions cooled to room temperature. No precipitates were observed at 60°C. In Test #1, visual precipitates formed early in the test upon cooling and the quantity increased over the course of the test. In Test #5, the precipitates took longer to form (several days), and the quantities were much smaller than in Test #1. In addition, the quantity of Test #5 precipitates was relatively unchanged throughout the test. ICP-AES analyses were performed to characterize the precipitates from both tests. Because of the larger precipitate formation observed in Test #1, additional analyses were performed in an effort to characterize the precipitate.

ICP-AES analysis was performed to determine the elemental compositions of the precipitates observed in Test #1. Samples from Day 7 and Day 29 were analyzed (Table 4-2). The precipitates were isolated by centrifuge and then thoroughly rinsed with RO water. The ICP-AES results indicated that the precipitate was composed largely of aluminum and boron. Calcium and sodium were also present in smaller amounts. Note that ICP analysis cannot detect the presence of either oxygen or hydrogen in materials. Laboratory tests were performed to produce a surrogate precipitate by titrating aluminum nitrate solution into a pH-9.5 solution containing 2800 mg/L boron and sodium hydroxide at 25°C. Nuclear magnetic resonance analysis was performed on this surrogate precipitate, which indicated that a complexation between aluminum and boron occurred when the solution cooled below 40°C.

**Table 4-2. Composition of Precipitates from Test #1**

Element	11/28 (Day 7) Precipitate (mg/kg)	12/20 (Day 29) Precipitate (mg/kg)
Al	219,000	220,000
B	84,200	245,000
Ca	23,300	8340
Cu	755	232
Mg	N/D <sup>a</sup>	N/D <sup>a</sup>
Silica	1740	7360
Zn	373	41
Na	23,200	55,300

<sup>a</sup>N/D = Not detected

Test #5 precipitates from Days 7 and 29 were also collected and taken for ICP-AES analysis. As shown in Table 4-3, the precipitate was largely composed of aluminum and boron, with smaller amounts of sodium and calcium.

**Table 4-3. Composition of Precipitates from Test #5**

Element	08/02 (Day 7) Precipitate (mg/kg)	08/24 (Day 29) Precipitate (mg/kg)
Al	143,000	122,000
B	119,000	125,000
Ca	43,200	42,000
Cu	1,790	944
Mg	N/D <sup>a</sup>	712
Silica	2,120	780
Zn	551	112
Na	25,200	20,500

<sup>a</sup>N/D = Not detected

When comparing the precipitates from Tests #1 and #5 (Table 4-4), it is seen that both have similar chemical compositions. Test #1 precipitate had a larger concentration of aluminum than in Test #5. Test #5 precipitate had a larger concentration of calcium. These results are supported by the relative amounts of aluminum and calcium in solution (Figures 4-10 and 4-11).

**Table 4-4. Distribution of Main Elemental Components of Precipitates from Tests #1 and #5**

Precipitate Sample	Al (%)	B (%)	Ca (%)	Na (%)	Other
<b>Test #1</b>					
11/28 (Day 7)	62	24	7	7	0
12/20 (Day 29)	41	46	2	10	1
Average	51	35	5	8	0.5
<b>Test #5</b>					
08/02 (Day 7)	43	36	13	8	0
08/24 (Day 29)	39	40	13	7	0
Average	41	38	13	8	0

Larger amounts of precipitate were obtained from Test #1, which allowed for more analyses. X-ray fluorescence (XRF) was another procedure used to determine the elemental composition of the precipitates from Test #1, and the results are available in the Test #1 data report (Ref. 2). The results indicated that the Test #1 precipitates were mainly composed of Na, Al, Ca, and Si. The accuracy of the results depends on how closely the comparative standards resemble the sample. Also, the sensitivity of XRF decreases with decreasing atomic weight, so it is normally difficult to identify an element with an atomic number that is less than that of carbon. Since boron cannot be detected by XRF, the elemental composition obtained from this procedure was in agreement with that obtained from the ICP-AES analysis.

ICP-AES and XRF analyses provided an elemental composition of the Test #1 precipitate, but did not offer any information about the structure. Analytical procedures, which include TEM and x-ray diffraction (XRD) analyses, were used to aid with further characterization of the precipitate obtained from Test #1 (Ref. 2). These procedures were mainly used to determine whether the solids physical structure was more consistent with microcrystalline flocculent or with amorphous hydrated gels. Upon examination of the results, it is likely that the precipitate was amorphous in nature.

## **4.2. Insulation**

In this section, post-test examinations of fiberglass (Section 4.2.1) and cal-sil (Section 4.2.2) are presented.

### **4.2.1. Fiberglass**

Fiberglass insulation was present in the tank in each test. In the fiberglass-only tests (Tests #1, #2, and #5) there was 4.58 ft<sup>3</sup> of shredded fiberglass in the tank. In Tests #3 and #4, there was 80% of that amount in the tank. In all of the tests, 75% of the fiberglass was submerged. Most of the submerged fiberglass was bundled in 3-in.-thick bags (or blankets) of fiberglass confined in SS mesh to prevent ingestion through the pump and to better control the placement of fiberglass in various flow regimes. Those blankets rested on the tank bottom, away from the tank drain. Other fiberglass samples were designated by their placement in high-flow and low-flow regions of the tank. In high-flow regions, the smaller blankets were attached to the submerged coupon rack (Figure 2-4), and they were exposed to direct flow from the recirculation flow headers. Blankets in low-flow regions did not experience direct water flow. Additional 4-in.-square envelopes of fiberglass (Figure 2-4) were also prepared for extraction during the course of the test. These samples were referred to as "sacrificial" samples. One sample, called the "birdcage," was constructed so that the fiberglass within it was loose and not compacted. The birdcage fiberglass sat on the tank bottom and was removed on Day 30. Also, a cylindrical blanket of fiberglass was placed around the tank drain screen. The unsubmerged fiberglass was placed in blankets and attached to the ends of suspended coupon racks. Some amount of fiber, especially short-fiber fragments, escaped the mesh bags and was deposited in other locations within the tank. This material was referred to as "fugitive" fiberglass.

An SEM image of clean fiberglass, before exposure to the test solution, is shown in Figure 4-17. This SEM image provides a visual baseline as a comparison for images from samples taken after the tests began. As can be seen, there are no deposits on the clean fiberglass. Over the course of each test, deposits were observed throughout the fiberglass samples. These deposits could be of chemical origin (i.e., solids that formed at the surface of the fiberglass because of chemical reactions between soluble chemical species and the fiberglass or because of precipitation of soluble species at that location) or physically retained or attached (i.e., deposits that existed as solid particles in the test solution and were captured by the fiberglass). Because there was not significant water flow through the fiber, particle migration into the fiberglass interior was not likely; however, physical retention and attachment of particles at the exterior of fiberglass were possible. Therefore, deposits found in the interior of the fiberglass samples were likely of chemical origin, whereas the deposits on the exterior could have been of either origin.



**Figure 4-17. Clean fiberglass before exposure to test chemicals.**

The amount of deposits varied between tests because of the differences in the chemical conditions. In some tests (Tests #1, #2, and #5), fiberglass was the only insulation material present, whereas in the other tests (Tests #3 and #4), the insulation present was a mixture of 20% fiberglass and 80% cal-sil (by volume). In addition, the chemicals used and the test pH varied between tests. The pertinent test conditions, insulation type, relative amounts of deposits in each test, and likely sources of deposits are summarized in Table 4-5. In addition to differences between tests, a time dependence of the deposits was observed, with the amount of deposits increasing as each test proceeded. Test #5 was an exception, where time dependence of the deposits was insignificant. Furthermore, differences between fiberglass sample locations within the tank were observed; the general trend was that the amount of deposits was greatest on the drain collar's outside exterior (farthest from the drain screen), followed by the drain collar's inside exterior (next to the drain screen), followed by the birdcage exterior, and then followed by

the high-flow fiberglass exterior. Descriptions of the deposits observed in each test are detailed in the following sections.

**Table 4-5. Relative Amounts of Particle Deposits in Fiberglass**

Test	pH and Chemicals <sup>a</sup>	Insulation	Likely Sources
1	pH = 9.3 to 9.5 H <sub>3</sub> BO <sub>3</sub> = 2,800 mg/L NaOH = 8,021 mg/L	100% fiberglass	High pH caused severe corrosion on aluminum. Corrosion products then precipitated on the fiberglass.
2	pH = 7.1 to 7.4 H <sub>3</sub> BO <sub>3</sub> = 2,800 mg/L TSP = 4,000 mg/L	100% fiberglass	Low pH caused less corrosion; however, TSP may have formed precipitates.
3	pH = 7.3 to 8.1 H <sub>3</sub> BO <sub>3</sub> = 2,800 mg/L TSP = 4,000 mg/L	20% fiberglass 80% cal-sil	TSP reacted with calcium from the cal-sil and formed calcium phosphate precipitates. In addition, flowing water suspended some of the cal-sil debris, which then deposited on the fiberglass. Cal-sil deposits were observed on the exterior surface and the amount of deposits was more than in Tests #1 and #2.
4	pH = 9.5 to 9.9 H <sub>3</sub> BO <sub>3</sub> = 2,800 mg/L NaOH = 8,951 mg/L	20% fiberglass 80% cal-sil	Cal-sil debris was suspended by the flowing water and deposited on the fiberglass. Corrosion was lower, possibly because of passivation of the metal coupon surfaces by silicate that originated from the cal-sil. Cal-sil deposits were observed on the exterior surface, and the amount of deposits was more than in Tests #1 and #2.
5	pH = 8.2 to 8.5 H <sub>3</sub> BO <sub>3</sub> = 6,848 mg/L Borax = 10,568 mg/L	100% fiberglass	Low corrosion and insignificant chemical precipitation. The amount of deposits was less than in Tests #1 and #2.

<sup>a</sup>H<sub>3</sub>BO<sub>3</sub> is reported in milligrams per liter as boron, TSP is reported in milligrams per liter as Na<sub>3</sub>PO<sub>4</sub>·12H<sub>2</sub>O, borax is reported in milligrams per liter as Na<sub>2</sub>B<sub>4</sub>O<sub>7</sub>·10H<sub>2</sub>O. Additional chemicals were present in the test solution (see Table A-4).

### Test #1

In Test #1, the most significant deposits observed on the fiberglass were thin crusts, as shown in Figure 4-18, and sheets of film (i.e., webbing) that stretched between multiple fibers, as shown in Figures 4-19 and 4-20. In these SEM images, it is important to note that all samples were partially or thoroughly desiccated before examination, which may have contributed to the cracking of the webbing shown in Figure 4-19. The EDS analysis shown in Figure 4-21 indicates that the thin crusts were composed primarily of sodium, aluminum, silicon, and oxygen, whereas the webbing was primarily composed of sodium, boron, and oxygen, as shown in Figure 4-22.

Lab diagnostic tests revealed that the webbing material was likely an artifact of the sampling and analysis procedure and may not have existed when the fiberglass was submerged in the tank. On removal from the tank, the fiberglass was wet with the tank solution, and it appears that the webbing formed as the tank solution evaporated. A sample of clean fiberglass dipped momentarily in the ICET Test #1 solution and allowed to dry exhibited similar webbing, as shown in Figure 4-23. Moreover, the EDS analysis of this webbing (shown in Figure 4-24) indicated that the webbing produced in bench-top experiments exhibited elemental composition similar to the webbing observed in the Test #1 fiberglass (the silicon peak is likely from the fiberglass in the background of the webbing). This webbing was not observed when a sample of clean fiberglass was dipped momentarily in the ICET Test #1 solution, rinsed gently with RO water, and allowed to dry, as shown in Figure 4-25, thus demonstrating that the residual liquid on the surface of the fiberglass was responsible for film formation and that the webbing was actually soluble. Additional diagnostic tests indicated that sodium hydroxide did not contribute to the formation of webbing material (see Figure 4-26). However, a sodium borate solution at pH 9.5 did result in webbing on the fiberglass (see Figures 4-27 and 4-28). The elemental composition of the webbing after it was dipped in sodium borate, as shown in Figure 4-29 was consistent with the elemental composition after it was dipped in the ICET Test #1 solution (see Figure 4-24).

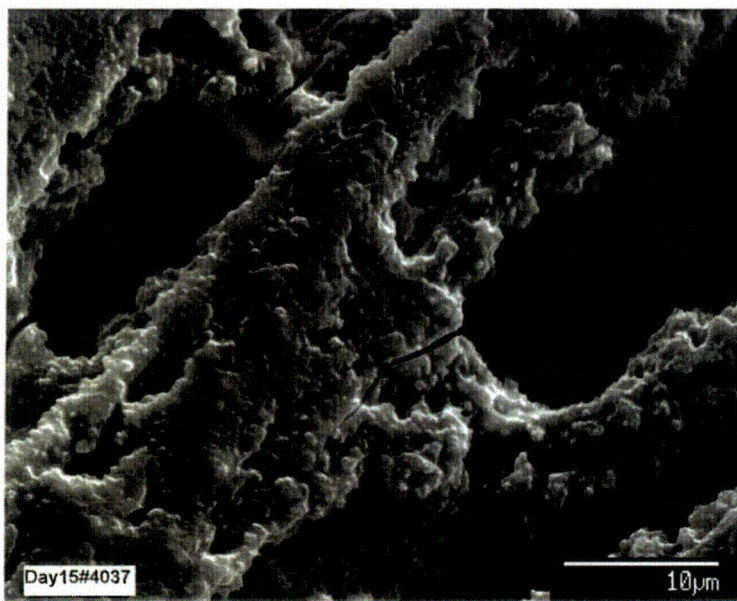


Figure 4-18. Day 15, sample #4 SEM image (#4037), magnified 2500 times; BSE close-up.

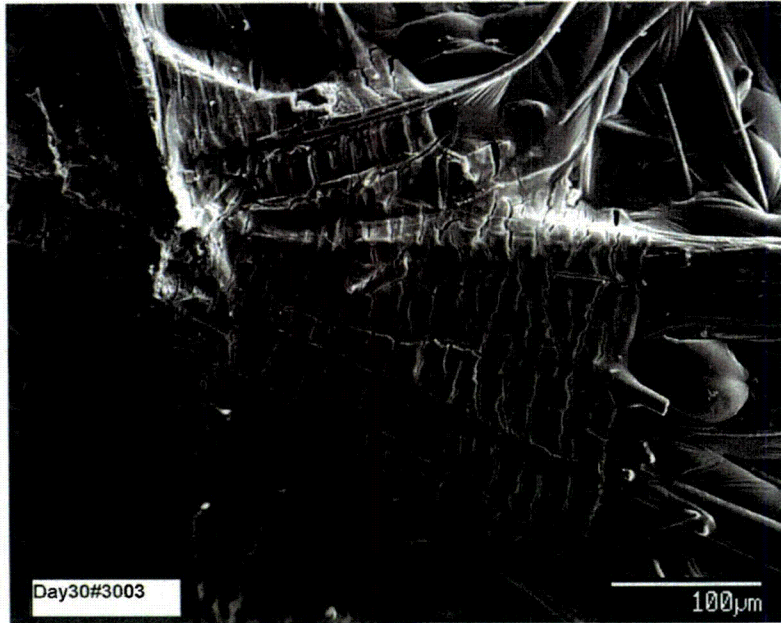


Figure 4-19. Day 30, sample #3 SEM image (#3003), magnified 250 times, of the fiberglass with surface coating.

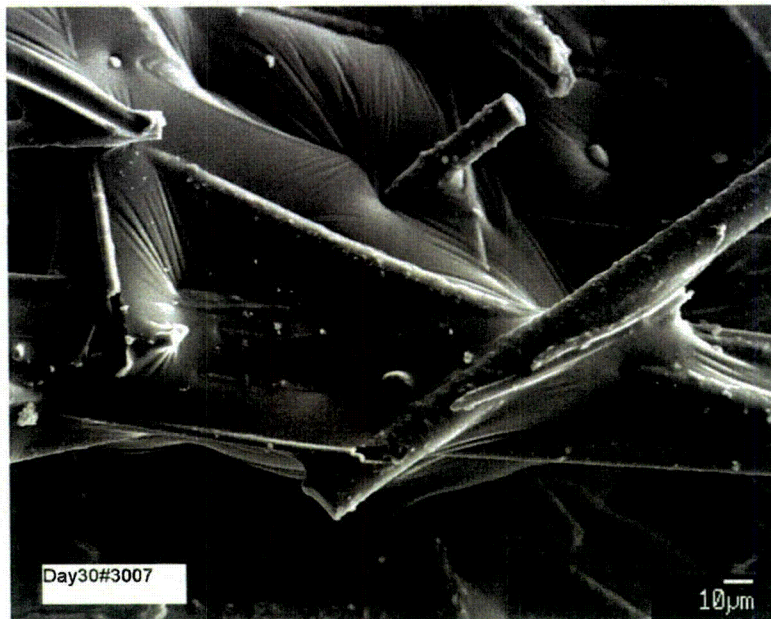


Figure 4-20. Day 30, sample #3 SEM image (#3007), magnified 500 times, of the film across the fibers.

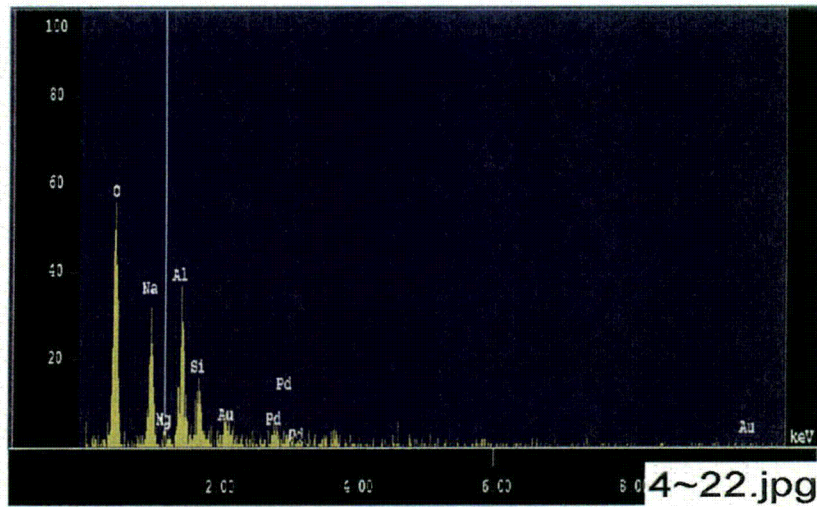


Figure 4-21. Day 15, sample #4 counting spectrum (EDS 4-22) for the crust on the fiberglass, as shown in Figure 4-18.

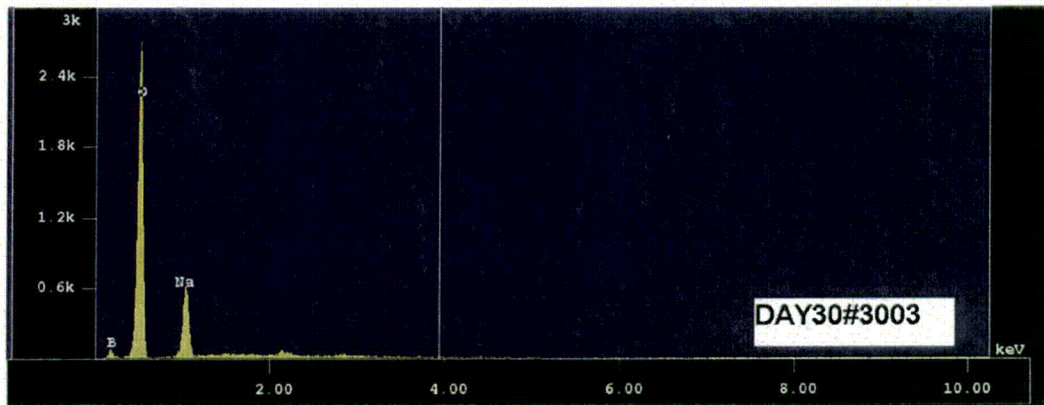


Figure 4-22. Day 30, sample #3 counting spectrum (EDS #3003) of the fractured coating, as shown in Figure 4-19.



Figure 4-23. ESEM image, magnified 100 times, of raw fiberglass dipped in ICET Test #1 solution. (rfbt105.tif, 7/28/05)

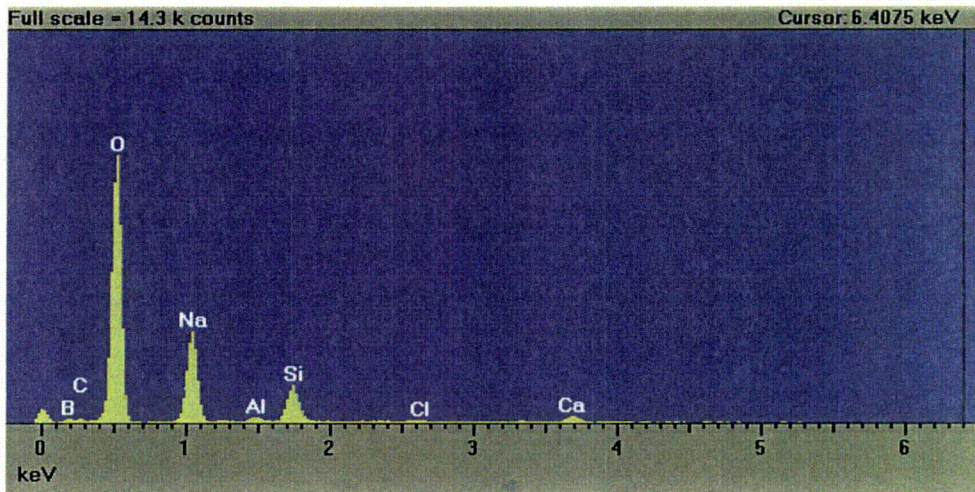


Figure 4-24. EDS counting spectrum for the film on fiberglass, as shown in Figure 4-23. (rfbt106.tif, 7/28/05)

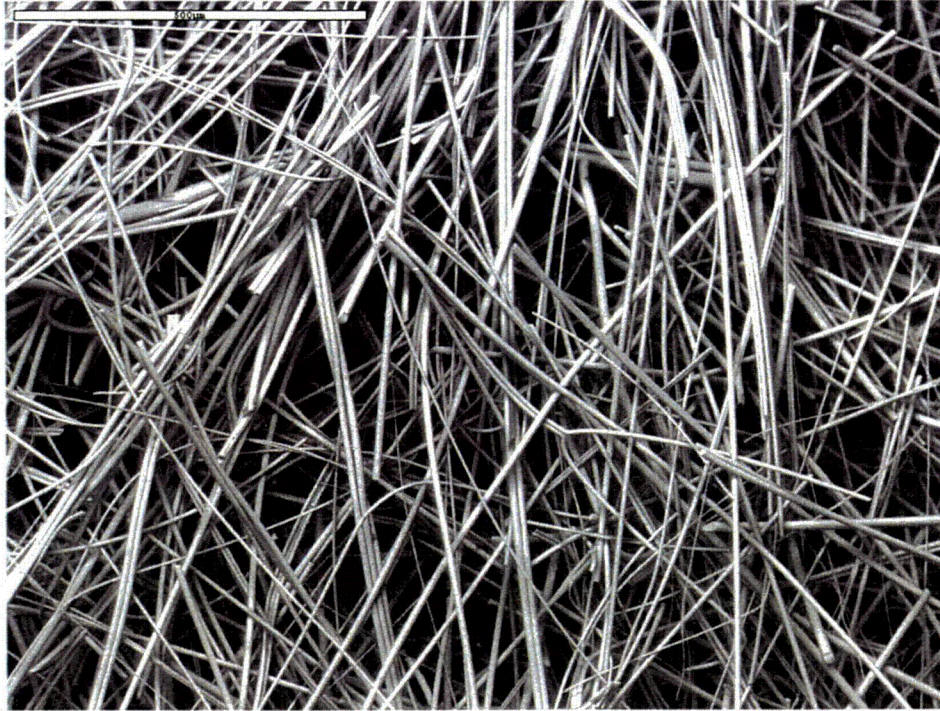


Figure 4-25. ESEM image, magnified 100 times, of raw fiberglass dipped in ICET Test #1 solution and then washed with RO water. (Difbrg15.tif, 8/3/05)



Figure 4-26. ESEM image, magnified 100 times, of raw fiberglass dipped in NaOH solution at pH 9.5. (OHFbrg07.tif, 8/3/05)



Figure 4-27. ESEM image, magnified 100 times, of raw fiberglass dipped in the solution containing 2800 mg/L boron and NaOH at pH 9.5. (Bofbrg09.tif, 8/3/05)

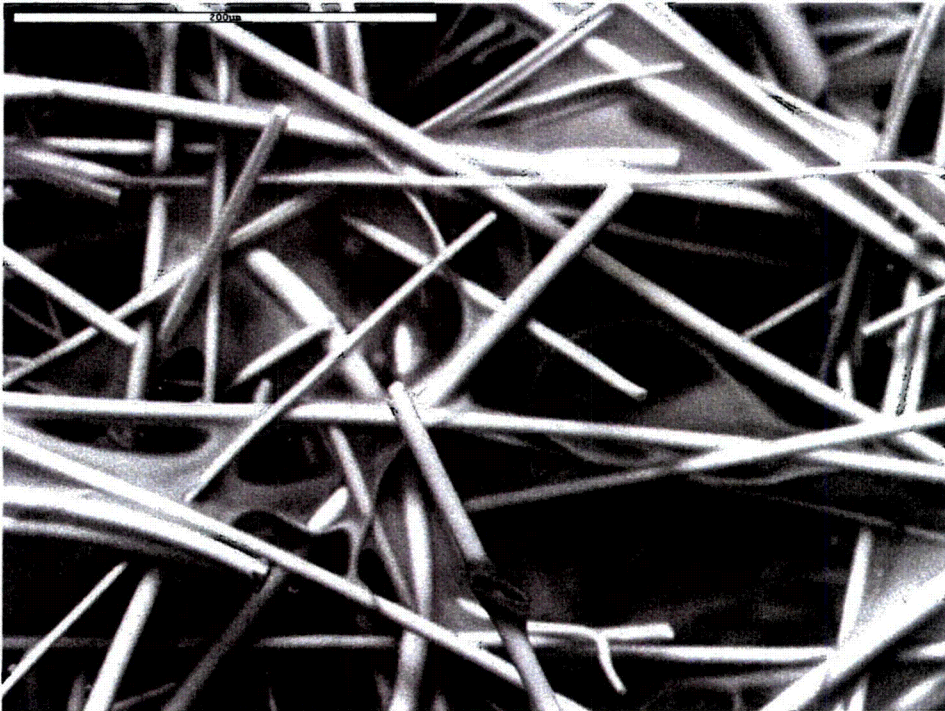


Figure 4-28. ESEM image, magnified 300 times, of raw fiberglass dipped in the solution containing 2800 mg/L boron and NaOH at pH 9.5. (rfgbn03.tif, 8/5/05)

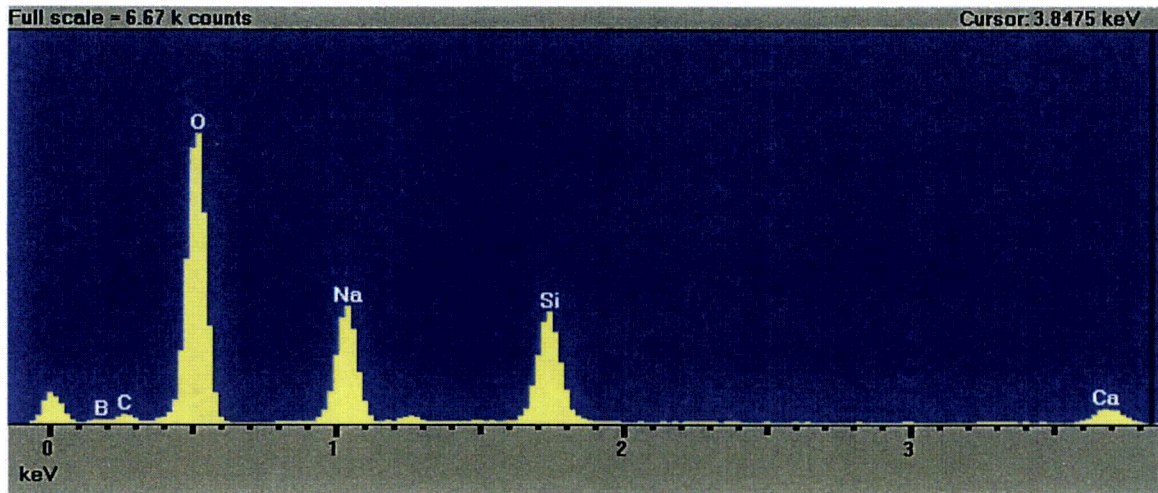


Figure 4-29. EDS counting spectrum for the film on fiberglass, as shown in Figure 4-28. (rfgbn05.tif, 8/5/05)

### Test #2

Fiberglass samples from four locations in the tank were examined in Test #2, including the low-flow area, high-flow area, birdcage, and drain collar. Both the interior and exterior regions of the fiberglass samples were examined in each location. In general, the amount of deposits increased as the test proceeded. Figures 4-30 through 4-33 show deposits in the interior and exterior regions of the high-flow, Day-30 fiberglass samples. The figures show that the deposits were pervasive throughout the fiberglass. However, the particulate deposits were more significant in the exterior fiberglass samples, whereas flocculent deposits were more prevalent in the interior fiberglass samples. When the probe SEM results were compared with the ESEM results, more significant flocculent deposits were found with probe SEM analysis (compare Figures 4-33 and 4-34, which are at approximately the same magnification), especially for the interior fiberglass samples. The possible reason is that ESEM samples were moist compared with the dry-probe SEM samples during the examination process, and the drying process may have caused the formation of the flocculent deposits, i.e., chemical precipitation. However, it is also possible that the flocculent deposits are chemical byproducts formed during the test. In addition, the EDS results from Figure 4-35 indicate numerous elemental constituents in these deposits, including oxygen, sodium, aluminum, phosphorus, calcium, and possibly silicon. These elements likely originated from the metal and concrete coupons, fiberglass, and testing solution.

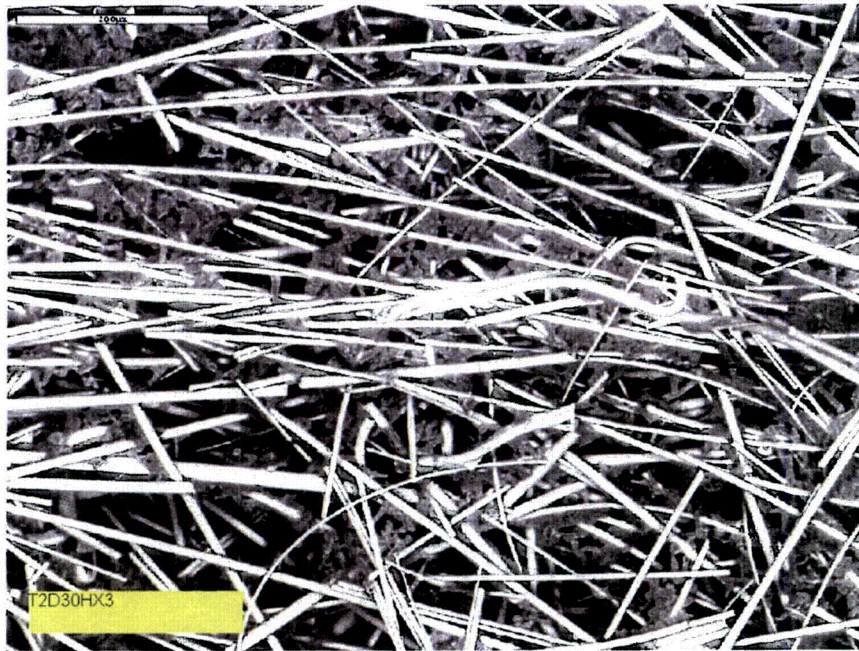


Figure 4-30. ESEM image for a Test #2, Day 30, high-flow exterior fiberglass sample.

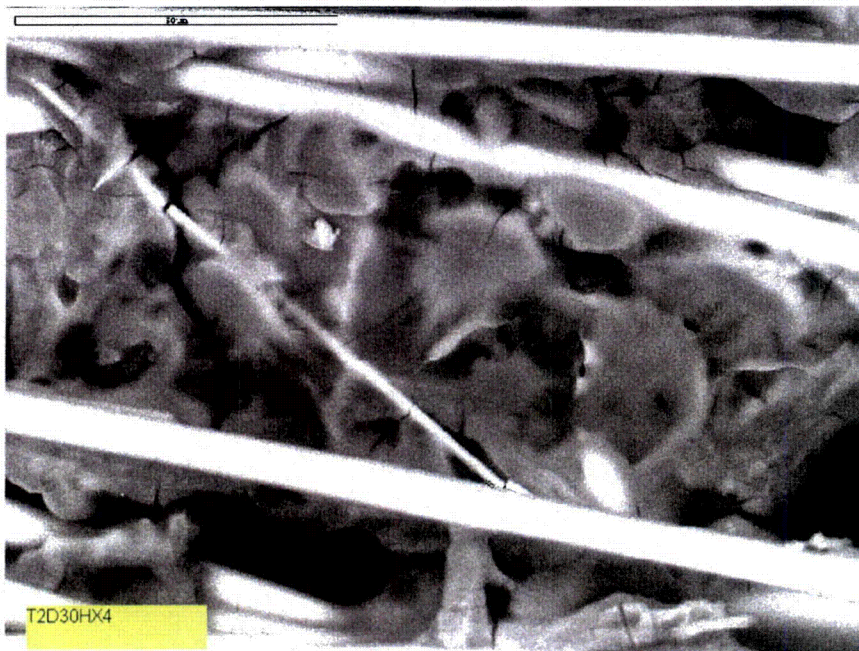


Figure 4-31. Higher-magnification ESEM image of a Test #2, Day 30, high-flow exterior fiberglass sample.

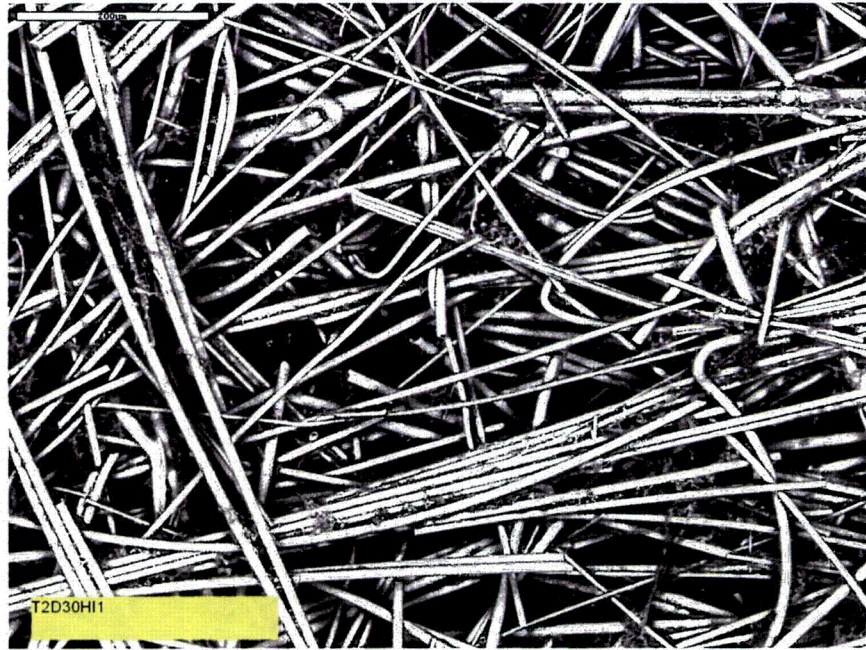


Figure 4-32. ESEM image for a Test #2, Day 30, high-flow interior fiberglass sample.

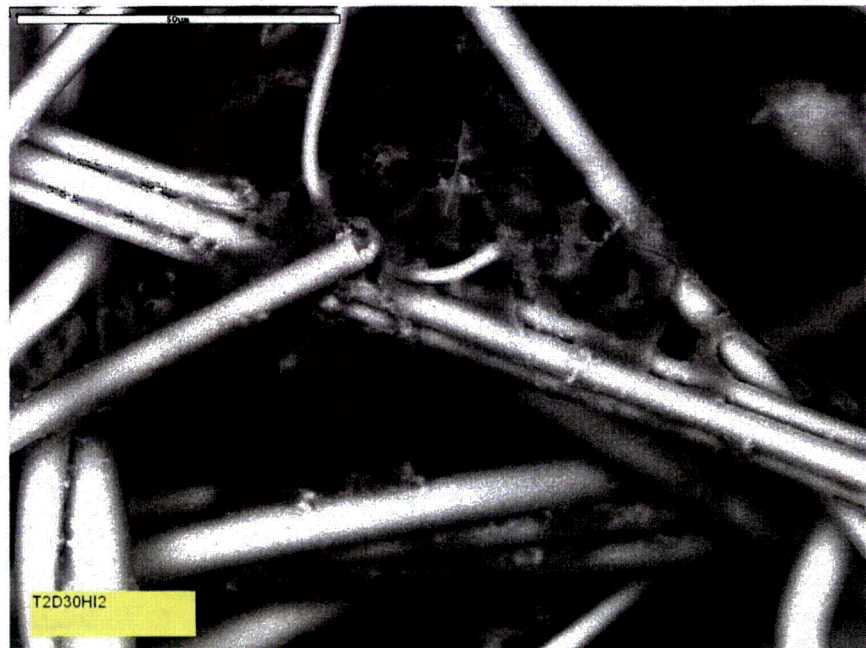


Figure 4-33. Higher-magnification ESEM image of a Test #2, Day 30, high-flow interior fiberglass sample.



Figure 4-34. Probe SEM image at 1000× magnification for a Test #2, Day 30, high-flow interior fiberglass sample. (T2D30\_HiFlo023)

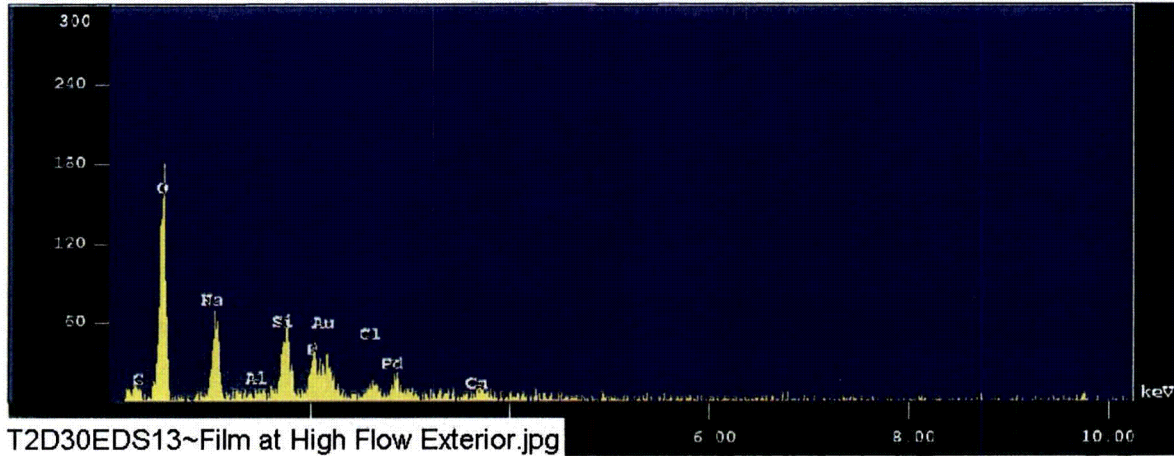


Figure 4-35. EDS counting spectrum for the deposits on a high-flow exterior fiberglass sample.

### Test #3

Tests #3 and Test #4 each had much greater amounts of deposits than Tests #1, #2, and #5. In addition, the amount of deposits increased as the test proceeded. The greatest amount of deposits was found on the exteriors of the Day-30 samples, as shown in Figure 4-36. The corresponding EDS is shown in Figure 4-37. Based on EDS analysis, the particulate deposits on the fiberglass exterior may be divided into two categories according to phosphorus and silicon content, as shown in Figures 4-38 and 4-39. Particulate deposits of lower phosphorus and higher silicon content were likely cal-sil particles. The particulate deposits with lower silicon and high phosphorus, calcium, and oxygen content were likely composed of calcium phosphate precipitates, and it is compositionally similar to the white gel found on the tank bottom at the end of the test. It is likely that calcium and phosphate precipitated when dissolved calcium from the cal-sil reacted with phosphate from the TSP. After precipitation, the calcium phosphate precipitates were transported to the fiberglass exterior by sedimentation and/or water flow depending on the location of the fiberglass sample within the tank. Both kinds of deposits (cal-sil and calcium phosphate precipitates) may be physically transported and/or deposited onto the fiberglass sample exterior in this manner.

In contrast to the exterior regions of the fiberglass, the interior fiberglass samples were relatively pristine, as shown in Figures 4-40 and 4-41. These results suggest that almost all of the particulate deposits were physically retained at the fiberglass exterior. Any deposits observed in the fiberglass interior likely were chemical byproducts in the test or formed by chemical precipitation during the sample-drying process for ESEM/SEM analysis (see Figure 4-42). EDS analysis indicates that the deposits in Figure 4-42 contained insignificant amounts of phosphorus (see Figure 4-43), meaning that the deposits were distinct from the white gel found in this test.



Figure 4-36. ESEM image of a Test #3, Day 30, exterior high-flow fiberglass sample, magnified 100 times. (t3hifx33, 5/11/05)

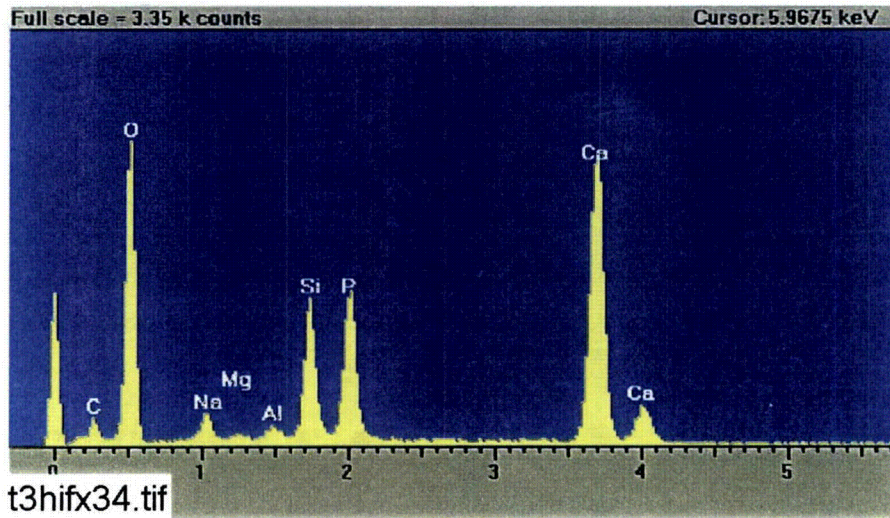


Figure 4-37. EDS counting spectrum for the large masses of particulate deposits shown in Figure 4-36. (t3hifx34, 5/11/05)

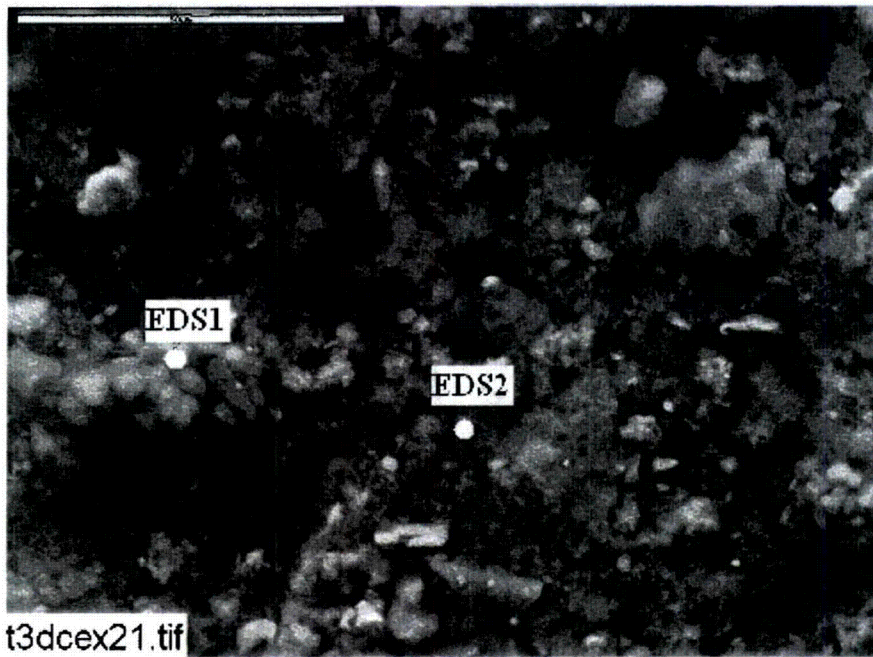


Figure 4-38. ESEM image of a Test #3, Day 30, exterior fiberglass sample on the drain collar (away from the drain screen), magnified 1000 times. (t3dcex21, 5/6/05)

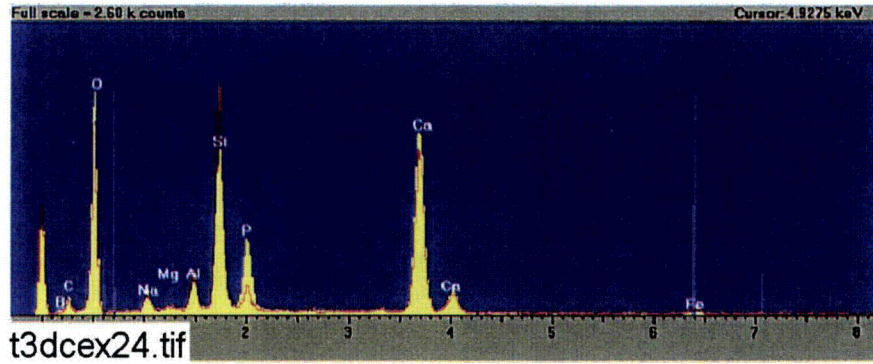


Figure 4-39. Comparison of EDS counting spectra between the light particle (EDS1, yellow) and the dark particle (EDS2, red) shown in Figure 4-38. (t3dcex24, 5/6/05)

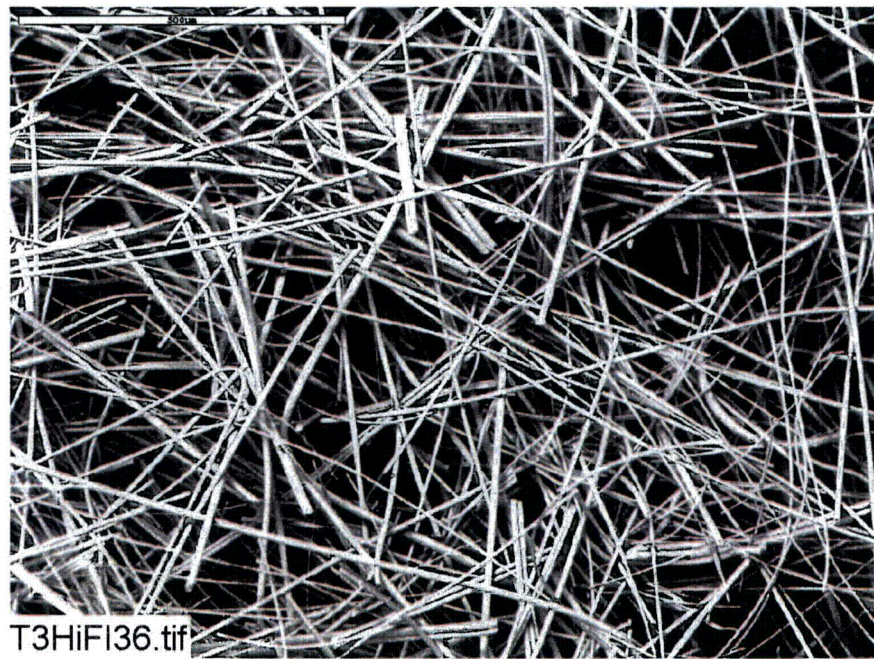


Figure 4-40. ESEM image of a Test #3, Day 30, interior high-flow fiberglass sample, magnified 100 times. (T3HiF136, 5/11/05)

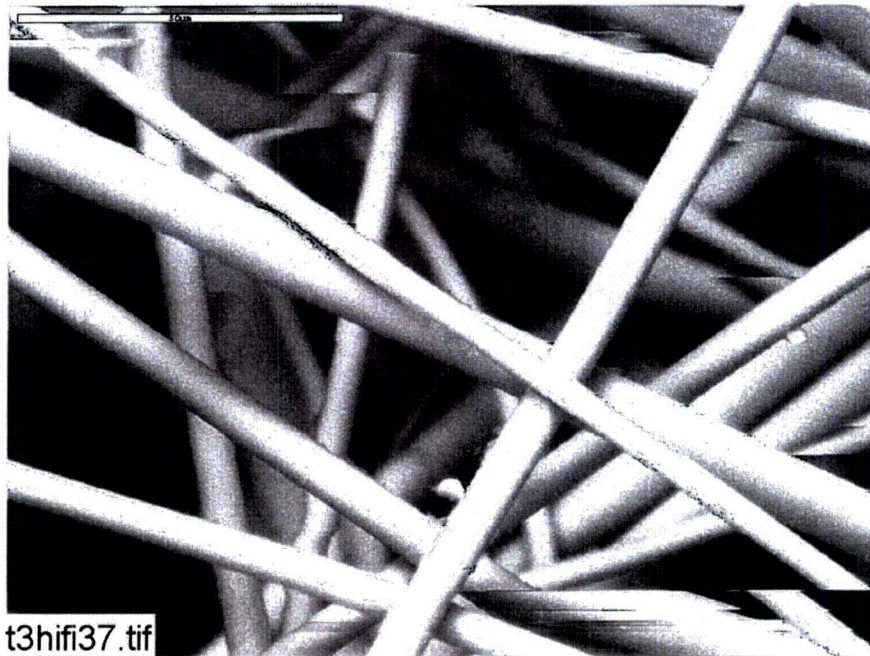


Figure 4-41. ESEM image of a Test #3, Day 30, interior high-flow fiberglass sample, magnified 1000 times. (t3hifi37, 5/11/05)



Figure 4-42. ESEM image of a Test #3, Day 15, high-flow interior fiberglass sample, magnified 2000 times. (T3D15HI3, 4/22/05)

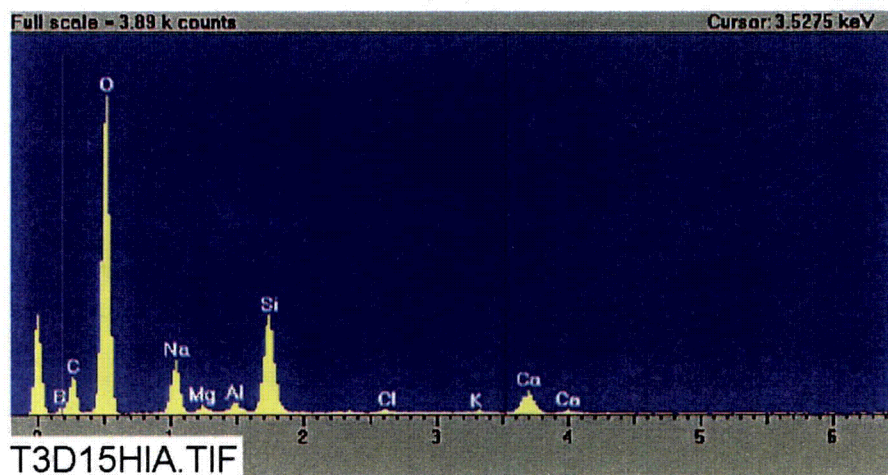


Figure 4-43. EDS counting spectrum for the flocculent deposits between the fibers on the ESEM image shown in Figure 4-42. (T3D15HIA, 4/22/05)

#### Test #4

The Test #4 fiberglass contained a large number of deposits, similar to Test #3. In Test #4, particulate deposits generally were found only on the exterior of the fiberglass, as shown in Figures 4-44, 4-45, 4-46, and 4-47. EDS analyses, as shown in Figure 4-48, indicate that these particulate deposits contain significant amounts of silicon and calcium, suggesting that they are from cal-sil debris. In contrast, the interior of fiberglass samples was relatively pristine, as shown in Figures 4-49 and 4-50. Only film deposits were observed. These deposits were likely formed by chemical precipitation when the samples were dehydrated. To investigate the formation of the film deposits, controlled experiments were performed by gently rinsing the interior fiberglass samples with several drops of RO water before an ESEM analysis was performed. Figures 4-51 and 4-52 show that after being rinsed with RO water, the film deposits disappeared from the fiberglass samples. These results suggest that the film is actually soluble, which is consistent with the explanation that the film was formed by chemical precipitation during the drying process of the fiberglass. In other words, although the ESEM analysis maintains samples in a moister state than does conventional SEM, the partial drying that took place during ESEM analysis was sufficient for some chemicals to precipitate and form the film deposits that were observed. This is consistent with the results obtained from the Test #1 flocculent deposits, which were presented earlier.



**Figure 4-44.** ESEM image, magnified 100 times, of a Test #4, Day 30, exterior high-flow fiberglass sample. (T4HFEx01.jpeg)



**Figure 4-45.** ESEM image, magnified 500 times, of a Test #4, Day 30, exterior high-flow fiberglass sample. (t4hfex07.jpg)

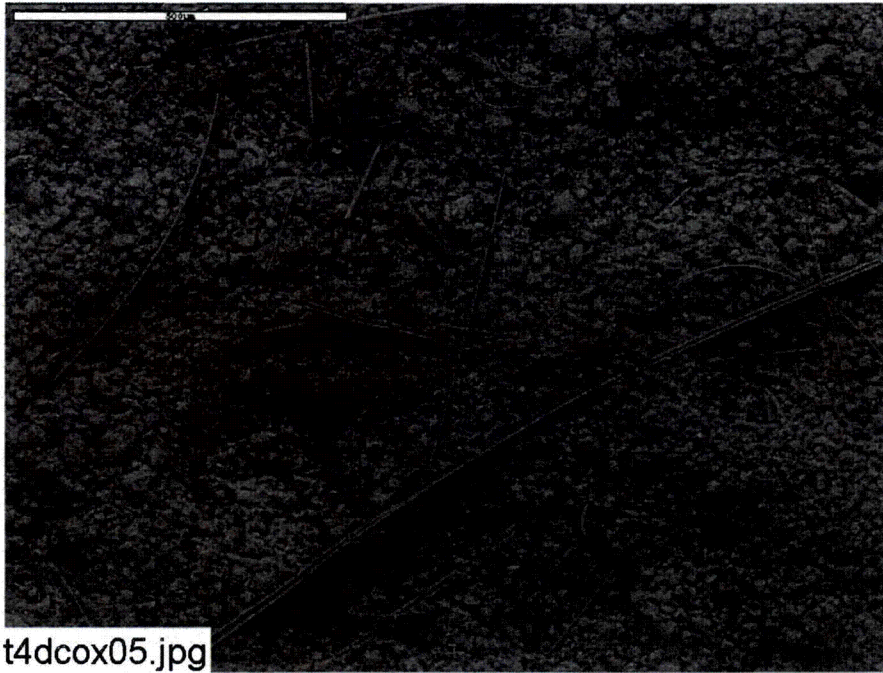


Figure 4-46. ESEM image, magnified 100 times, of a Test #4, Day 30, exterior fiberglass sample on the drain collar (away from the drain screen). (t4dcox05.jpg)

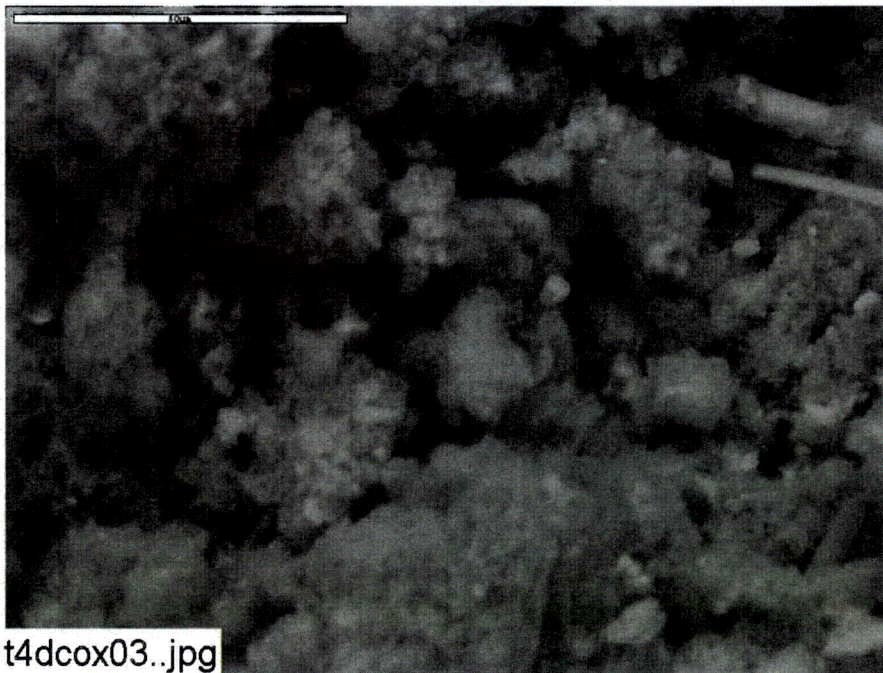


Figure 4-47. ESEM image, magnified 1000 times, of a Test #4, Day 30, exterior fiberglass sample on the drain collar (away from the drain screen). (t4dcox03.jpg)

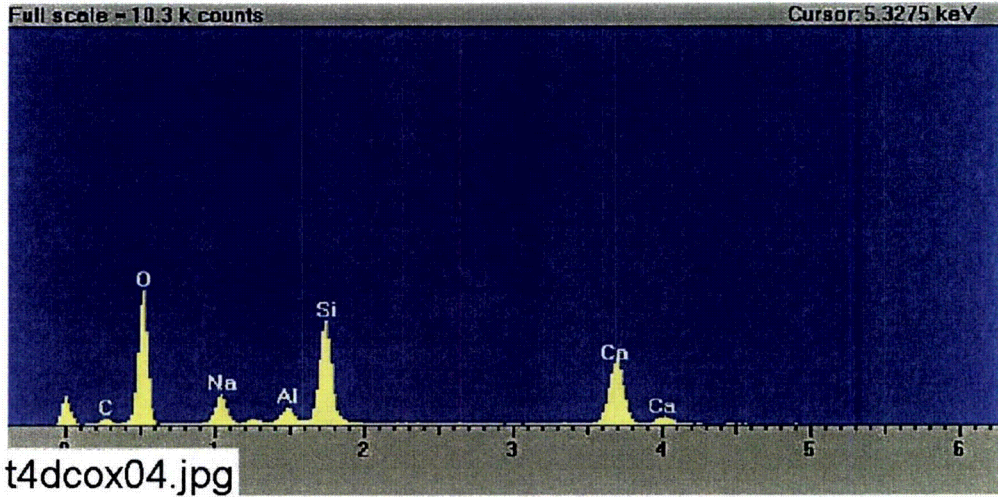


Figure 4-48. EDS counting spectrum for the large mass of particulate deposits on fiberglass shown in Figure 4-47. (t4dcox04.jpg)

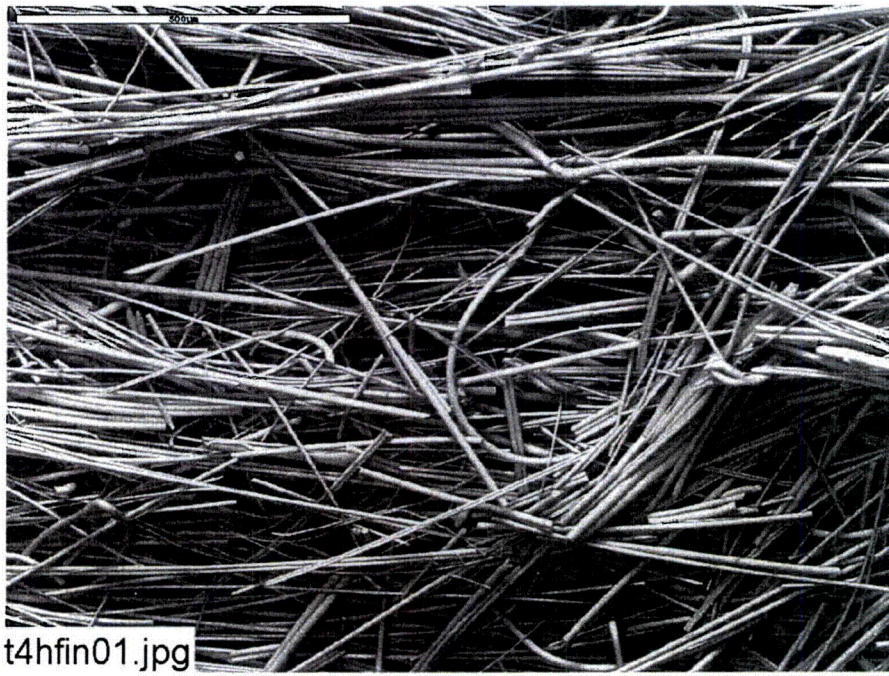
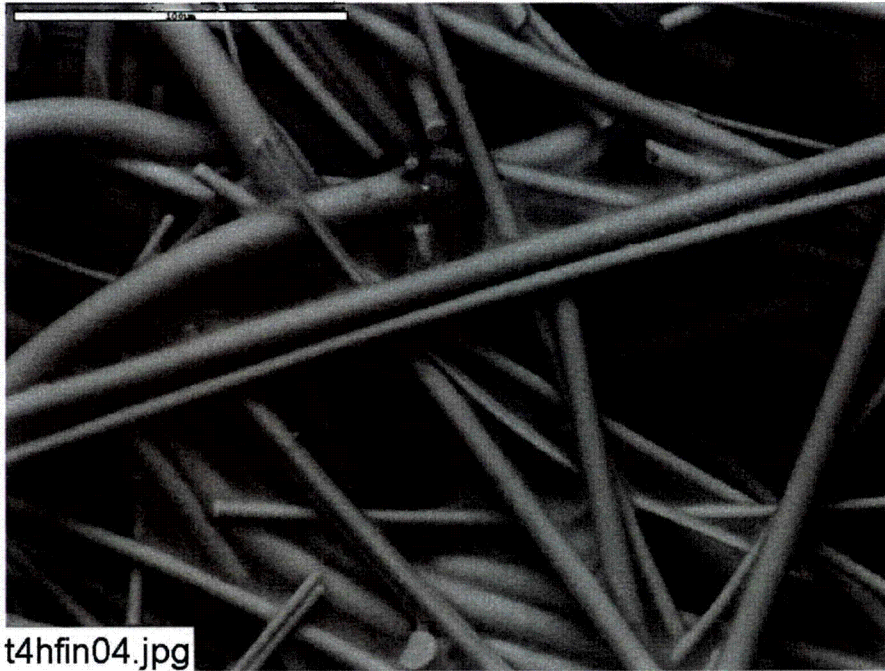
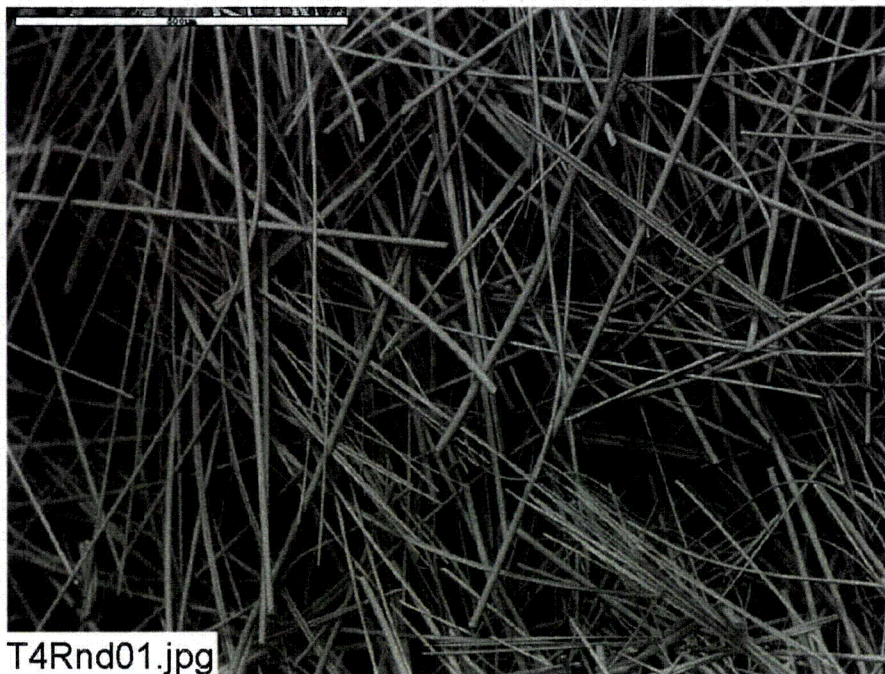


Figure 4-49. ESEM image, magnified 100 times, of a Test #4, Day 30, interior high-flow fiberglass sample. (t4hfin01.jpg)



**Figure 4-50.** ESEM image, magnified 500 times, for a Test #4, Day 30, interior high-flow fiberglass sample. (t4hfin04.jpg)



**Figure 4-51.** ESEM image, magnified 100 times, of a Test #4, Day 30, interior high-flow fiberglass sample. The sample was gently pre-rinsed with RO water. (T4Rnd01.jpg)

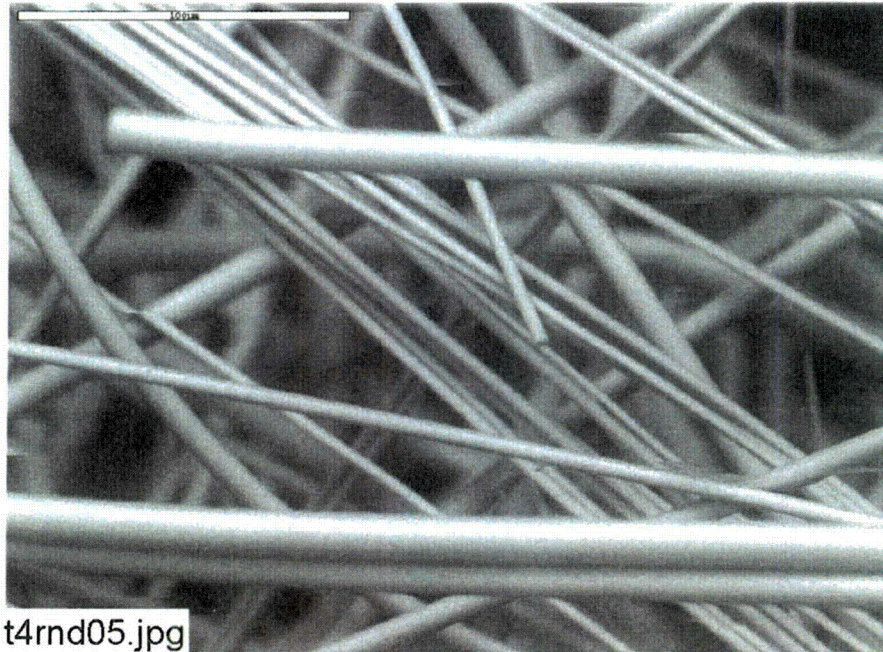


**Figure 4-52.** ESEM image, magnified 500 times, for a Test #4, Day 30, interior high-flow fiberglass sample. The sample was gently pre-rinsed with RO water. (t4rnd05.jpg)

#### Test #5

ICET Test #5 had the smallest amount of deposits in the fiberglass of any of the ICET tests. Day-30, high-flow fiberglass exterior samples are shown in Figures 4-53 and 4-54. The samples were relatively pristine, and they had the fewest particulate deposits. Similarly, interior samples shown in Figures 4-55, 4-56, and 4-57 were also relatively pristine. Only flocculent deposits were observed. The lack of deposits is likely because the smallest amount (compared to the other tests) of chemicals were added to the test solution. The flocculent deposits in the fiberglass interior were composed primarily of oxygen, sodium, calcium, magnesium, aluminum, and possibly silicon, as shown in Figure 4-58. These deposits likely were formed by chemical precipitation during dehydration of the samples, after the samples were removed from the tank, as demonstrated in the Test #4 results.



**Figure 4-53.** ESEM image, magnified 100 times, of a Test #5, Day 30, high-flow exterior fiberglass sample. (T5D30HX1.jpeg)

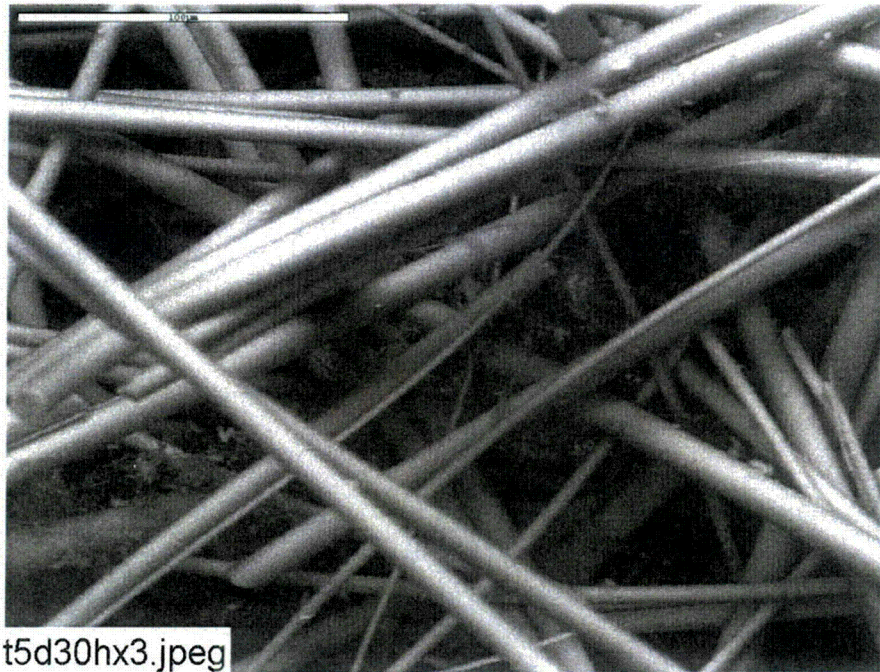


**Figure 4-54.** ESEM image, magnified 500 times, of a Test #5, Day 30, high-flow exterior fiberglass sample. (t5d30hx3.jpeg)



Figure 4-55. ESEM image, magnified 100 times, of a Test #5, Day 30, high-flow interior fiberglass sample. (T5D30HI4.jpg)

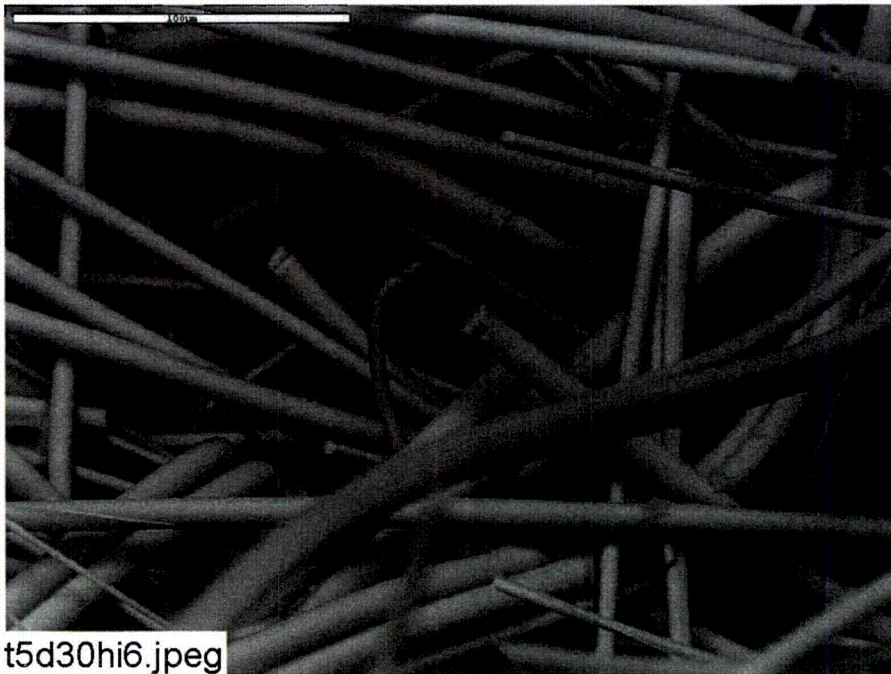


Figure 4-56. ESEM image, magnified 500 times, of a Test #5, Day 30, high-flow interior fiberglass sample. (t5d30hi6.jpg)

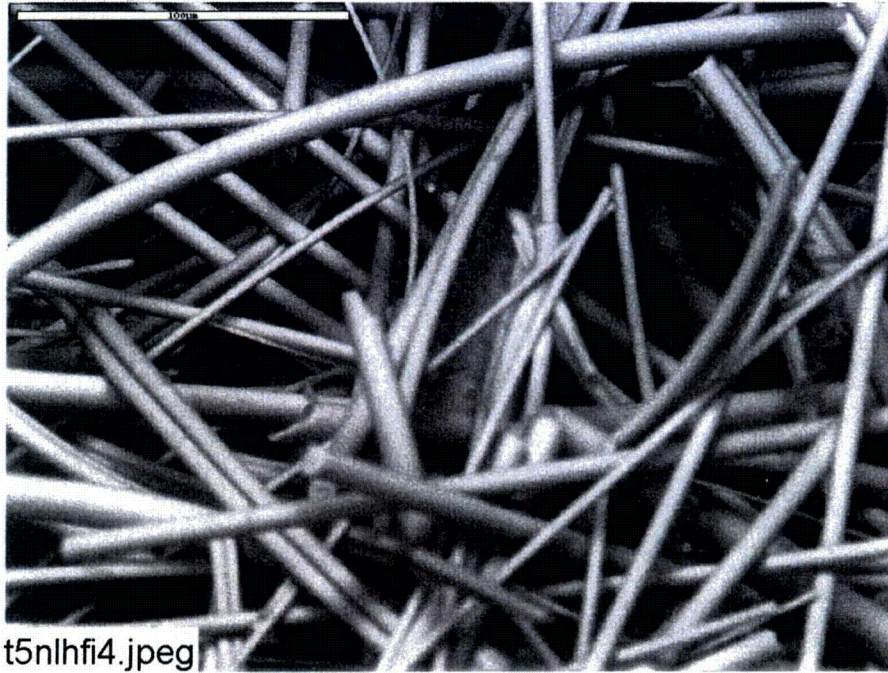


Figure 4-57. ESEM image, magnified 500 times, of a Test #5, Day 30 high-flow interior fiberglass sample in a nylon mesh.

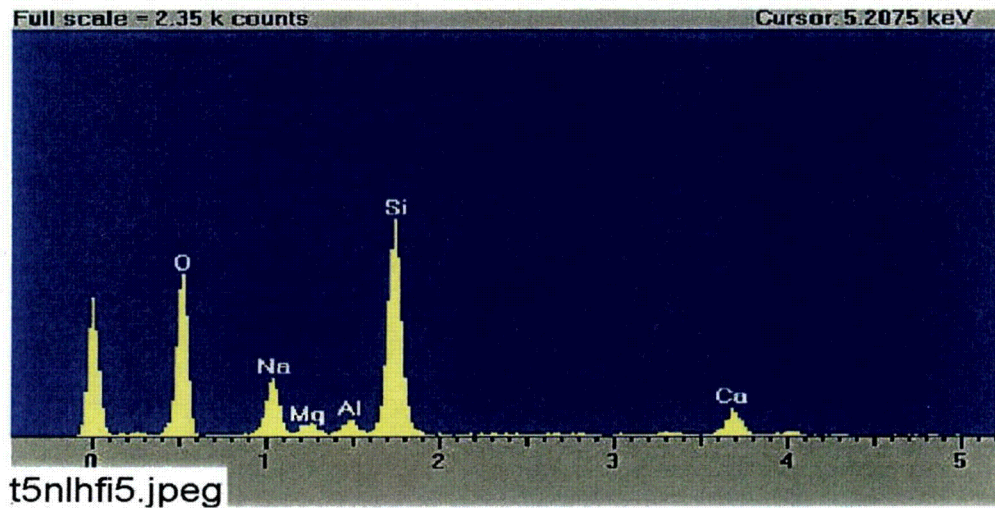


Figure 4-58. EDS counting spectrum for the deposits between the fibers shown in Figure 4-57.

#### 4.2.2. Cal-Sil

In ICET Tests #3 and #4, 80% of the fiberglass was replaced with cal-sil. The cal-sil was divided into 4 size categories, in pieces that were roughly cubes. Of the total cal-sil, 14% was over 3 in., 19% was 1–3 in., 5% was less than 1 in., and 62% was “dust.” The dust consisted of cal-sil pieces that were ground into a fine powder (Figure 2-6). With the exception of the dust, the cal-sil pieces were contained within SS mesh (Figure 2-5) and apportioned into submerged (75%

of the total) and unsubmerged (25% of the total) samples. The unsubmerged cal-sil was placed on the ends of suspended coupon racks. The dust was put into the tank solution before the test started.

The cal-sil released significant concentrations of calcium and silicate to the test solutions (see References 4 and 5). The released calcium and silicate may react with other chemical species in the test solutions, such as phosphate anions and aluminum cations. Because TSP was used in Test #3, a significant amount of phosphorus was found on the exterior of the submerged cal-sil samples in Test #3, in which phosphorus was likely present as calcium phosphate precipitate. However, almost no phosphorus was present in the interior of the submerged cal-sil. The result may be explained by the limited phosphate diffusion into the cal-sil interior. In Test #4, no phosphorus was found on the submerged cal-sil samples because TSP was not used. However, silicate released from cal-sil may have formed a passivation on the submerged aluminum coupon surface. As a result, the corrosion process was significantly decreased, as compared with Test #1 (see Section 4.4.3).

### **Unused Cal-Sil Samples**

As a base-line analysis, the unused unbaked and baked cal-sil samples were examined by SEM, XRD, and XRF. Figures 4-59 and 4-60 show the SEM images of unused unbaked and baked cal-sil, respectively. The amount of fiber in baked cal-sil appears to be less than in unbaked cal-sil, suggesting that the fibers were organic material that was burned off during the baking process. XRD and XRF results show the crystal structure and the chemical composition of the unused unbaked and unused baked cal-sil samples. Based on XRD results, as shown in Figures 4-61 and 4-62, both unused unbaked and unused baked cal-sil samples contained crystalline substances of tobermorite [ $\text{Ca}_{2.25}(\text{Si}_3\text{O}_{7.5}(\text{OH})_{1.5})(\text{H}_2\text{O})$ ] and calcite ( $\text{CaCO}_3$ ). XRF results are presented in Table 4-5. The XRF analysis involves heating the sample to 80°C, during which all elements are oxidized to their highest oxidation state. Therefore, the results are reported as percent composition of oxides of various metals, but they give an indication of the elements that were detected in the sample. The results in Table 4-5 indicate that the dominant elements in cal-sil include silicon, calcium, and small amounts of aluminum, iron, sodium, manganese, titanium, phosphorus, and magnesium. As a result, silicon and calcium may be leaching out of the cal-sil to the test solution during Tests #3 and #4.

No significant difference was observed in elemental composition between unbaked and baked unused cal-sil, as shown in Table 4-6. Carbon content is an exception, because it cannot be quantified by XRF analysis. After being baked in a laboratory oven at 260°C for 72 hours, the unbaked cal-sil color changed from yellow to pink. The possible property changes of cal-sil after being baked include loss of water and oxidation of reduced species, such as organic carbon, Fe(0) and Fe(II), as well as possible mineral and crystal structural changes. Specifically, oxidation of Fe(0) and Fe(II) into  $\text{Fe}_2\text{O}_3$  is likely responsible for the baked cal-sil turning pink.

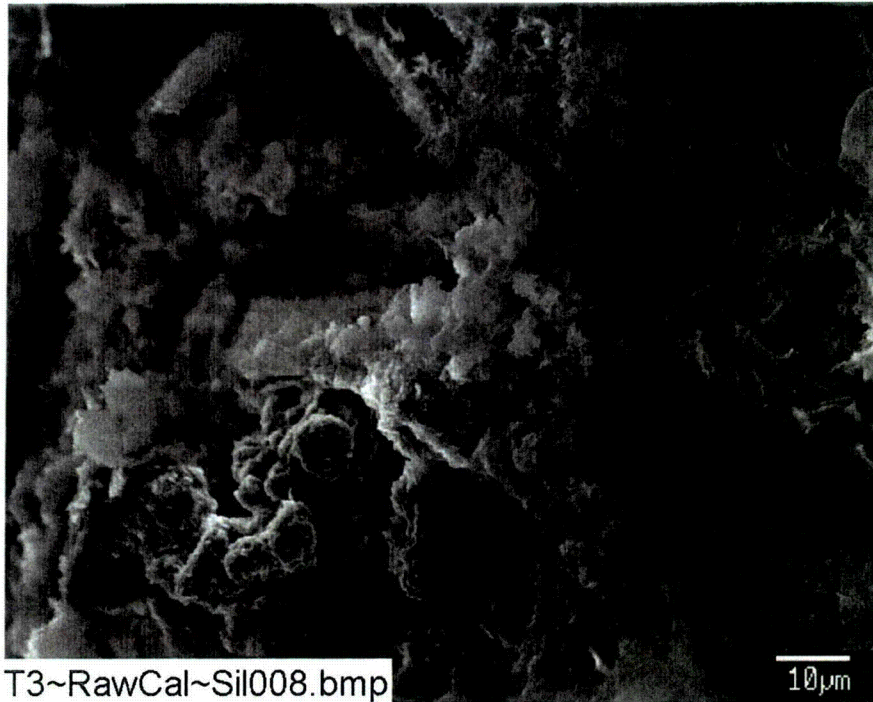


Figure 4-59. SEM image, magnified 1000 times, of an unused, unbaked cal-sil sample. (T3~RawCal\_Sil008)

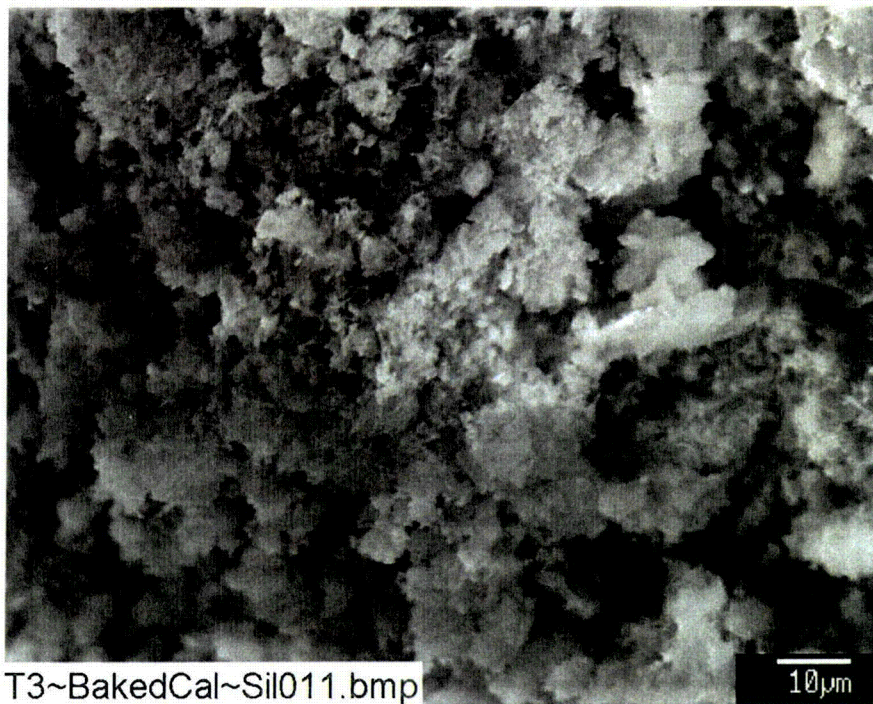


Figure 4-60. SEM image, magnified 1000 times, of an unused, baked cal-sil sample. (T3~BakedCal\_Sil011)



**Table 4-6. Dry Mass Composition (%) of Unused Cal-Sil Samples by XRF Analysis**

<b>Compound</b>	<b>Unbaked Cal-Sil</b>	<b>Baked Cal-Sil</b>
SiO <sub>2</sub>	38.34	33.87
TiO <sub>2</sub>	0.18	0.36
Al <sub>2</sub> O <sub>3</sub>	5.02	4.27
Fe <sub>2</sub> O <sub>3</sub>	2.54	2.07
FeO	0.00	0.00
MnO	0.06	0.05
MgO	0.79	1.35
CaO	34.76	34.66
Na <sub>2</sub> O	2.32	2.27
K <sub>2</sub> O	0.42	0.35
P <sub>2</sub> O <sub>5</sub>	0.15	0.12
H <sub>2</sub> O(-)	0.35	0.56
H <sub>2</sub> O(+) CO <sub>2</sub>	18.75	1.59
Total	103.67	81.50

**Test #3, Day 30, Submerged Cal-Sil Samples**

TSP was injected into the test solution in Test #3 but not in Test #4. A Day-30 baked cal-sil sample that had been submerged in the high-flow region and a Day-30 unbaked cal-sil sample that had been submerged in the birdcage were examined. The exterior surface of the baked cal-sil samples from the high-flow region was examined by ESEM/EDS, and the results are shown in Figures 4-63, 4-64, and 4-65. These results show a significant amount of phosphorus, which is presumably because of the formation of a calcium phosphate precipitate. A comparison of Figures 4-64 and 4-65 indicates that Figure 4-64 has a phosphorus peak bigger than the silicon peak, and the situation is reversed in Figure 4-65. This suggests that the lighter-colored material in Figure 4-63 is predominantly the calcium phosphate precipitate on top of the cal-sil, whereas the darker-colored material is predominantly the background cal-sil. Smaller amounts of phosphorus were found on the exterior of the unbaked cal-sil in the birdcage sample, as shown in Figures 4-66 and 4-67, but the presence of phosphorus was still evident. However, almost no phosphorus was present in the interior of the unbaked cal-sil, as shown in Figures 4-68 and 4-69. The interior cal-sil sample was obtained by breaking a chunk of cal-sil in half and examining the interior surface with SEM. The lack of phosphorus may be explained by the limited phosphate diffusion into the cal-sil interior. The EDS results are used as evidence that phosphate may react with calcium in Test #3 and form calcium phosphate precipitates in the bulk solution and on the submerged cal-sil exterior surface, both baked and unbaked.

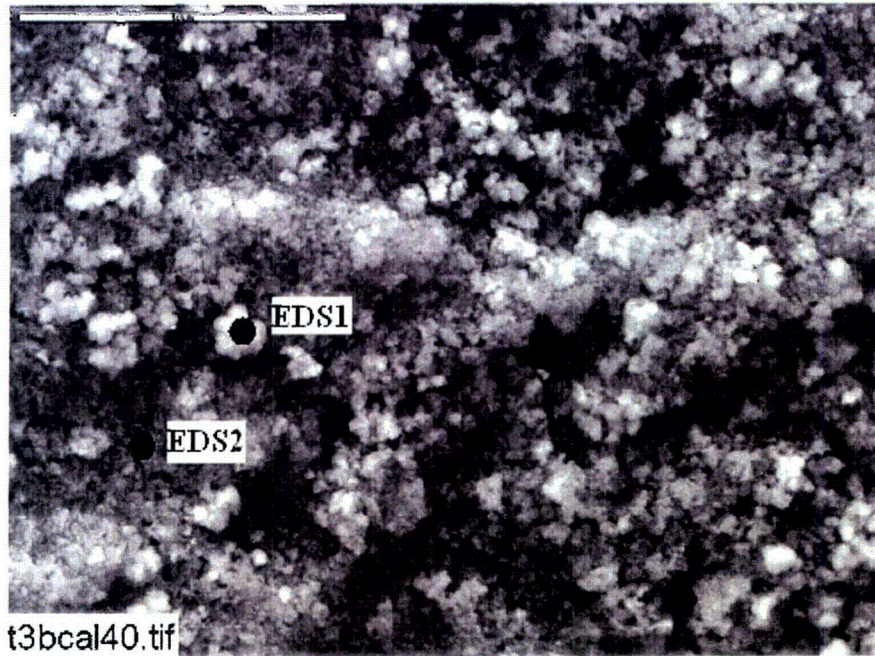


Figure 4-63. Annotated ESEM image, magnified 1000 times, of the exterior of a Test #3, Day 30, submerged high-flow baked cal-sil sample. (t3bcal40)

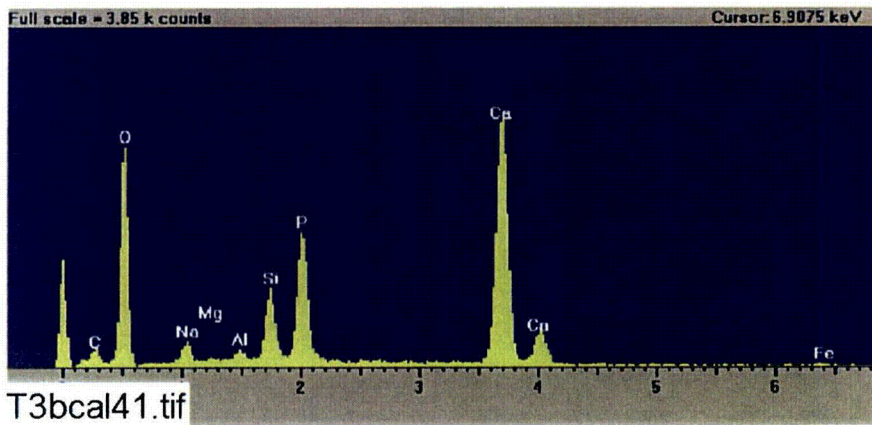


Figure 4-64. EDS counting spectrum for the light particles (EDS1) shown in Figure 4-63. (T3bcal41)

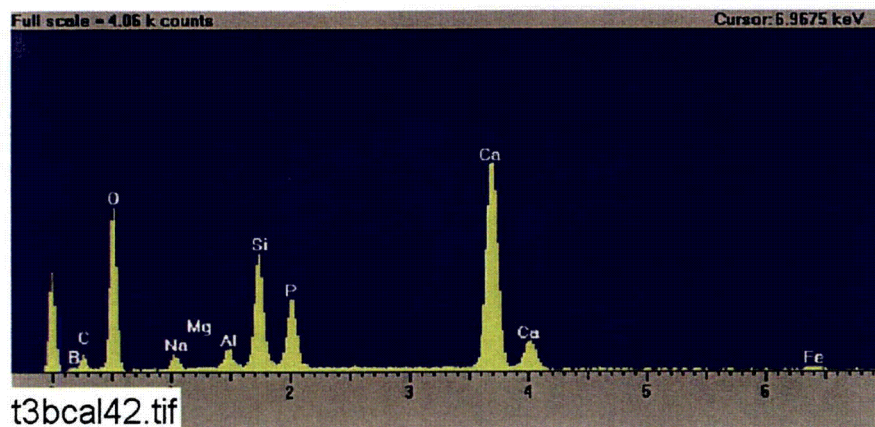


Figure 4-65. EDS counting spectrum for the dark particles (EDS2) shown in Figure 4-63. (t3bcal42)

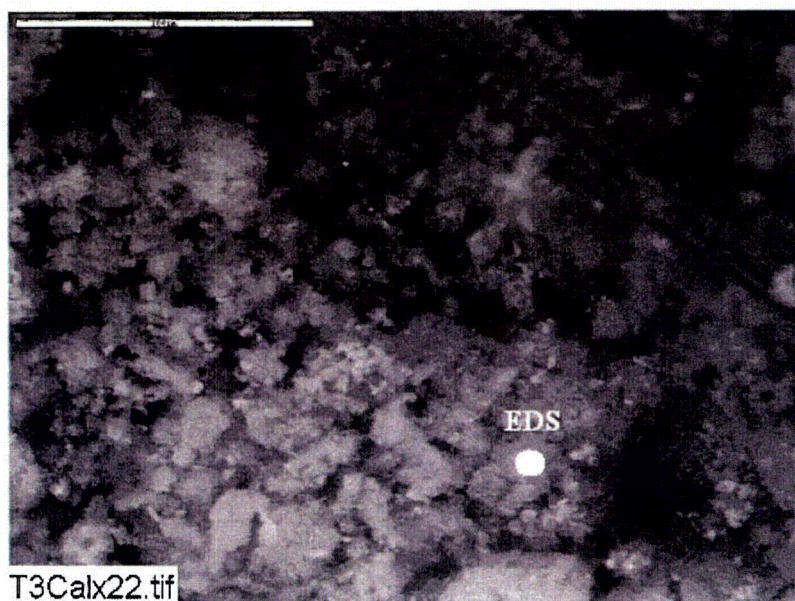


Figure 4-66. Annotated ESEM image, magnified 500 times, of the exterior of a Test #3, Day 30, unbaked cal-sil sample submerged in the birdcage. (T3Calx22)

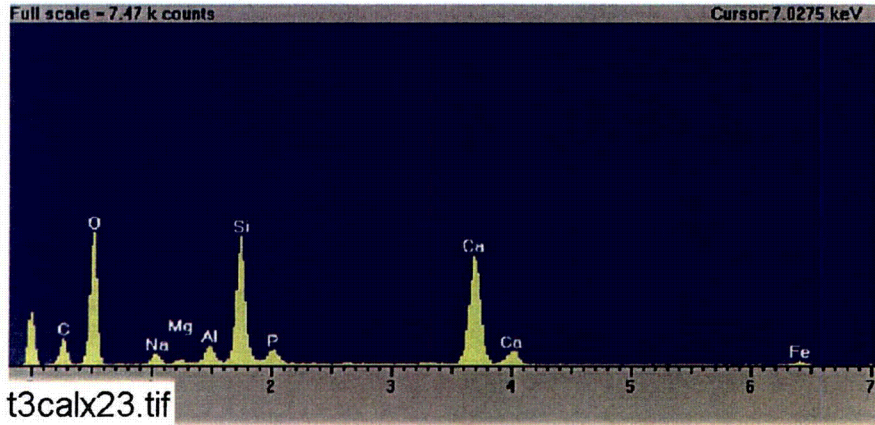


Figure 4-67. EDS counting spectrum for the particles shown in Figure 4-66. (t3calx23)

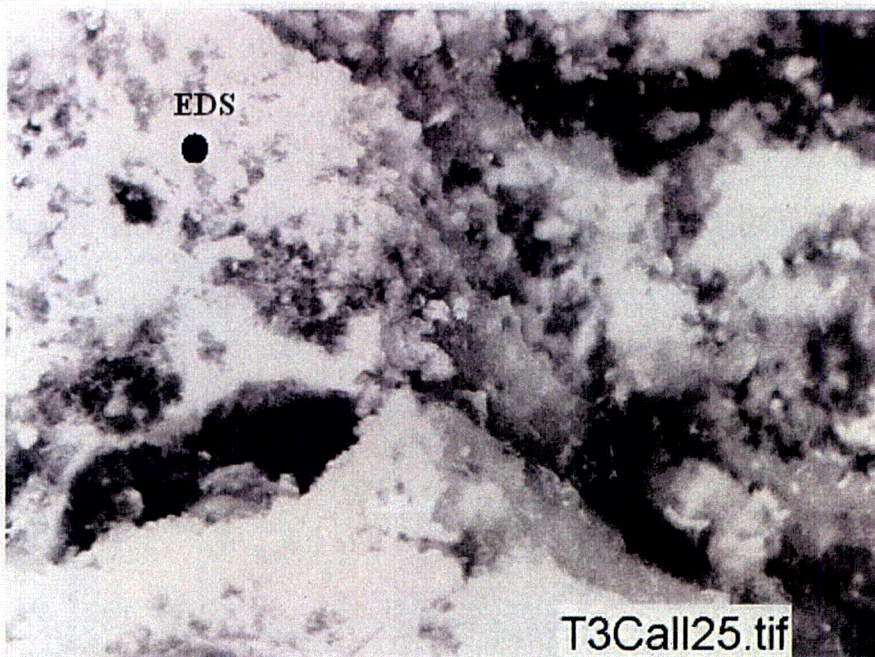


Figure 4-68. Annotated ESEM image, magnified 500 times, of the interior of a Test #3, Day 30, unbaked cal-sil sample submerged in the birdcage. (T3Call25)

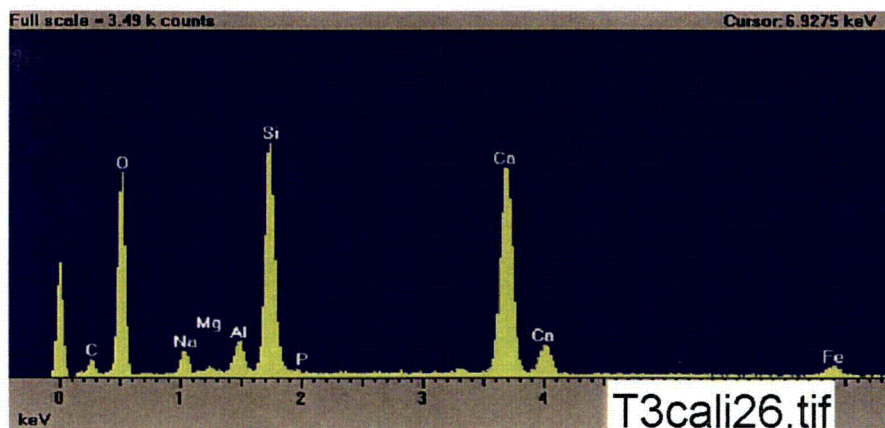


Figure 4-69. EDS counting spectrum for the particles shown in Figure 4-68. (T3cali26)

#### Test #4, Day 30, Submerged Cal-Sil Samples

No TSP was used in Test #4. Consequently, ESEM/EDS results showed no phosphorus on the exterior (Figures 4-70 and 4-71) or the interior cal-sil samples (Figures 4-72 and 4-73). The elements present in the Test #4 cal-sil are similar to the Test #3 cal-sil, with the exception of phosphorus and sodium. Phosphorus is observed on the exterior of the cal-sil samples in Test #3, but no phosphorus is observed in Test #4 because no TSP was used in Test #4. Comparing EDS results from Test #3 and Test #4, the sodium peak in Test #4 relative to other elements appears to be higher than in Test #3. This result is likely because of the relative differences in the aqueous sodium concentrations in the tests. In Test #3, 725 mg/L of sodium was added in the form of TSP, and in Test #4, 5520 mg/L of sodium was added in the form of NaOH. Residual sodium left on the samples during the drying and preparation process could leave the Test #4 samples with higher sodium than the Test #3 samples. In addition, sodium was present in solution as a dissolved ion throughout the duration of the tests (unlike phosphate) and was able to diffuse to the interior of the cal-sil (the cal-sil was essentially soaked in a sodium solution for 30 days) and so appears in relatively equal amounts in the interior and exterior.

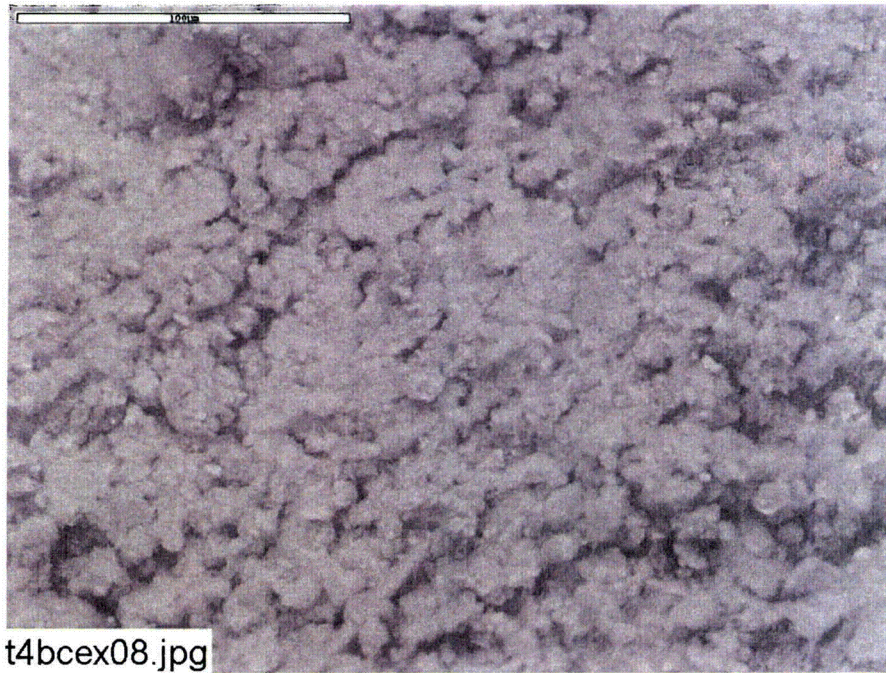


Figure 4-70. ESEM image, magnified 500 times, of a Test #4, Day 30, low-flow exterior baked cal-sil sample. (t4bcex08.jpg)

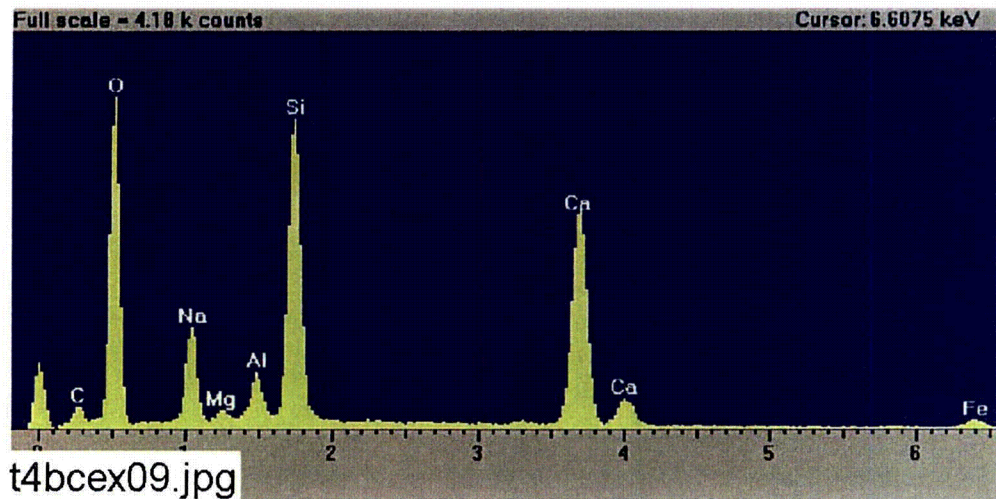
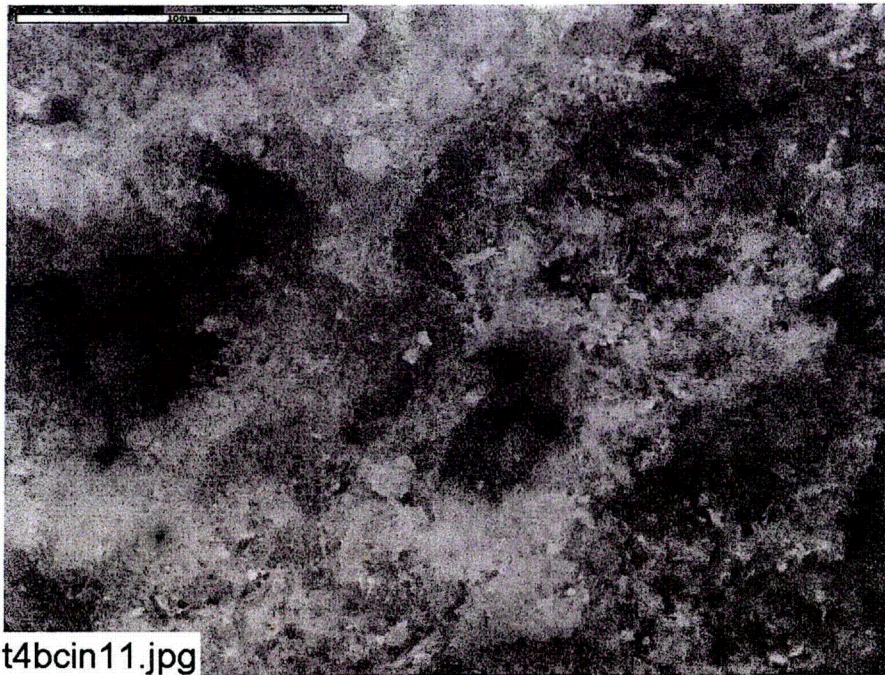
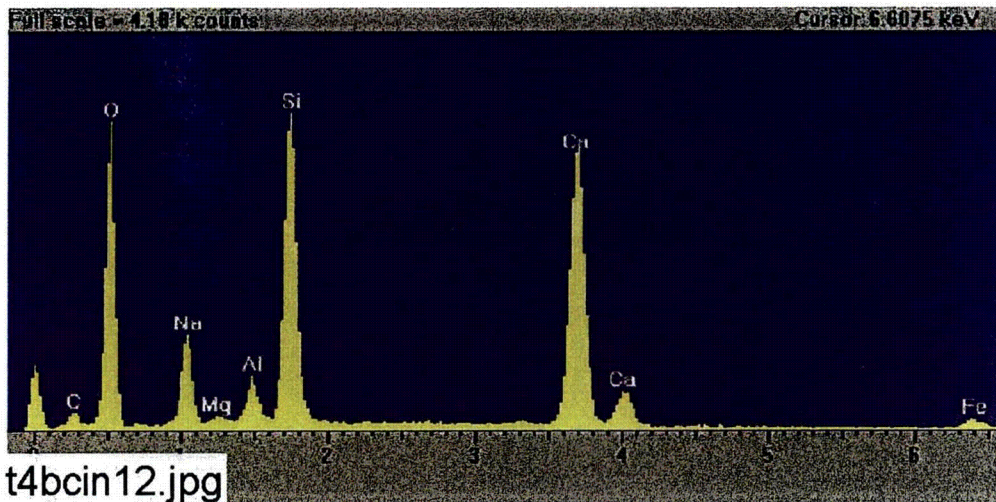


Figure 4-71. EDS counting spectrum for the whole image shown in Figure 4-70. (t4bcex09.jpg)



t4bcin11.jpg

Figure 4-72. ESEM image, magnified 500 times, of a Test #4, Day 30, low-flow interior baked cal-sil sample. (t4bcin11.jpg)



t4bcin12.jpg

Figure 4-73. EDS counting spectrum for the whole image shown in Figure 4-72. (t4bcin12.jpg)

### 4.3. Sediment

According to photographic evidence and SEM/EDS analysis, the sediment samples from the five ICET tests were composed mainly of debris of insulation material (i.e., fiberglass and/or cal-sil), dirt, corrosion products, and chemical precipitates. However, because of the differences in solution conditions (i.e., pH and trisodium phosphate) and the insulation materials, the relative compositions and amounts of the sediments varied among the tests. As shown in Table 4-6, the

largest amount of sediment was observed in Tests #3 and #4. Test #5 yielded the smallest amount of sediment.

As shown in Table 4-7, XRF analysis determined that silicon (Si) was the dominant element in the sediments of Tests #1, #2, and #5 because fiberglass was the sole insulation material used in these tests. Table 4-8 lists XRF results of unused insulation samples for reference. The XRF result for silicon (Si) is consistent with the SEM results showing large portions of fiberglass debris in the sediments. The fiber debris present at the bottom of the ICET tank represents fiberglass that escaped the stainless-steel mesh bags that were constructed to hold the primary volume of this debris type. The detection of quartz in XRD results of Tests #1, #2, and #5 sediment samples (Figures 4-78, 4-83, and 4-98) further verified the presence of some fiberglass debris in the sediments. However, in Tests #3 and #4, calcium content was higher than silicon in the sediment because 80% of the fiberglass was replaced by cal-sil as the insulation material in those two tests. As a result, cal-sil debris contributed largely to the sediments, as shown in the SEM/EDS results. The XRD results (Figures 4-89 and 4-94) indicate that Test #3 and Test #4 sediment contained crystalline of calcite ( $\text{CaCO}_3$ ) and tobermorite in two forms,  $[\text{Ca}_{2.25}(\text{Si}_3\text{O}_{7.5}(\text{OH})_{1.5})(\text{H}_2\text{O})]$  and  $\text{Ca}_4(\text{Si}_6\text{O}_{15}(\text{OH})_2)(\text{H}_2\text{O})_5$ , which match the XRD results of unused, baked and unused, unbaked cal-sil samples. This result suggests that the sediment obtained from Tests #3 and #4 was mostly attributable to the addition of the cal-sil material.

In addition, because of the injection of trisodium phosphate in Tests #2 and #3, a significantly higher phosphorus content was found in the sediments of Tests #2 and #3 than in the other tests. The presence of aluminum, calcium, iron, magnesium, and manganese in the sediments are likely a result of corrosion products of metallic and concrete coupons and/or from the leaching of insulation materials.

**Table 4-7. Elemental Composition of the Sediment Samples from Different Tests Based on XRF Analysis**

Element	Test #1 (%)	Test #2 (%)	Test #3 (%)	Test #4 (%)	Test #5 (%)
Si	27.0	17.5	16.9	16.0	29.8
Ti	0.1	0.1	0.1	0.1	0.1
Al	3.3	8.5	2.6	2.5	3.2
Fe	1.4	0.5	1.6	1.5	0.9
Mn	0.2	0.1	0.0	0.0	0.1
Mg	1.3	0.9	0.4	0.4	1.1
Ca	3.9	3.6	19.4	20.4	3.9
Na	8.7	2.9	1.6	3.7	6.9
K	0.7	0.6	0.4	0.2	0.9
P	0.0	4.4	1.3	0.1	0.0
Wet Sediment Recovered (g)	292	256	78,000	86,000	89

**Table 4-8. Elemental Composition of the Fiberglass Samples Based on XRF Analysis**

<b>Element</b>	<b>Clean Fiberglass</b>	<b>Unbaked Cal-sil</b>	<b>Baked Cal-Sil</b>
Si	29.2	15.8	17.9
Ti	--	0.2	0.1
Al	1.9	2.3	2.7
Fe	--	1.5	1.8
Mn	--	0.1	0.1
Mg	2.1	0.8	0.5
Ca	5.9	24.8	24.8
Na	11.7	1.7	1.7
K	--	0.3	0.3
P	--	0.1	0.1

#### **4.3.1. Test #1 Sediment**

Figure 4-74 is a photograph of the sediment sample from the bottom of the tank after completion of Test #1. The photograph shows that a large portion of the sediment is fiberglass debris, which is consistent with SEM images in Figures 4-75, 4-76, and 4-77. Besides fiberglass debris, the particulate materials in the sediment mixture likely are from corrosion products, dirt, and chemical precipitates. A total of 292 g of wet sediment were recovered from the tank following the test.

In addition to the photograph and SEM images, XRD was used to determine the composition and the structure of some solid polycrystalline substances. As shown in Figure 4-78, the XRD spectrum indicates the presence of quartz in the sediment, which is consistent with the photograph and SEM images showing fiberglass debris in the sediment. Another possible crystal, sigloite, is not likely present in the sediment because the sigloite XRD peaks do not totally match the sample spectrum.

To further characterize other properties of the Test #1 sediment, the ratio between dry and wet sediment mass was determined and the qualitative resuspension and settling behavior of the sediment was performed. The ratio of dry to moist sediment mass was determined to be between 0.4 and 0.5. The sediment was shown to resuspend upon agitation and provide a turbidity measurement of 77 NTU after 40 minutes. Comparing this result to that of clean tap water (0.8 NTU), it can be concluded that a significant concentration of particles remained in solution after 40 minutes.